

Measurement of the $W\gamma$ and $Z\gamma$ inclusive cross sections in pp collisions at $\sqrt{s} = 7$ TeV and limits on anomalous triple gauge boson couplings

S. Chatrchyan *et al.*^{*}

(CMS Collaboration)

(Received 31 August 2013; published 13 May 2014)

Measurements of $W\gamma$ and $Z\gamma$ production in proton-proton collisions at $\sqrt{s} = 7$ TeV are used to extract limits on anomalous triple gauge couplings. The results are based on data recorded by the CMS experiment at the LHC that correspond to an integrated luminosity of 5.0 fb^{-1} . The cross sections are measured for photon transverse momenta $p_T^\gamma > 15 \text{ GeV}$, and for separations between photons and final-state charged leptons in the pseudorapidity-azimuthal plane of $\Delta R(\ell, \gamma) > 0.7$ in $\ell\nu\gamma$ and $\ell\ell\gamma$ final states, where ℓ refers either to an electron or a muon. A dilepton invariant mass requirement of $m_{\ell\ell} > 50 \text{ GeV}$ is imposed for the $Z\gamma$ process. No deviations are observed relative to predictions from the standard model, and limits are set on anomalous $WW\gamma$, $ZZ\gamma$, and $Z\gamma\gamma$ triple gauge couplings.

DOI: 10.1103/PhysRevD.89.092005

PACS numbers: 14.70.-e, 12.15.-y, 13.40.Em, 13.85.Qk

I. INTRODUCTION

The standard model (SM) has been enormously successful in describing the electroweak (EW) and strong interactions. However, important questions remain unanswered regarding possible extensions of the SM that incorporate new interactions and new particles. The self-interactions of the electroweak gauge bosons comprise an important and sensitive probe of the SM, as their form and strength are determined by the underlying $SU(2) \times U(1)$ gauge symmetry. A precise measurement of the production of pairs of EW bosons (“diboson” events) provides direct information on the triple gauge couplings (TGCs), and any deviation of these couplings from their SM values would be indicative of new physics. Even if the new phenomena involve the presence of objects that can only be produced at large energy scales, i.e., beyond the reach of the Large Hadron Collider (LHC), they can nevertheless induce changes in the TGCs. In addition, since diboson processes represent the primary background to the SM Higgs production, their precise measurement is important for an accurate evaluation of Higgs boson production at the LHC, particularly in association with gauge bosons.

Aside from $\gamma\gamma$ production, the EW $W\gamma$ and $Z\gamma$ production processes at hadron colliders provide the largest and cleanest yields, as backgrounds to $W\gamma$ and $Z\gamma$ production can be significantly suppressed through the identification of the massive W and Z vector bosons via their leptonic decay modes. Measurements from LEP [1–4], the Tevatron [5–9], and initial analyses at the LHC [10–12] have already

explored some of the parameter space of anomalous TGCs (ATGCs) in $W\gamma$ and $Z\gamma$ processes.

We describe an analysis of inclusive $W\gamma$ and $Z\gamma$ events, collectively referred to as “ $V\gamma$ ” production, based on the leptonic decays $W \rightarrow e\nu$, $W \rightarrow \mu\nu$, $Z \rightarrow ee$, and $Z \rightarrow \mu\mu$, observed in pp collisions at a center-of-mass energy of 7 TeV. The data, corresponding to an integrated luminosity $L = 5.0 \text{ fb}^{-1}$, were collected in 2011 with the Compact Muon Solenoid (CMS) detector at the LHC. The previous results from pp collisions at $\sqrt{s} = 7$ TeV at the LHC were limited by the statistics of the data samples, and this analysis achieves a significant improvement in precision.

$V\gamma$ production can be represented by the Feynman diagrams of Fig. 1. Three processes contribute: (a) initial-state radiation, where a photon is radiated by one of the incoming virtual partons; (b) final-state radiation, where a photon is radiated by one of the charged leptons from V decay; and (c) TGC at the $WW\gamma$ vertex in $W\gamma$ production, and at the $ZZ\gamma$ and $Z\gamma\gamma$ vertices in $Z\gamma$ production. In the SM, contributions from the TGC process are expected only for $W\gamma$ production, because neutral TGCs are forbidden at tree level [13,14].

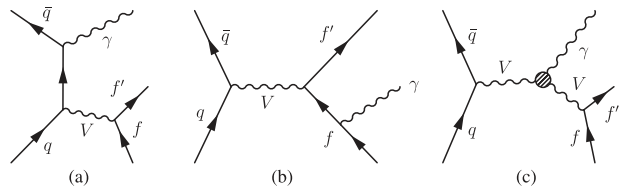


FIG. 1. The three lowest-order diagrams for $V\gamma$ production, with V corresponding to both virtual and on-shell γ , W , and Z bosons. The three diagrams reflect contributions from (a) initial-state radiation, (b) final-state radiation, and (c) TGC. The TGC diagram does not contribute at the lowest order to SM $Z\gamma$ production, since photons do not couple to particles without electric charge.

* Full author list given at the end of the article.

This paper is organized as follows: Brief descriptions of the CMS detector and Monte Carlo (MC) simulations are given in Sec. II. Selection criteria used to identify the final states are given in Sec. III. Dominant backgrounds to $V\gamma$ production are described in Sec. IV, along with methods used to estimate background contributions. Measurements of cross sections and limits on ATGCs are given, respectively, in Secs. V and VI, and the results are summarized in Sec. VII.

II. CMS DETECTOR AND MONTE CARLO SIMULATION

The central feature of the CMS apparatus is a superconducting solenoid, which is 13 m long and 6 m in diameter, and provides an axial magnetic field of 3.8 T. The bore of the solenoid is instrumented with detectors that provide excellent performance for reconstructing hadrons, electrons, muons, and photons. Charged particle trajectories are measured with silicon pixel and strip trackers that cover all azimuthal angles $0 < \phi < 2\pi$ and pseudorapidities $|\eta| < 2.5$, where η is defined as $-\ln[\tan(\theta/2)]$, with θ being the polar angle of the trajectory of the particle relative to the counterclockwise beam direction. A lead tungstate crystal electromagnetic calorimeter (ECAL) and a brass/scintillator hadron calorimeter (HCAL) surround the tracking volume. Muons are identified and measured in gas-ionization detectors embedded in the steel flux-return yoke outside of the solenoid. The detector coverage is nearly hermetic, providing thereby accurate measurements of the imbalance in momentum in the plane transverse to the beam direction. A two-tier trigger system selects the most interesting pp collisions for use in analyses. A more detailed description of the CMS detector can be found in Ref. [15].

The main background to $W\gamma$ and $Z\gamma$ production arises from $W + \text{jets}$ and $Z + \text{jets}$ events, respectively, in which one of the jets is misidentified as a photon. To minimize systematic uncertainties associated with the modeling of parton fragmentation through MC simulation, this background is estimated from multijet events in data, as described in Sec. IV. The background contributions from other processes, such as $t\bar{t}$, $\gamma + \text{jets}$, and multijet production, are relatively small, and are estimated using MC simulation.

The MC samples for the signal processes $W\gamma + n \text{jets}$ and $Z\gamma + n \text{jets}$, where $n < 3$, are generated with MADGRAPH v5.1.4.2 [16] and interfaced to PYTHIA v6.424 [17] for parton showering and hadronization. The kinematic distributions for these processes are cross-checked with expectations from SHERPA v1.2.2 [18], and the predictions from the two programs are found to agree. The signal samples are normalized to the predictions of next-to-leading-order (NLO) quantum chromodynamics from the MCFM v6.5 generator [19,20] using the CTEQ6.6 NLO parton distribution functions (PDF) [21].

Backgrounds from $t\bar{t}$, $W + \text{jets}$, $Z + \text{jets}$, WW , and $\gamma\gamma$ events are also simulated with the MADGRAPH program interfaced with PYTHIA. Multijet, $\gamma + \text{jets}$, and WZ and ZZ diboson events are generated using the stand-alone PYTHIA MC program and have negligible impact on the analysis. All these MC event samples, generated using the CTEQ6L1 leading-order (LO) PDF [22], are passed through a detailed simulation of the CMS detector based on GEANT4 [23] and reconstructed with the same software that is used for data.

III. SELECTION OF CANDIDATE EVENTS

The requirements for selecting isolated muons follow closely the standard CMS muon identification criteria [24]. However, electron and photon selection criteria are optimized specifically for this analysis and are described in greater detail in the following subsections, as are the reconstruction of transverse momentum imbalance or the “missing” transverse momentum (E_T), all trigger requirements, and the selections used to enhance the purity of signal.

The presence of pileup from additional overlapping interactions is taken into account in the analysis and cross-checked by studying the effectiveness of the selection criteria, separately, for small and large pileup rates in data. There are on average 5.8 overlapping interactions per collision for low-pileup data, and 9.6 interactions for high-pileup data, which correspond, respectively, to integrated luminosities of $L \approx 2.2 \text{ fb}^{-1}$ (referred to subsequently as run 2011A) and $L \approx 2.7 \text{ fb}^{-1}$ (referred to as run 2011B).

A. Electron identification and selection

Electrons are identified as “superclusters” (SCs) of energy deposition [25] in the ECAL fiducial volume that are matched to tracks from the silicon tracker. Tracks are reconstructed using a Gaussian sum filter algorithm that takes into account possible energy loss due to bremsstrahlung in the tracker. The SCs are required to be located within the acceptance of the tracker ($|\eta| < 2.5$). Standard electron reconstruction in the transition regions between the central barrel (EB) and the end cap (EE) sections of the ECAL ($1.44 < |\eta| < 1.57$) has reduced efficiency, and any electron candidates found in these regions are therefore excluded from consideration. The reconstructed electron tracks are required to have hits observed along their trajectories in all layers of the inner tracker. Electron candidates must have $p_T > 35$ and $> 20 \text{ GeV}$ for the $W\gamma$ and $Z\gamma$ analyses, respectively.

Particles misidentified as electrons are suppressed through the use of an energy-weighted width quantity in pseudorapidity ($\sigma_{\eta\eta}$) that reflects the dispersion of energy in η (“shower shape”) in a 5×5 matrix of the 25 crystals centered about the crystal containing the largest energy in

the SC [25]. The $\sigma_{\eta\eta}$ parameter is defined through a mean $\bar{\eta} = \sum \eta_i w_i / \sum w_i$ as follows:

$$\sigma_{\eta\eta}^2 = \frac{\sum (\eta_i - \bar{\eta})^2 w_i}{\sum w_i}, \quad i = 1, \dots, 25, \quad (1)$$

where the sum runs over all the elements of the 5×5 matrix, and $\eta_i = 0.0174 \hat{\eta}_i$, with $\hat{\eta}_i$ denoting the η index of the i th crystal; the individual weights w_i are given by $4.7 + \ln(E_i/E_T)$, unless any of the w_i are found to be negative, in which case they are set to zero. In the ensuing analysis, the value of $\sigma_{\eta\eta}$ is required to be consistent with expectations for electromagnetic showers, and the discriminant is used to suppress the background as well as to assess the contribution from the signal and background in fits to the data discussed in Sec. IVA 1.

In addition, the η and ϕ coordinates of the particle trajectories extrapolated to the ECAL are required to match those of the SC, and limits are imposed on the amount of HCAL energy deposited within the spatial cone $\Delta R = \sqrt{(\Delta\phi)^2 + (\Delta\eta)^2} < 0.15$ relative to the axis of the ECAL cluster. To reduce background from $\gamma \rightarrow e^+e^-$ conversions in the tracker material, the electron candidates are required to have no “partner” tracks within 2 mm of the extrapolated point in the transverse plane where both tracks are parallel to each other (near the hypothesized point of the photon conversion), and the difference in the cotangents of their polar angles must satisfy $|\Delta \cot\theta| > 0.02$. To ensure that an electron trajectory is consistent with originating from the primary interaction vertex, taken to be the one with the largest scalar sum of the p_T^2 of its associated tracks in the case of multiple vertices, the distances of closest approach are required to be $|d_z| < 0.1$ cm and $|d_T| < 0.02$ cm for the longitudinal and transverse coordinates, respectively.

To reduce background from jets misidentified as electrons, the electron candidates are required to be isolated from other energy depositions in the detector. The electron selection criteria are obtained by optimizing signal and background levels using simulated samples. This optimization is done separately for the EB and EE sections. Different criteria are used for the $W\gamma \rightarrow ev\gamma$ and $Z\gamma \rightarrow ee\gamma$ channels because of the different trigger requirements and relative background levels. For the $Z\gamma$ analysis, a relative isolation parameter (I_r) is calculated for each electron candidate through a separate sum of scalar p_T in the ECAL, HCAL, and tracker (TRK), all defined relative to the axis of the electron, but without including its p_T , within a cone of $\Delta R < 0.3$. In computing TRK isolation for electrons, each of the contributing tracks is required to have $p_T > 0.7$ GeV and to be consistent with originating from within $|d_z| < 0.2$ cm of the primary interaction vertex. This sum, reduced by $\rho \times \pi \times 0.3^2$ to account for the pileup contributions to the isolation parameter, and divided by the p_T of the electron candidate, defines the I_r for each subdetector. Here ρ is the mean energy (in GeV) per unit

area of (η, ϕ) for background from pileup, computed event by event using the FASTJET package [26].

The $W\gamma$ analysis uses individual I_r contributions from the three subdetectors. Also, to minimize the contributions from $Z\gamma$ events, a less restrictive selection is applied to the additional electron. The efficiencies for these criteria are measured in $Z \rightarrow ee$ data and in MC simulation, using the “tag and probe” technique of Ref. [27]. An efficiency correction of $\approx 3\%$ is applied to the MC simulation to match the performance observed in data.

B. Photon identification and selection

Photon candidates in the fiducial volume of the ECAL detector are reconstructed as SCs with efficiencies very close to 100% for $p_T^\gamma > 15$ GeV, as estimated from MC simulation. The photon energy scale is measured using $Z \rightarrow \mu\mu$ events, following the “PHOSPHOR” procedure described in Refs. [28,29].

As in the previous CMS analysis of $V\gamma$ final states [11], we reduce the rate of jets misreconstructed as photons by using stringent photon identification criteria, including isolation and requirements on the shapes of electromagnetic (EM) showers. In particular, (i) the ratio of HCAL to ECAL energies deposited within a cone of $\Delta R = 0.15$ relative to the axis of the seed ECAL crystal must be < 0.05 ; (ii) the value of $\sigma_{\eta\eta}$ must be < 0.011 in the barrel and < 0.030 in the end cap; and (iii) to reduce background from misidentified electrons, photon candidates are rejected if there are hits present in the first two inner layers of the silicon pixel detector that can originate from an electron trajectory that extrapolates to the location of the deposited energy in an ECAL SC of $E_T > 4$ GeV. This requirement is referred to as the pixel veto.

However, unlike in the previous analysis [11], the pileup conditions during run 2011 require modifications to photon isolation criteria to achieve reliable modeling of pileup effects. In particular, for photon candidates, the scalar sum of the p_T for all tracks originating from within $|d_z| < 0.1$ cm of the primary vertex, that have $|d_T| < 0.02$ cm, and that are located within a $0.05 < \Delta R < 0.4$ annulus of the direction of each photon candidate, are required to have $p_T^{\text{TRK}} < 2 \text{ GeV} + 0.001 \times p_T^\gamma + A_{\text{eff}} \times \rho$, where A_{eff} is the effective area used to correct each photon shower for event pileup. This procedure ensures that the isolation requirement does not exhibit a remaining dependence on pileup. For each photon candidate, the scalar sum of the p_T deposited in the ECAL in an annulus $0.06 < \Delta R < 0.40$, excluding a rectangular strip of $\Delta\eta \times \Delta\phi = 0.04 \times 0.40$ to reduce the impact of energy leakage from any converted $\gamma \rightarrow e^+e^-$ showers, is computed. The isolation in the ECAL is required to have $p_T^{\text{ECAL}} < 4.2 \text{ GeV} + 0.006 \times p_T^\gamma + A_{\text{eff}} \times \rho$, and finally, the isolation criterion in the HCAL is $p_T^{\text{HCAL}} < 2.2 \text{ GeV} + 0.0025 \times p_T^\gamma + A_{\text{eff}} \times \rho$. The expected values of A_{eff} are defined by the ratio of slopes obtained in fits of the isolation and ρ

TABLE I. The values of A_{eff} , in units of $\Delta\eta \times \Delta\phi$, used to correct contributions from pileup to the summed p_T accompanying photon candidates in the tracker and the two calorimeters, separately for photons observed in the barrel and end-cap regions of the ECAL.

Isolation	Barrel	End cap
Tracker	0.0167	0.032
ECAL	0.183	0.090
HCAL	0.062	0.180

parameters to a linear dependence on the number of vertices observed in data. These are summarized in Table I, separately for the three isolation parameters, calculated for EM showers observed in the barrel and end-cap regions of the ECAL.

To estimate the efficiency of requirements on the shape and isolation of EM showers, we use the similarity of photon and electron showers to select common shower parameters based on electron showers, but we use the isolation criteria that consider differences between the photon and electron characteristics. The results for data and MC simulation, as a function of p_T^γ and η^γ , are shown in Fig. 2. The efficiencies obtained using generator-level information in $Z \rightarrow ee$ and in $\gamma + \text{jets}$ simulations are also shown in Fig. 2. The difference between these efficiencies is taken as an estimate of systematic uncertainty in the photon identification efficiency, based on results from $Z \rightarrow ee$ data. The ratios of efficiency in data to that in simulation, both measured by the tag-and-probe method (squares), and of efficiency in $Z \rightarrow ee$ simulation to that in the $\gamma + \text{jets}$ simulation, obtained from generator-level information (triangles) as a function of p_T , integrated over the full range of η , are shown in Fig. 3. We find that the efficiencies in data and MC simulation agree to within 3% accuracy. As for the case of electrons and muons, we reweight the simulated events to reduce the residual discrepancy in modeling efficiency as a function of p_T^γ and η^γ .

The efficiency of the pixel veto is obtained from $Z \rightarrow \mu\mu\gamma$ data, where the photon arises from final-state radiation. The purity of such photon candidates is estimated to exceed 99.6%, and they are therefore chosen for checking photon identification efficiency, energy scale, and energy resolution. We find that the efficiency of the pixel veto corresponds to 97% and 89% for photons in the barrel and end-cap regions of the ECAL, respectively.

C. Muon identification and selection

Muons are reconstructed off-line by matching particle trajectories in the tracker and the muon system. The candidates must have $p_T > 35$ and > 20 GeV for the $W\gamma$ and $Z\gamma$ analyses, respectively. We require muon candidates to pass the standard CMS isolated muon selection criteria

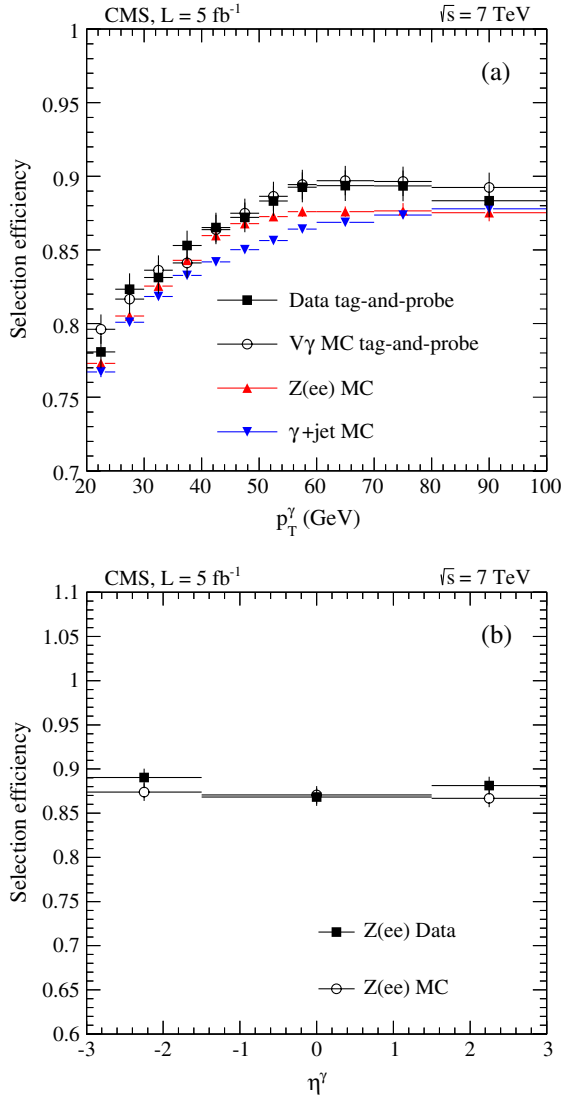


FIG. 2 (color online). Efficiency of photon selection, as a function of (a) photon transverse momentum and (b) photon pseudorapidity.

[24], with minor changes in requirements on the distance of closest approach of the muon track to the primary vertex. We require $|d_z| < 0.1$ cm in the longitudinal direction and $|d_T| < 0.02$ cm in the transverse plane. The efficiencies for these criteria are measured in data and in MC simulation using a tag-and-probe technique applied to $Z \rightarrow \mu\mu$ events. An efficiency correction of $\approx 3\%$ is also applied to the MC simulation to match the performance found in muon data.

D. Reconstruction of E_T

Neutrinos from $W \rightarrow \ell\nu$ decay are not detected directly, but they give rise to an imbalance in reconstructed transverse momentum in an event. This quantity is computed using objects reconstructed with the particle-flow algorithm [30], which generates a list of four-vectors of particles

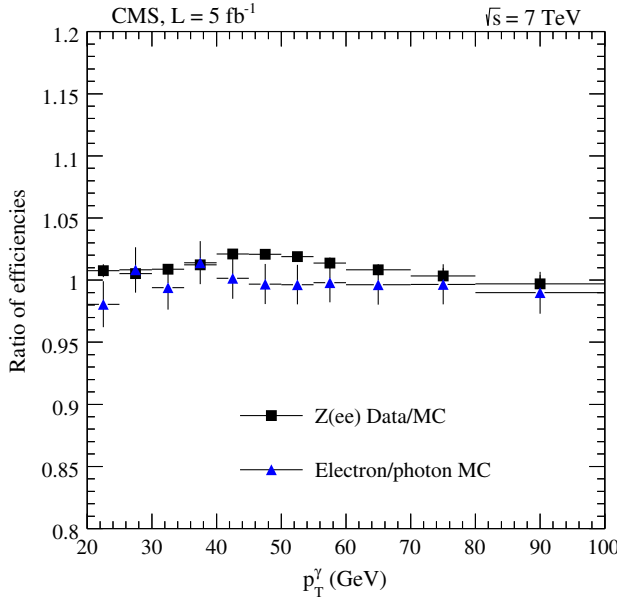


FIG. 3 (color online). Ratio of efficiencies for selecting photons in data relative to MC simulation, obtained through the tag-and-probe method, and the ratio of electron to photon efficiencies, obtained at the MC generator level, with both sets of ratios given as a function of the transverse momentum of the photon.

based on information from all subsystems of the CMS detector. The E_T for each event is defined by the magnitude of the vector sum of the transverse momenta of all the reconstructed particles.

E. Trigger requirements

The $W\gamma \rightarrow \ell\nu\gamma$ and $Z\gamma \rightarrow \ell\ell\gamma$ events are selected using unprescaled isolated lepton triggers. The p_T thresholds and isolation criteria imposed on lepton candidates at the trigger level changed with time to accommodate the instantaneous luminosity and are less stringent than the off-line requirements.

For the $W\gamma \rightarrow e\nu\gamma$ channel, we use an isolated single-electron trigger, requiring electrons with $|\eta| < 3$ and a p_T threshold of 32 GeV, except for the first part of run 2011A ($L = 0.2 \text{ fb}^{-1}$), where the threshold is 27 GeV. In addition, for the last part ($L = 1.9 \text{ fb}^{-1}$) of run 2011A and the entire run 2011B, a selection is implemented on the transverse mass (M_T^W) of the system consisting of the electron candidate and the E_T , requiring $M_T^W = \sqrt{2p_T^\ell E_T(1 - \cos \Delta\phi(\ell, E_T))} > 50 \text{ GeV}$, where $\Delta\phi$ is the angle between the p_T^ℓ and the E_T vectors. The trigger used for the $Z\gamma \rightarrow ee\gamma$ events requires two isolated electron candidates with p_T thresholds of 17 GeV on the leading (highest- p_T) candidate and 8 GeV on the trailing candidate.

The trigger for $W\gamma \rightarrow \mu\nu\gamma$ events requires an isolated muon with $p_T > 30 \text{ GeV}$ and $|\eta| < 2.1$. The dimuon trigger used to collect $Z\gamma \rightarrow \mu\mu\gamma$ events does not require

the two muons to be isolated and has coverage for $|\eta| < 2.4$. For most of the data, the muon p_T thresholds are 13 GeV for the leading and 8 GeV for the trailing candidates. For the first part of run 2011A ($L = 0.2 \text{ fb}^{-1}$) and for most of the remaining data, these thresholds are 7 GeV for each muon candidate, except for the last part of run 2011B ($L = 0.8 \text{ fb}^{-1}$), where these increase to 17 and 8 GeV, respectively.

F. $W\gamma$ event selections

The $W\gamma \rightarrow \ell\nu\gamma$ process is characterized by a prompt, energetic, and isolated lepton, a prompt isolated photon, and significant E_T that reflects the escaping neutrino. Both electrons and muons are required to have $p_T > 35 \text{ GeV}$, and photons are required to have $p_T > 15 \text{ GeV}$. The maximum allowed $|\eta|$ values for electrons, photons, and muons are 2.5, 2.5, and 2.1, respectively. We require the photon to be separated from the lepton by $\Delta R(\ell, \gamma) > 0.7$. To minimize contributions from $Z\gamma \rightarrow \ell\ell\gamma$ production, we reject events that have a second reconstructed lepton of the same flavor. This veto is implemented only for electrons that have $p_T > 20 \text{ GeV}$, $|\eta| < 2.5$, and pass looser electron selections, and for muons that have $p_T > 10 \text{ GeV}$ and $|\eta| < 2.4$.

To suppress background processes without genuine E_T , we require events to have $M_T^W > 70 \text{ GeV}$. We find that the E_T distribution is well modeled, but we apply a small efficiency correction to reduce the residual disagreement. The efficiencies of the M_T^W selection in data and simulation agree at the 1% level. The full set of $\ell\nu\gamma$ selections yields 7470 electron and 10 809 muon candidates in the data. The selection criteria used to define the $W\gamma$ sample are summarized in Table II.

G. $Z\gamma$ event selections

Accepted $Z\gamma$ events are characterized by two prompt, energetic, and isolated leptons and an isolated, prompt photon. Both electrons and muons are required to have $p_T > 20 \text{ GeV}$, and the photons are required to have $p_T > 15 \text{ GeV}$. The maximum $|\eta|$ values for accepted electrons, photons, and muons are 2.5, 2.5, and 2.4, respectively. We require photons to be separated from leptons by imposing a $\Delta R(\ell, \gamma) > 0.7$ requirement. Finally, the invariant mass of the two leptons is required to satisfy $m_{\ell\ell} > 50 \text{ GeV}$. Applying all these selections yields 4108 $Z\gamma \rightarrow ee\gamma$ and 6463 $Z\gamma \rightarrow \mu\mu\gamma$ candidates. The selection criteria used to define the $Z\gamma$ sample are summarized in Table II.

IV. BACKGROUND ESTIMATES

The dominant background for both $W\gamma$ and $Z\gamma$ production arises from events in which jets, originating mostly from $W + \text{jets}$ and $Z + \text{jets}$ events, respectively, are misidentified as photons. We estimate the background from

TABLE II. Summary of selection criteria used to define the $W\gamma$ and $Z\gamma$ samples.

Selection	$W\gamma \rightarrow e\nu\gamma$	$W\gamma \rightarrow \mu\nu\gamma$	$Z\gamma \rightarrow ee\gamma$	$Z\gamma \rightarrow \mu\mu\gamma$
Trigger	Single electron	Single muon	Dielectron	Dimuon
p_T^ℓ (GeV)	>35	>35	>20	>20
$ \eta^\ell $	EB or EE	<2.1	EB or EE	<2.4
p_T^γ (GeV)	>15	>15	>15	>15
$ \eta^\gamma $	EB or EE	EB or EE	EB or EE	EB or EE
$\Delta R(\ell, \gamma)$	>0.7	>0.7	>0.7	>0.7
M_T^W (GeV)	>70	>70		
$m_{\ell\ell}$ (GeV)			>50	>50
Other criterion	Only one lepton	Only one lepton		

these sources as a function of p_T^γ using the two methods described in Sec. IV A.

For the $W\gamma$ channel, a second major background arises from Drell-Yan ($q\bar{q} \rightarrow \ell^+\ell^-$) and EW diboson production, when one electron is misidentified as a photon. This background is estimated from data as described in Sec. IV B.

Other backgrounds to $V\gamma$ processes include (i) jets misidentified as leptons in $\gamma +$ jet production; (ii) $V\gamma$ events, with V decaying into $\tau\nu$ or $\tau\tau$, and subsequently $\tau \rightarrow \ell\nu\nu$; (iii) $t\bar{t}\gamma$ events; and (iv) $Z\gamma$ events, where one of the leptons from Z decay is not reconstructed properly. All these backgrounds are small relative to the contribution from $V +$ jets and are estimated using MC simulation.

A. Jets misidentified as photons

1. Template method

The template method relies on a maximum-likelihood fit to the distribution of $\sigma_{\eta\eta}$ in data to estimate the background from misidentified jets in the selected $V\gamma$ samples. The fit makes use of the expected distributions (“templates”) for genuine photons and misidentified jets. For isolated prompt photons, the $\sigma_{\eta\eta}$ distribution is very narrow and symmetric, while for photons produced in hadron decays, the $\sigma_{\eta\eta}$ distribution is asymmetric, with a slow falloff at large values. The distribution in $\sigma_{\eta\eta}$ for signal photons is obtained from simulated $W\gamma$ events. The $\sigma_{\eta\eta}$ distribution of electrons from Z -boson decays in data is observed to be shifted to smaller values relative to simulated events. The shift is 0.9×10^{-4} and 2.0×10^{-4} for the EB and EE regions, respectively, and corresponds to 1% and 0.8% shifts in the average of the simulated photon $\sigma_{\eta\eta}$ values, which are corrected for the shift relative to data.

The $\sigma_{\eta\eta}$ templates for background are defined by events in a background-enriched isolation sideband of data. These photon candidates are selected using the photon identification criteria described in Sec. III B, but without the $\sigma_{\eta\eta}$ selection, and with inverted TRK isolation requirements: (i) $2 \text{ GeV} < p_T^{\text{TRK}} - 0.001 \times p_T^\gamma - 0.0167 \times \rho < 5 \text{ GeV}$, for $|\eta_\gamma| < 1.4442$, and (ii) $2 \text{ GeV} < p_T^{\text{TRK}} - 0.001 \times p_T^\gamma - 0.0320 \times \rho < 3 \text{ GeV}$, for $1.566 < |\eta_\gamma| < 2.5$. These

requirements ensure that the contributions from genuine photons are negligible, while the isolation requirements remain close to those used for the selection of photons and thereby provide jets with large EM energy fractions that have properties similar to those of genuine photons. We observe that $\sigma_{\eta\eta}$ is largely uncorrelated with the isolation parameter in simulated multijet events, so that the distribution observed for background from jets that are misidentified as photons (i.e., with inverted tracker isolation criteria) is expected to be the same as that for jets misidentified as isolated photons.

Because of the M_T^W requirement in selected $W\gamma$ events, the presence of significant E_T can bias the estimation of the background. We therefore investigate possible correlations between the distribution in $\sigma_{\eta\eta}$ for background events and the projection of E_T along the p_T of jets misidentified as photons. In particular, we define $\sigma_{\eta\eta}$ templates for background using events in data with $E_T > 10 \text{ GeV}$ and with the direction of the E_T vector along the photonlike jet. The estimated systematic uncertainty is obtained from the smallest bin in p_T^γ ($15 < p_T^\gamma < 20 \text{ GeV}$), as this is the bin that contains most of the background (Fig. 4) and corresponds to the largest control sample for input to the $\sigma_{\eta\eta}$ template representing the background. Based on the modified templates, we assign a systematic uncertainty that reflects the largest discrepancy relative to the nominal yield, which is found to be 13% and 7% for the barrel and end cap, respectively. A more detailed discussion of systematic uncertainties in the background estimate is given in Sec. V D.

The systematic uncertainty in electron misidentification is estimated through changes made in the modeling of signal and background, the electron and photon energy resolutions, and the distributions for pileup in MC simulations.

The function fitted to the observed distribution of $\sigma_{\eta\eta}$ is the sum of contributions from signal (S) and background (B):

$$N_S S(\sigma_{\eta\eta}) + N_B B(\sigma_{\eta\eta}) = N \left[\frac{N_S}{N} S(\sigma_{\eta\eta}) + \left(1 - \frac{N_S}{N}\right) B(\sigma_{\eta\eta}) \right], \quad (2)$$

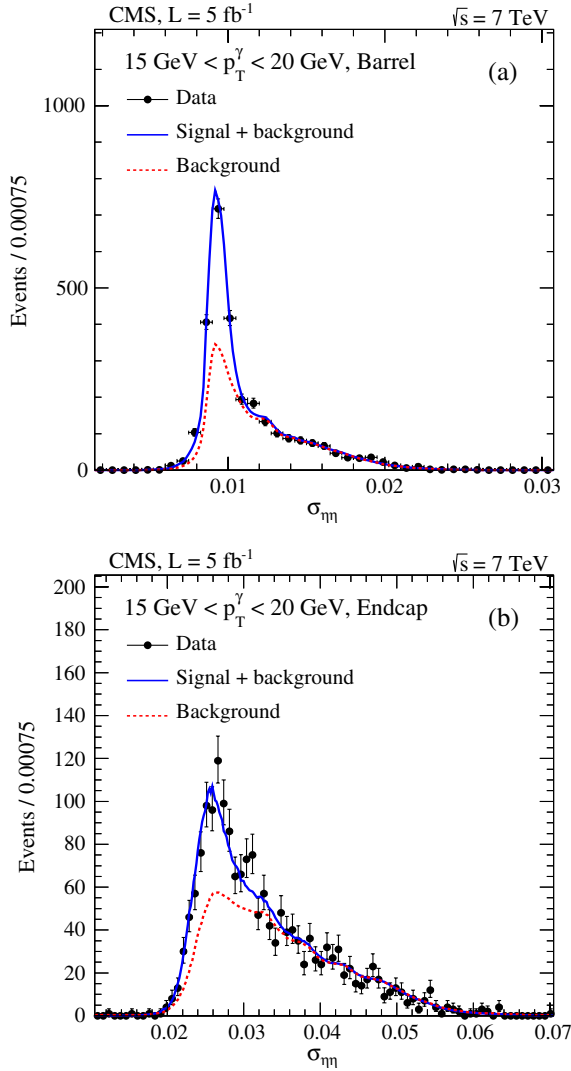


FIG. 4 (color online). Fit to the $\sigma_{\eta\eta}$ distribution for photon candidates with $15 < p_T^\gamma < 20$ GeV in data with signal and background templates in the (a) barrel and (b) end caps.

where N , N_S , and N_B are the total number of events and the number of signal and background candidates in data for any given bin of p_T^γ , respectively. The functions $S(\sigma_{\eta\eta})$ and $B(\sigma_{\eta\eta})$ represent the expected signal and background distributions in $\sigma_{\eta\eta}$. These distributions are smoothed using a kernel-density estimator [31], or through direct interpolation when the statistical uncertainties are small, which makes it possible to use unbinned fits to the data in regions where statistics are poor while preserving the good performance of the fit. The fit uses an unbinned extended likelihood [32] function (L) to minimize $-\ln L$ as a function of the signal fraction $f_S = N_S/N$:

$$-\ln L = (N_S + N_B) - \ln[f_S S(\sigma_{\eta\eta}) + (1 - f_S) B(\sigma_{\eta\eta})]. \quad (3)$$

2. Ratio method

We use a second method, referred to as the “ratio method,” to infer the $V +$ jets background as a cross-check of the results obtained with the template method at large p_T^γ , where the template method is subject to larger statistical uncertainties. The ratio method uses $\gamma +$ jets and multijet data to extract the misidentification rate, taking into account the quark/gluon composition of the jets in $V +$ jets events.

The ratio method exploits a category of jets that have properties similar to electromagnetic objects in the ECAL and are called photonlike jets. Photonlike jets are jets selected through the presence of photons that pass all photon selection criteria, but fail either the photon isolation or $\sigma_{\eta\eta}$ requirements. However, these kinds of jets are still more isolated and have higher EM fractions than most generic jets.

The ratio method provides a ratio R_p of the probability for a jet to pass photon selection criteria and that of passing photonlike requirements. Once R_p is known, the number of jets that satisfy the final photon selection criteria (N_{V+jets}) can be estimated as the product of R_p and the number of photonlike jets in data.

We measure R_p separately for each p_T^γ bin of the analysis for both the barrel and end-cap regions of the ECAL, using “diphoton” events, defined by the presence of either two photon candidates that pass the final photon selections, or of one photon candidate that passes the final selections and one that passes only photonlike jet selections. To reduce

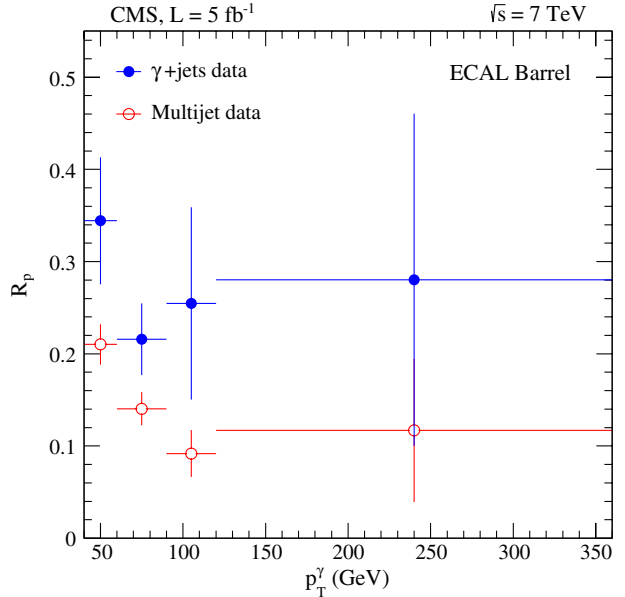


FIG. 5 (color online). The R_p ratio (described in text) as a function of the p_T of photon candidates for the barrel region of the ECAL in $\gamma +$ jets and multijet data. The difference in R_p values for the two processes is attributed to the fact that jets in $\gamma +$ jets events are dominated by quark fragmentation, while jets in multijet events are dominated by gluon fragmentation.

TABLE III. Yield of misidentified photons from jets in $W +$ jets events and their symmetrized associated systematic uncertainties as a function of p_T^γ in the $W\gamma \rightarrow \ell\nu\gamma$ analyses. The results are specified in the second column by the number of events expected in the $e\nu\gamma$ and $\mu\nu\gamma$ channels, and by the uncertainties from each of the sources in the rest of the columns.

p_T^γ (GeV)	Yield from $W +$ jets events	Shape of γ shower	Systematic uncertainties on yields ($e\nu\gamma/\mu\nu\gamma$)			Diff. between jet $\rightarrow \gamma$ predictions
			Shape of jet shower	Sampling of distributions	Correlation of γ and E_T	
15–20	1450/2760	9.3/21	83/159	19/36	130/250	
20–25	650/1100	5.2/20	37/63	11/19	54/94	
25–30	365/520	3.7/9.4	21/30	9.4/14	33/43	
30–35	220/330	10.5/3.3	12/19	7.5/11	19/29	
35–40	160/200	3.4/2.8	10/12	6.2/7.9	14/16	
40–60	220/270	3.5/0.7	19/23	5.1/6.3	19/24	22/4.4
60–90	77/100	1.4/0.9	10/13	3.0/3.8	6.6/8.5	7.7/1.6
90–120	26/21	2.0/2.3	5.3/4.1	0.9/0.9	2.4/1.8	2.6/0.4
120–500	15/38	4.3/2.1	7.6/26	1.1/0.7	1.0/3.9	1.5/0.6
Totals	3180/5350	17/30	98/179	27/45	280/470	34/7.0
			300/510			

correlations induced by the diphoton production kinematics, we require that the photons corresponding to each diphoton candidate be in the same η region and p_T^γ bin. A two-dimensional fit is performed based on templates of distributions in $\sigma_{\eta\eta}$ of each photon candidate to estimate R_p , and thereby subtract the contribution from genuine photons to the photonlike jet yield. As only 5%–10% of genuine photons in multijet events pass photonlike jet requirements, we correct the distribution in R_p using MC simulation of multijet events and check the correction through $Z \rightarrow ee$ data and simulation.

The observed R_p values for the barrel region of the ECAL are given in Fig. 5 as a function of p_T^γ . The difference between the two sets of R_p values extracted in different ways indicates the sensitivity of the method to whether the photonlike jet originates from hadronization of a quark or a gluon. We use the simulation of the

gluon-to-quark jet ratio in $W +$ jets and $Z +$ jets events to correct R_p as a function of the p_T of the photonlike jet. We find the predictions from the ratio method to be consistent with those from the template method, and we consider their difference as an additional source of systematic uncertainty in the analysis.

B. Background from electrons misidentified as photons in $\ell\nu\gamma$ events

The criterion that differentiates electrons from photons is the presence in the pixel detector of a track that is associated with a shower in the ECAL. We use $Z \rightarrow ee$ data to measure the probability ($P_{e \rightarrow \gamma}$) for an electron not to have a matching track by requiring one of the electrons to pass stringent electron identification criteria, and then by checking how often the other electron passes the full photon selection criteria, including the requirement of

TABLE IV. Yield of misidentified photons from jets in $Z +$ jets events and their symmetrized associated systematic uncertainties as a function of p_T^γ in the $Z\gamma \rightarrow \ell\ell\gamma$ analyses. The results are specified by the numbers of events expected in the $ee\gamma$ and $\mu\mu\gamma$ channels, and by the uncertainties from each of the sources.

p_T^γ (GeV)	Yield from $Z +$ jets events	Shape of γ shower	Systematic uncertainties on yields ($ee\gamma/\mu\mu\gamma$)			Diff. between jet $\rightarrow \gamma$ prediction
			Shape of jet shower	Sampling of distributions		
15–20	460/710	11/50	27/41	6.4/16		
20–25	200/310	6.8/23	11/18	3.7/6.7		
25–30	82/130	3.7/7.6	4.7/7.6	2.3/3.0		
30–35	51/82	2.8/10	2.9/4.7	1.9/1.8		
35–40	46/54	3.0/4.0	2.6/3.6	1.8/1.2		
40–60	40/72	3.8/11	2.3/5.8	0.9/1.5		11/9.5
60–90	18/25	3.0/6.5	1.1/3.6	0.7/0.6		4.8/3.2
90–120	0.0/14	0.0/3.8	0.0/1.9	0.0/0.3		0.0/4.4
120–500	5.3/6.6	4.6/13	0.4/1.4	0.1/0.2		1.4/3.6
Totals	910/1400	16/59	30/46	8.3/18		17/12
			38/77			

TABLE V. Summary of parameters used in the measurement of the $W\gamma$ cross section.

Parameter	$e\nu\gamma$ channel	$\mu\nu\gamma$ channel
$N^{\ell\nu\gamma}$	7470	10809
$N_B^{W+\text{jets}}$	$3180 \pm 50(\text{stat}) \pm 300(\text{syst})$	$5350 \pm 60(\text{stat}) \pm 510(\text{syst})$
N_B^{eeX}	$690 \pm 20(\text{stat}) \pm 50(\text{syst})$	$91 \pm 1(\text{stat}) \pm 5(\text{syst})$
N_B^{other}	$410 \pm 20(\text{stat}) \pm 30(\text{syst})$	$400 \pm 20(\text{stat}) \pm 30(\text{syst})$
$N_S^{\ell\nu\gamma}$	$3200 \pm 100(\text{stat}) \pm 320(\text{syst})$	$4970 \pm 120(\text{stat}) \pm 530(\text{syst})$
A_S	$0.108 \pm 0.001(\text{stat})$	$0.087 \pm 0.001(\text{stat})$
$A_S \cdot \epsilon_{\text{MC}} (W\gamma \rightarrow \ell\nu\gamma)$	$0.0187 \pm 0.0010(\text{syst})$	$0.0270 \pm 0.0014(\text{syst})$
ρ_{eff}	$0.940 \pm 0.027(\text{syst})$	$0.990 \pm 0.025(\text{syst})$
$L (\text{fb}^{-1})$	$5.0 \pm 0.1(\text{syst})$	$5.0 \pm 0.1(\text{syst})$

having no associated track in the pixel detector. Fitting to the $m_{\ell\ell}$ distribution using a convolution of Breit-Wigner and Crystal Ball [33] functions to describe the signal and a falling exponential function for background, we obtain the probability for an electron to have no associated track as $P_{e \rightarrow \gamma} = 0.014 \pm 0.003(\text{syst})$ and $0.028 \pm 0.004(\text{syst})$ for the barrel and the end cap regions, respectively.

To estimate the background from sources where an electron is misidentified as a photon in the $\mu\nu\gamma$ channel, we select events that pass all event selection criteria, except that the presence of a track in the pixel detector associated with the photon candidate is ignored. The contribution from genuine electrons misidentified as photons can therefore be calculated as

$$N_{e \rightarrow \gamma} = N_{\mu\nu e} \times \frac{P_{e \rightarrow \gamma}}{1 - P_{e \rightarrow \gamma}}, \quad (4)$$

where $N_{e \rightarrow \gamma}$ is the background from misidentified electrons and $N_{\mu\nu e}$ is the number of events selected without any requirement on the pixel track. The systematic uncertainties associated with this measurement are discussed in detail in Sec. V D.

The background in the $e\nu\gamma$ channel is dominated by $Z + \text{jets}$ events, where one of the electrons from $Z \rightarrow ee$ decays is misidentified as a photon. To estimate the $Z \rightarrow ee$ contribution to the $W\gamma \rightarrow e\nu\gamma$ signal, we apply the full selection criteria and fit the invariant mass of the photon and electron candidates with a Breit-Wigner function convolved with a Crystal Ball function for the Z boson and an exponential form for the background. Contributions to $e\nu\gamma$ events from other sources with genuine electrons misidentified as photons (e.g., $t\bar{t} + \text{jets}$ and diboson processes) are estimated using MC simulation, in which a photon candidate is matched spatially to the generator-level electron.

C. Total background

The background from jets that are misidentified as photons is summarized as a function of p_T of the photon in Table III for $\ell\nu\gamma$ events and in Table IV for $\ell\ell\gamma$ events, and the sums are listed as $N_B^{W+\text{jets}}$ in Table V and as $N_B^{Z+\text{jets}}$ in Table VI. The background from electrons in selected $\ell\nu\gamma$ events that are misidentified as photons, N_B^{eeX} , is summarized in Table III for both the $e\nu\gamma$ and $\mu\nu\gamma$ channels. The N_B^{other} in Tables V and VI indicates the rest of the

TABLE VI. Summary of parameters used in the measurement of the $Z\gamma$ cross section.

Parameter	$e\nu\gamma$ channel	$\mu\nu\gamma$ channel
$N^{\ell\ell\gamma}$	4108	6463
$N_B^{Z+\text{jets}}$	$910 \pm 50(\text{stat}) \pm 40(\text{syst})$	$1400 \pm 60(\text{stat}) \pm 80(\text{syst})$
N_B^{other}	$40 \pm 3(\text{stat})$	$24 \pm 2(\text{stat})$
$N_S^{\ell\ell\gamma}$	$3160 \pm 80(\text{stat}) \pm 90(\text{syst})$	$5030 \pm 100(\text{stat}) \pm 210(\text{syst})$
A_S	$0.249 \pm 0.001(\text{stat})$	$0.286 \pm 0.001(\text{stat})$
$A_S \cdot \epsilon_{\text{MC}} (Z\gamma \rightarrow \ell\ell\gamma)$	$0.1319 \pm 0.0018(\text{syst})$	$0.1963 \pm 0.0013(\text{stat})$
ρ_{eff}	$0.929 \pm 0.047(\text{syst})$	$0.945 \pm 0.016(\text{syst})$
$L (\text{fb}^{-1})$	$5.0 \pm 0.1(\text{syst})$	$5.0 \pm 0.1(\text{syst})$

background contributions estimated from simulation. For the $e\nu\gamma$ channel, the largest contribution to N_B^{other} (53%) is from $Z\gamma$ events, and the next largest is from $\gamma + \text{jets}$ with a contribution of 33%. For the $\mu\nu\gamma$ channel, the dominant background to N_B^{other} is from $Z\gamma$, with a contribution of 84%. All the specific parameters will be discussed in more detail in Secs. V D–V F.

V. RESULTS

A. The $W\gamma$ process and radiation-amplitude zeros

For photon transverse momenta > 15 GeV and angular separations between the charged leptons and photons of $\Delta R > 0.7$, the $W\gamma$ production cross section at NLO for each leptonic decay channel is expected to be 31.8 ± 1.8 pb [19,20]. This cross-section point is used to normalize the p_T^γ distributions for the signal in Fig. 6, which shows good agreement of the data with the expectations from the SM.

The three leading-order $W\gamma$ production diagrams in Fig. 1 interfere with each other, resulting in a vanishing of the yield at specific regions of phase space. Such phenomena are referred to as radiation-amplitude zeros (RAZs) [34–38], and the effect was first observed by the D0 Collaboration [6] using the charge-signed rapidity difference $Q_\ell \times \Delta\eta$ between the photon candidate and the charged lepton candidate from $W \rightarrow \ell\nu$ decays [39]. In the SM, the minimum is at $Q_\ell \times \Delta\eta = 0$ for pp collisions. Anomalous $W\gamma$ contributions can affect the distribution in $Q_\ell \times \Delta\eta$ and make the minimum less pronounced. The differential yield as a function of charge-signed rapidity difference, shown in Fig. 7(a) for $W\gamma$ events normalized to the yield of signal in data, is obtained with the additional requirements of having no accompanying jets with $p_T > 30$ GeV and a transverse three-body mass, or cluster mass [39] of the photon, lepton, and E_T system > 110 GeV. The three-body mass $M_T(\ell\gamma E_T)$ is calculated as

$$M_T(\ell\gamma E_T)^2 = [(M_{\ell\gamma}^2 + |\mathbf{p}_T(\gamma) + \mathbf{p}_T(\ell)|^2)^{1/2} + E_T]^2 - |\mathbf{p}_T(\gamma) + \mathbf{p}_T(\ell) + \mathbf{E}_T|^2,$$

where $M_{\ell\gamma}$ denotes the invariant mass of the $\ell\gamma$ system, and $\mathbf{p}_T(i)$, $i = \gamma, \ell$, and E_T are the projections of the photon, lepton, and E_T vectors on the transverse plane, respectively. Figure 7(b) shows the background-subtracted data. The shaded bars indicate statistical and systematic uncertainties on the MC prediction. The distributions demonstrate the characteristic RAZ expected for $W\gamma$ production. Both figures indicate no significant difference between data and expectations from SM MC simulations.

B. The $Z\gamma$ process

The cross section for $Z\gamma$ production at NLO in the SM, for $p_T^\gamma > 15$ GeV, $\Delta R(\ell, \gamma) > 0.7$ between the photon and either of the charged leptons from the $Z \rightarrow \ell^+\ell^-$ decay,

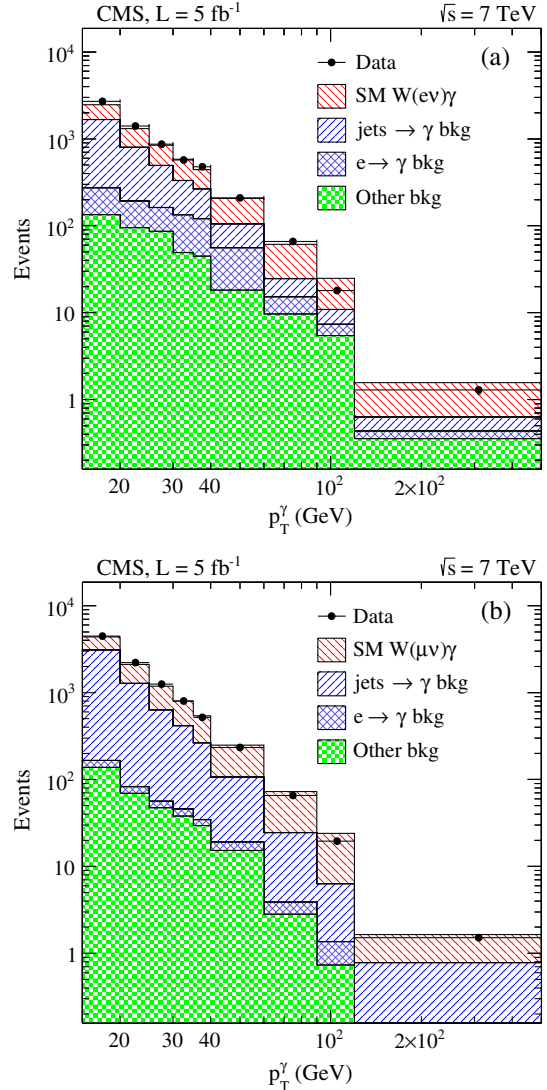


FIG. 6 (color online). Distributions in p_T^γ for $W\gamma$ candidate events in data, with signal and background MC simulation contributions to (a) $W\gamma \rightarrow e\nu\gamma$ and (b) $W\gamma \rightarrow \mu\nu\gamma$ channels shown for comparison.

and $m_{\ell\ell} > 50$ GeV, is predicted to be 5.45 ± 0.27 pb [19,20]. After applying all selection criteria, the p_T^γ distributions for data and contributions expected from MC simulation are shown for $e\nu\gamma$ and $\mu\nu\gamma$ final states in Figs. 8(a) and 8(b), respectively. Again, good agreement is found between data and the SM predictions.

C. Production cross sections

The cross section for any signal process of interest can be written as

$$\sigma_S = \frac{N_S}{A_S \cdot \epsilon_S \cdot L}, \quad (5)$$

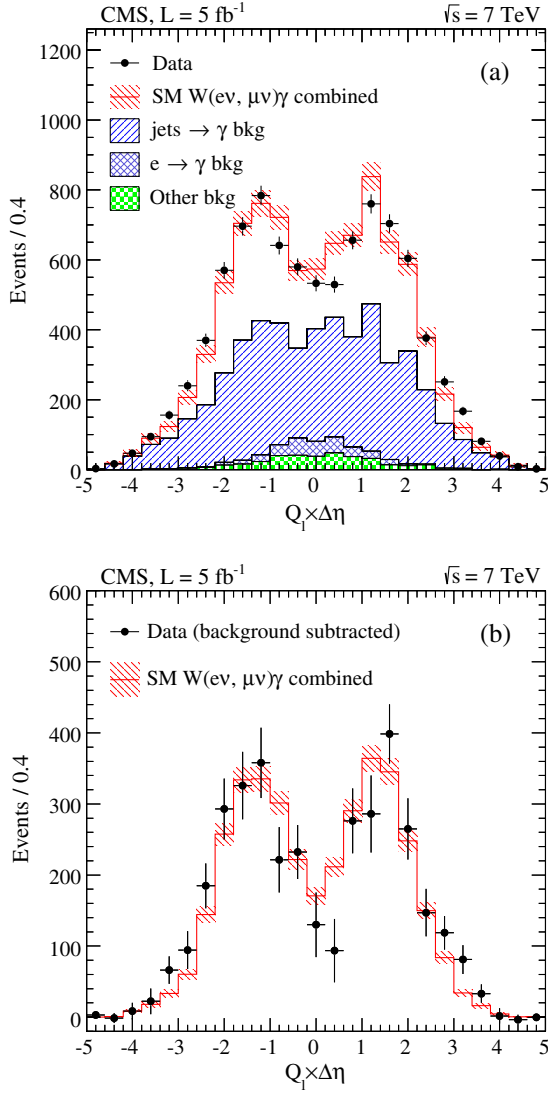


FIG. 7 (color online). Charge-signed rapidity difference $Q_\ell \times \Delta\eta$ between the photon candidate and a lepton for $W\gamma$ candidates in data (filled circles) and expected SM signal and backgrounds (shaded regions) normalized to (a) data, and (b) background-subtracted data. The hatched bands illustrate the full uncertainty in the MC prediction.

where N_S is the number of observed signal events, A_S is the geometric and kinematic acceptance of the detector, ϵ_S is the selection efficiency for signal events in the region of acceptance, and L is the integrated luminosity. The value of A_S in our analyses is calculated through MC simulation and is affected by the choice of PDF and other uncertainties of the model, while the value of ϵ_S is sensitive to uncertainties in the simulation, triggering, and reconstruction. To reduce uncertainties in efficiency, we apply corrections to the efficiencies obtained from MC simulation, which reflect ratios of efficiencies $\rho_{\text{eff}} = \epsilon_{\text{data}}/\epsilon_{\text{MC}}$ obtained by measuring the efficiency in the same way for data and simulation. The product $A_S \times \epsilon_S$ can then be replaced by the product

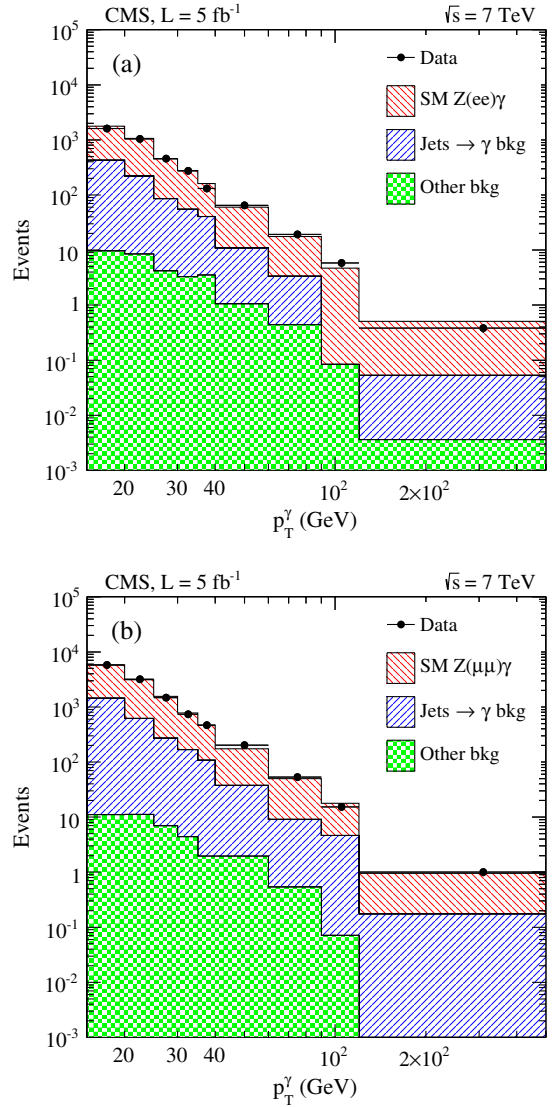


FIG. 8 (color online). Distributions in p_T^γ for $Z\gamma$ candidate events in data, with signal and background MC simulation contributions to the (a) $Z\gamma \rightarrow ee\gamma$ and (b) $Z\gamma \rightarrow \mu\mu\gamma$ channels shown for comparison.

$\mathcal{F}_S \times \rho_{\text{eff}}$, where $\mathcal{F}_S \equiv A_S \times \epsilon_{\text{MC}}$ corresponds to the fraction of generated signal events selected in the simulation.

Equation (5) can therefore be rewritten as

$$\sigma_S = \frac{N - N_B}{\mathcal{F}_S \cdot \rho_{\text{eff}} \cdot L}, \quad (6)$$

in which we replace the number of signal events N_S by subtracting the estimated number of background events N_B from the observed number of selected events N .

We calculate \mathcal{F}_S using MC simulation, with \mathcal{F}_S defined by $N_{\text{accept}}/N_{\text{gen}}$, where N_{accept} is the number of signal events that pass all selection requirements in the MC simulation of signal, and N_{gen} is the number of MC-generated events restricted to $p_T^\gamma > 15$ GeV and

$\Delta R(\ell, \gamma) > 0.7$ for $W\gamma$, and with an additional requirement, $m_{\ell\ell} > 50$ GeV, for $Z\gamma$.

D. Systematic uncertainties

Systematic uncertainties are grouped into five categories. The first group includes uncertainties that affect the signal, such as uncertainties on lepton and photon energy scales. We assess the systematic uncertainties in the electron and photon energy scales separately to account for the differences in the clustering procedure, the response of the ECAL, and calibrations between the electrons and photons. The estimated uncertainty is 0.5% in the EB and 3% in the EE for electrons, and 1% in the EB and 3% in the EE for photons. The uncertainties in the two scales are conservatively treated as fully correlated. For the muon channel, the muon momentum is changed by 0.2%. The systematic effect on the measured cross section is obtained by reevaluating N_S for such changes in each source of systematic uncertainty. To extract the systematic effect of the energy scale on the signal yield, the data-driven background estimation is performed using signal and background templates modified to use the varied energy scale. This ensures that migrations of photons and misidentified photonlike jets across the low- p_T^γ boundaries are properly taken into account for this systematic uncertainty.

In the second group, we combine uncertainties that affect the product of the acceptance, reconstruction, and identification efficiencies of final-state objects, as determined from simulation. These include uncertainties in the lepton and photon energy resolution, effects from pileup, and uncertainties in the PDF. The uncertainty in the product of acceptance and efficiency ($A_S \times \epsilon_S$) is determined from MC simulation of the $V\gamma$ signal and is affected by the lepton and photon energy resolution through the migration of events in and out of the acceptance. The electron energy resolution is determined from data using the observed width of the Z boson peak in the $Z \rightarrow ee$ events, following the same procedure as employed in Ref. [40]. To estimate the effect of electron resolution on $A_S \times \epsilon_S$, each electron candidate's energy is smeared randomly by the energy resolution determined from data before applying the standard selections. The photon energy resolution is determined simultaneously with the photon energy scale from data, following the description in Refs. [28,29]. The systematic effect of photon resolution on $A_S \times \epsilon_S$ is calculated by smearing the reconstructed photon energy in simulation to match that in data.

The number of pileup interactions per event is estimated from data using a convolution procedure that extracts the estimated pileup from the instantaneous bunch luminosity. The total inelastic pp scattering cross section is used to estimate the number of pileup interactions expected in a given bunch crossing, with a systematic uncertainty from modeling of the pileup interactions obtained by changing the total inelastic cross section within its uncertainties [41]

to determine the impact on $A_S \times \epsilon_S$. The uncertainties from the choice of PDF are estimated using the CTEQ6.6 PDF set [21]. The uncertainty in the modeling of the signal is taken from the difference in acceptance between MCFM and MADGRAPH predictions.

The third group of uncertainties includes the systematic sources affecting the relative ρ_{eff} correction factors for efficiencies of the trigger, reconstruction, and identification requirements in simulations and data. Among these sources are the uncertainties in lepton triggers, lepton and photon reconstruction and identification, and E_T for the $W\gamma$ process. The uncertainties in lepton and photon efficiencies are estimated by changing the modeling of the background and the range of the fits used in the tag-and-probe method.

The fourth category of uncertainties comprises the contributions from the background. These are dominated

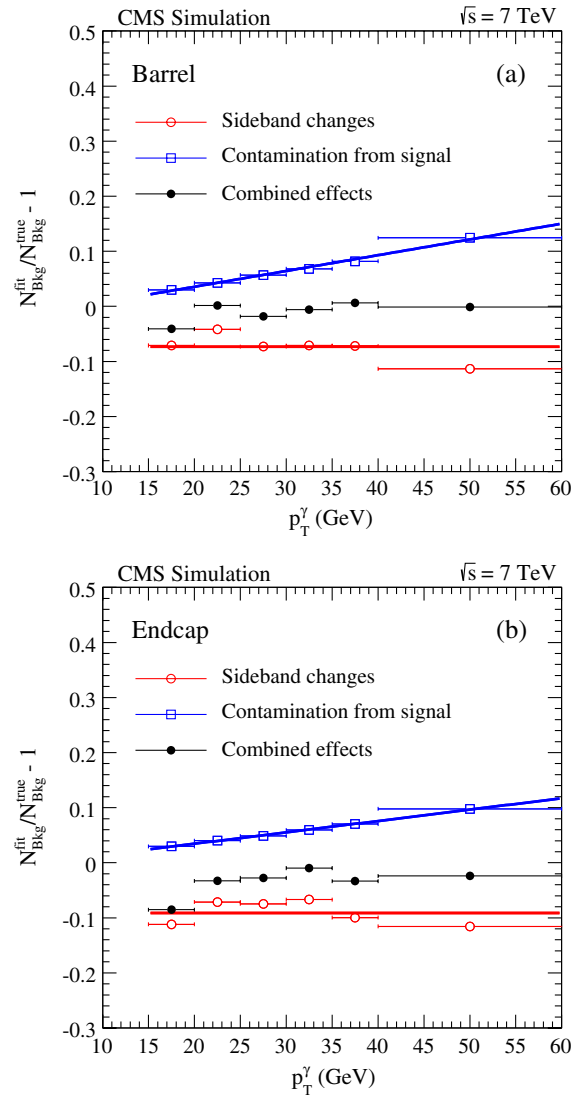


FIG. 9 (color online). Bias in the background contamination related to the background templates for $\sigma_{\eta\eta}$, as a function of p_T^γ , for the (a) barrel and (b) end-cap regions of ECAL.

TABLE VII. Summary of systematic uncertainties in the measurement of $W\gamma$ cross sections, separated into the main groups of sources for the $e\nu\gamma$ and $\mu\nu\gamma$ channels; “n/a” stands for “not applicable.”

		$e\nu\gamma$	$\mu\nu\gamma$
Source (Group 1)	Uncertainties		
e/γ energy scale	[e : 0.5%; γ : 1% (EB), 3% (EE)]	2.9%	n/a
γ energy scale	[1% (EB), 3% (EE)]	n/a	2.9%
μp_T scale	(0.2%)	n/a	0.6%
Total uncertainty in N_{sig}		2.9%	3.0%
Source (Group 2)	Uncertainties	Effect from $\mathcal{F}_S = A_S \cdot \epsilon_S$	
e/γ energy resolution	[1% (EB), 3% (EE)]	0.3%	n/a
γ energy resolution	[1% (EB), 3% (EE)]	n/a	0.1%
μp_T resolution	(0.6%)	n/a	0.1%
Pileup	(Shift pileup distribution by $\pm 5\%$)	2.4%	0.8%
PDF		0.9%	0.9%
Modeling of signal		5.0%	5.0%
Total uncertainty in $\mathcal{F}_S = A_S \cdot \epsilon_S$		5.6%	5.1%
Source (Group 3)	Uncertainties	Effect from ρ_{eff}	
Lepton reconstruction		0.4%	1.5%
Lepton trigger		0.1%	0.9%
Lepton ID and isolation		2.5%	0.9%
E_T selection		1.4%	1.5%
γ identification and isolation	[0.5% (EB), 1.0% (EE)]	0.5%	0.5%
Total uncertainty in ρ_{eff}		2.9%	2.5%
Source (Group 4)		Effect from background yield	
Template method		9.3%	10.2%
Electron misidentification		1.5%	0.1%
MC prediction		0.8%	0.5%
Total uncertainty due to background		9.5%	10.2%
Source (Group 5)			
Luminosity		2.2%	2.2%

by uncertainties in estimating the $W + \text{jets}$ and $Z + \text{jets}$ backgrounds from data. The difference in $\sigma_{\eta\eta}$ distributions between data and simulated events (Sec. IV A 1) is attributed to systematic uncertainties in signal templates, which are used to calculate the background estimate and measure its effect on the final result. To infer the background from photonlike jets that pass the full photon-isolation criteria, we use the $\sigma_{\eta\eta}$ distributions obtained by reversing the original isolation requirement for the tracker. The possible correlation of $\sigma_{\eta\eta}$ with tracker isolation and a contribution from genuine photons that pass the reversed isolation requirement can cause bias in the estimation of background. The first issue is investigated by comparing the sideband and true $\sigma_{\eta\eta}$ distributions in simulated multijet events, where genuine photons can be distinguished from jets. The resulting bias on the background estimation is shown by the open circles in Fig. 9. The second issue, concerning the contamination of the background template by signal, is investigated by comparing the sideband $\sigma_{\eta\eta}$ distributions of simulated samples, both with and without admixtures of genuine photons. The results of the bias studies are shown by the open squares in Fig. 9, and the

overall effect, given by the filled black circles, is found to be small.

Since smoothing is used to define a continuous function for describing the $\sigma_{\eta\eta}$ distribution for background, the effect of statistical sampling of the background probability density requires an appreciation of the features of the underlying distribution. This is studied as follows: The simulation is used to generate a distribution for background, which can be used to generate a template. These new distributions are also smoothed and used to fit the background fraction in data. The results of fits using each such distribution are saved, and the standard deviation associated with the statistical fluctuation in the template is taken as a systematic uncertainty. The systematic uncertainties from different inputs in the estimation of background from $W + \text{jets}$ and $Z + \text{jets}$ events were shown in Tables III and IV, respectively.

The uncertainties in background from electrons misidentified as photons in $W\gamma$ candidate events are estimated by taking the difference in $P_{e \rightarrow \gamma}$ between the measurement described in Sec. IV B and that obtained using a simple counting method. The uncertainties for lesser contributions

TABLE VIII. Summary of systematic uncertainties for the measurement of the $Z\gamma$ cross section; “n/a” stands for “not applicable.”

	$e\bar{e}\gamma$	$\mu\bar{\mu}\gamma$
Source (Group 1)	Uncertainties	Effect from N_{sig}
e/γ energy scale	[e: 0.5%; γ : 1% (EB), 3% (EE)] (0.2%)	3.0% n/a n/a
μp_T scale	[1% (EB), 3% (EE)]	n/a 0.6%
γ energy scale		n/a 4.2%
Total uncertainty in N_{sig}		3.0% 4.2%
Source (Group 2)	Uncertainties	Effect from $\mathcal{F}_S = A_S \cdot \epsilon_S$
e/γ energy resolution	[1% (EB), 3% (EE)]	0.2% n/a
γ energy resolution	[1% (EB), 3% (EE)] (0.6%)	n/a 0.1% n/a 0.2%
μp_T resolution		
Pileup	Shift pileup distribution by $\pm 5\%$	0.6% 1.1% 0.6% 1.4%
PDF		0.4% 1.1% 0.5% 1.3%
Modeling of signal		
Total uncertainty in $\mathcal{F}_S = A_S \cdot \epsilon_S$		
Source (Group 3)	Uncertainties	Effect from ρ_{eff}
Lepton reconstruction		0.8% 0.1% 5.0% 0.5% 5.1%
Lepton trigger		1.0% 1.0% 1.8% 1.0% 2.5%
Lepton ID and isolation		
Photon ID and isolation	[0.5% (EB), 1.0% (EE)]	
Total uncertainty in ρ_{eff}		
Source (Group 4)		Effect from background yield
Template method		1.2% 1.2%
Total uncertainty due to background		1.5% 1.5%
Source (Group 5)		
Luminosity		2.2% 2.2%

to background are defined by the statistical uncertainties in the samples used for their simulation. Finally, the systematic uncertainty in the measured integrated luminosity is 2.2% [42].

E. $W\gamma$ cross section

In the summary of parameters used in the measurement of the $p\bar{p} \rightarrow W\gamma$ cross sections listed in Table V, $N^{\ell\nu\gamma}$ is the number of observed events, $N_S^{\ell\nu\gamma}$ is the number of observed

signal events after background subtraction, and $A_S \times \epsilon_S$, ρ_{eff} , and L are as described in Sec. V C. A summary of all systematic uncertainties in the measured $W\gamma$ cross sections is given in Table VII, separately for electron and muon channels.

The measured cross sections are

$$\begin{aligned} \sigma(p\bar{p} \rightarrow W\gamma) \times \mathcal{B}(W \rightarrow e\nu) \\ = 36.6 \pm 1.2(\text{stat}) \pm 4.3(\text{syst}) \pm 0.8(\text{lum}) \text{ pb}, \end{aligned}$$

TABLE IX. Summary of the measured cross sections and predictions for $p_T^\gamma > 60$ and > 90 GeV for $W\gamma$ and $Z\gamma$ production.

Process	p_T^γ (GeV)	$\sigma \times \mathcal{B}$ (pb)	Theory (pb)
$W\gamma \rightarrow e\nu\gamma$	> 60	$0.77 \pm 0.07(\text{stat}) \pm 0.13(\text{syst}) \pm 0.02(\text{lum})$	0.58 ± 0.08
$W\gamma \rightarrow \mu\nu\gamma$	> 60	$0.76 \pm 0.06(\text{stat}) \pm 0.08(\text{syst}) \pm 0.02(\text{lum})$	0.58 ± 0.08
$W\gamma \rightarrow \ell\nu\gamma$	> 60	$0.76 \pm 0.05(\text{stat}) \pm 0.08(\text{syst}) \pm 0.02(\text{lum})$	0.58 ± 0.08
$W\gamma \rightarrow e\nu\gamma$	> 90	$0.17 \pm 0.03(\text{stat}) \pm 0.04(\text{syst}) \pm 0.01(\text{lum})$	0.17 ± 0.03
$W\gamma \rightarrow \mu\nu\gamma$	> 90	$0.25 \pm 0.04(\text{stat}) \pm 0.05(\text{syst}) \pm 0.01(\text{lum})$	0.17 ± 0.03
$W\gamma \rightarrow \ell\nu\gamma$	> 90	$0.20 \pm 0.03(\text{stat}) \pm 0.04(\text{syst}) \pm 0.01(\text{lum})$	0.17 ± 0.03
$Z\gamma \rightarrow e\bar{e}\gamma$	> 60	$0.14 \pm 0.02(\text{stat}) \pm 0.02(\text{syst}) \pm 0.01(\text{lum})$	0.12 ± 0.01
$Z\gamma \rightarrow \mu\bar{\mu}\gamma$	> 60	$0.14 \pm 0.01(\text{stat}) \pm 0.02(\text{syst}) \pm 0.01(\text{lum})$	0.12 ± 0.01
$Z\gamma \rightarrow \ell\bar{\ell}\gamma$	> 60	$0.14 \pm 0.01(\text{stat}) \pm 0.01(\text{syst}) \pm 0.01(\text{lum})$	0.12 ± 0.01
$Z\gamma \rightarrow e\bar{e}\gamma$	> 90	$0.047 \pm 0.013(\text{stat}) \pm 0.010(\text{syst}) \pm 0.001(\text{lum})$	0.040 ± 0.004
$Z\gamma \rightarrow \mu\bar{\mu}\gamma$	> 90	$0.046 \pm 0.008(\text{stat}) \pm 0.010(\text{syst}) \pm 0.001(\text{lum})$	0.040 ± 0.004
$Z\gamma \rightarrow \ell\bar{\ell}\gamma$	> 90	$0.046 \pm 0.007(\text{stat}) \pm 0.009(\text{syst}) \pm 0.001(\text{lum})$	0.040 ± 0.004

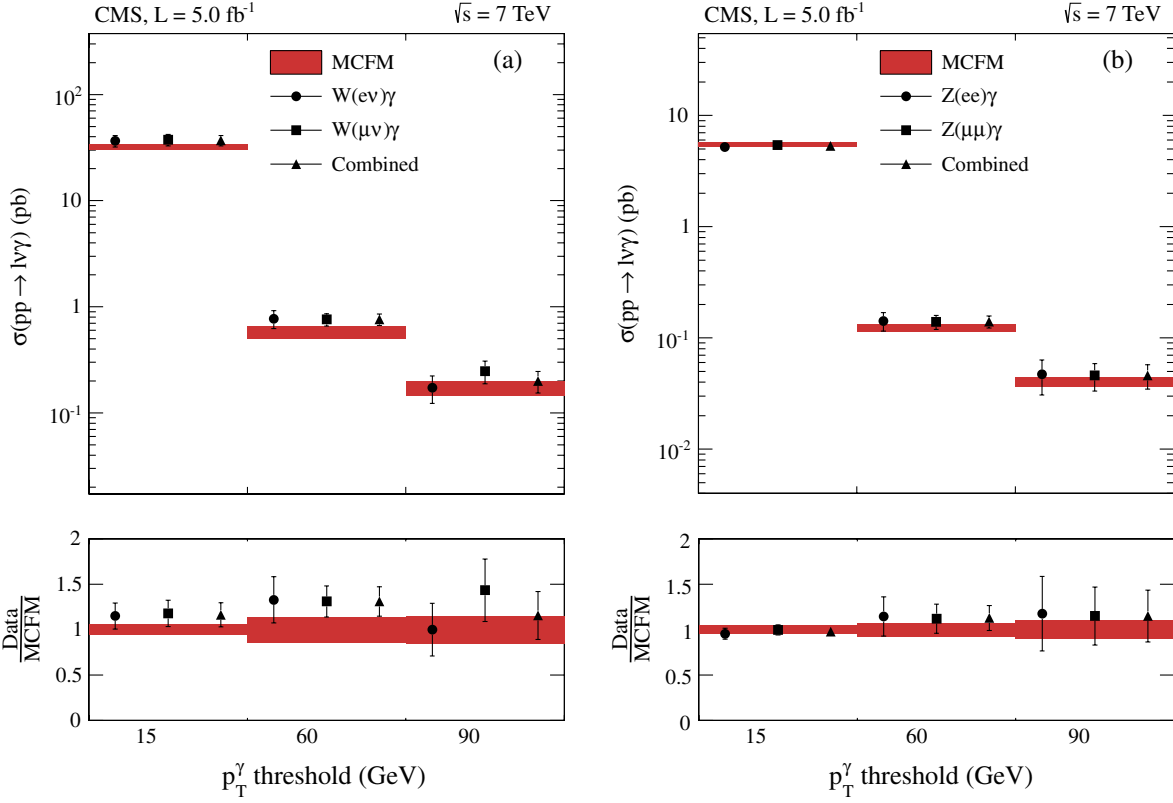


FIG. 10 (color online). A summary of measured cross sections for three p_T^γ thresholds, compared to SM predictions for (a) $W\gamma$ and (b) $Z\gamma$ production.

$$\begin{aligned} \sigma(pp \rightarrow W\gamma) \times \mathcal{B}(W \rightarrow \mu\nu) \\ = 37.5 \pm 0.9(\text{stat}) \pm 4.5(\text{syst}) \pm 0.8(\text{lum}) \text{ pb}. \end{aligned}$$

The mean of these cross sections, obtained using a best linear unbiased estimator (BLUE) [43], is

$$\begin{aligned} \sigma(pp \rightarrow W\gamma) \times \mathcal{B}(W \rightarrow \ell\nu) \\ = 37.0 \pm 0.8(\text{stat}) \pm 4.0(\text{syst}) \pm 0.8(\text{lum}) \text{ pb}. \end{aligned}$$

All three results are consistent within uncertainties with the NLO prediction of 31.8 ± 1.8 pb, computed with MCFM. The uncertainty on the prediction is obtained using the CTEQ6.6 PDF set [21].

F. $Z\gamma$ cross section

In the summary of parameters used in the measurement of the $pp \rightarrow Z\gamma$ cross section listed in Table VI, $N^{\ell\ell\gamma}$ is the number of observed events, and $N_S^{\ell\ell\gamma}$ is the number of observed signal events after background subtraction. The systematic uncertainties for the measurement of the $Z\gamma$ cross sections are listed in Table VIII. The cross sections for the two channels are

$$\begin{aligned} \sigma(pp \rightarrow Z\gamma) \times \mathcal{B}(Z \rightarrow ee) \\ = 5.20 \pm 0.13(\text{stat}) \pm 0.32(\text{syst}) \pm 0.11(\text{lum}) \text{ pb}, \end{aligned}$$

$$\begin{aligned} \sigma(pp \rightarrow Z\gamma) \times \mathcal{B}(Z \rightarrow \mu\mu) \\ = 5.43 \pm 0.10(\text{stat}) \pm 0.29(\text{syst}) \pm 0.12(\text{lum}) \text{ pb}, \end{aligned}$$

and their mean, extracted using the BLUE method is

$$\begin{aligned} \sigma(pp \rightarrow Z\gamma) \times \mathcal{B}(Z \rightarrow \ell\ell) \\ = 5.33 \pm 0.08(\text{stat}) \pm 0.25(\text{syst}) \pm 0.12(\text{lum}) \text{ pb}. \end{aligned}$$

All three results are also consistent within the uncertainties with the theoretical NLO cross section of 5.45 ± 0.27 pb, computed with MCFM. The uncertainty on the prediction is obtained using the CTEQ6.6 PDF set [21].

G. Ratio of $W\gamma$ and $Z\gamma$ production cross sections

We calculate the ratio of the $W\gamma$ and $Z\gamma$ cross sections using the BLUE method to account for correlated systematic uncertainties between individual channels for both measurements and predictions. The MCFM prediction of 5.8 ± 0.1 is consistent with the measured ratio, $6.9 \pm 0.2(\text{stat}) \pm 0.5(\text{syst})$.

H. Comparisons to MCFM predictions

Finally, we present a summary of the $W\gamma$ and $Z\gamma$ cross sections measured with larger requirements on the minimum photon p_T^γ . After accounting for all systematic uncertainties for $p_T^\gamma > 60$ and > 90 GeV, we find no significant disagreement with the MCFM predictions for the $V\gamma$ processes. These cross sections, predictions, and their uncertainties are summarized in Table IX and in Fig. 10.

VI. ANOMALOUS TRIPLE GAUGE COUPLINGS IN $W\gamma$ AND $Z\gamma$ PRODUCTION

A. $WW\gamma$ coupling

The most general Lorentz-invariant, effective Lagrangian that describes $WW\gamma$ and WWZ couplings has 14 independent parameters [44,45], seven for each triple-boson vertex. Assuming charge conjugation (C) and parity (P) invariance for the effective EW Lagrangian (\mathcal{L}_{WWV}), normalized by its EW coupling strength (g_{WWV}), leaves only six independent couplings for describing the $WW\gamma$ and WWZ vertices:

$$\frac{\mathcal{L}_{WWV}}{g_{WWV}} = ig_1^V(W_{\mu\nu}^\dagger W^\mu V^\nu - W_\mu^\dagger V_\nu W^{\mu\nu}) + i\kappa_V W_\mu^\dagger W_\nu V^{\mu\nu} + \frac{i\lambda_V}{M_W^2} W_{\delta\mu}^\dagger W_\nu^\mu V^{\nu\delta}, \quad (7)$$

where $V = \gamma$ or Z , W^μ are the W^\pm fields, $W_{\mu\nu} = \partial_\mu W_\nu - \partial_\nu W_\mu$, with the overall couplings given by $g_{WW\gamma} = -e$ and $g_{WWZ} = -e \cot \theta_W$, where θ_W is the weak mixing angle. Assuming electromagnetic gauge

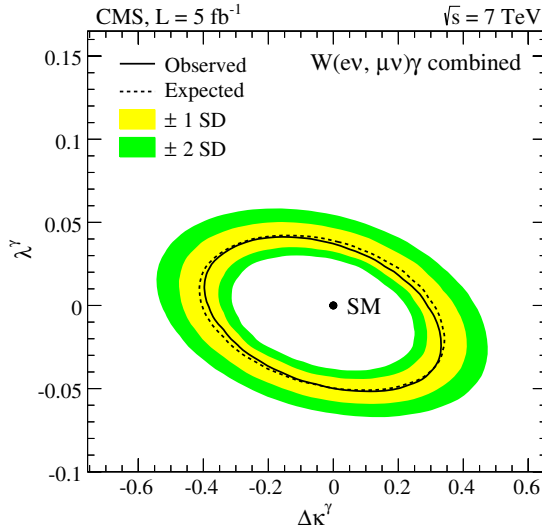


FIG. 11 (color online). Observed (solid curve) and expected (dashed curve) 95% C.L. exclusion contours for anomalous $WW\gamma$ couplings, with ± 1 and ± 2 standard deviation contours from uncertainties in the measurements indicated by light and dark shaded bands, respectively.

invariance, $g_1^\gamma = 1$; the remaining parameters that describe the $WW\gamma$ and WWZ couplings are g_1^Z , κ_Z , κ_γ , λ_Z , and λ_γ . In the SM, $\lambda_Z = \lambda_\gamma = 0$ and $g_1^Z = \kappa_Z = \kappa_\gamma = 1$. In this analysis, we follow the convention that describes the couplings in terms of their deviation from the SM values: $\Delta g_1^Z \equiv g_1^Z - 1$, $\Delta \kappa_Z \equiv \kappa_Z - 1$, and $\Delta \kappa_\gamma \equiv \kappa_\gamma - 1$. Invariance under $SU(2)_L \times U(1)_Y$ transformations reduces these to three independent couplings:

$$\Delta \kappa_Z = \Delta g_1^Z - \Delta \kappa_\gamma \cdot \tan^2 \theta_W, \quad \lambda = \lambda_\gamma = \lambda_Z, \quad (8)$$

where $\Delta \kappa_\gamma$ and λ_γ are determined from $W\gamma$ production.

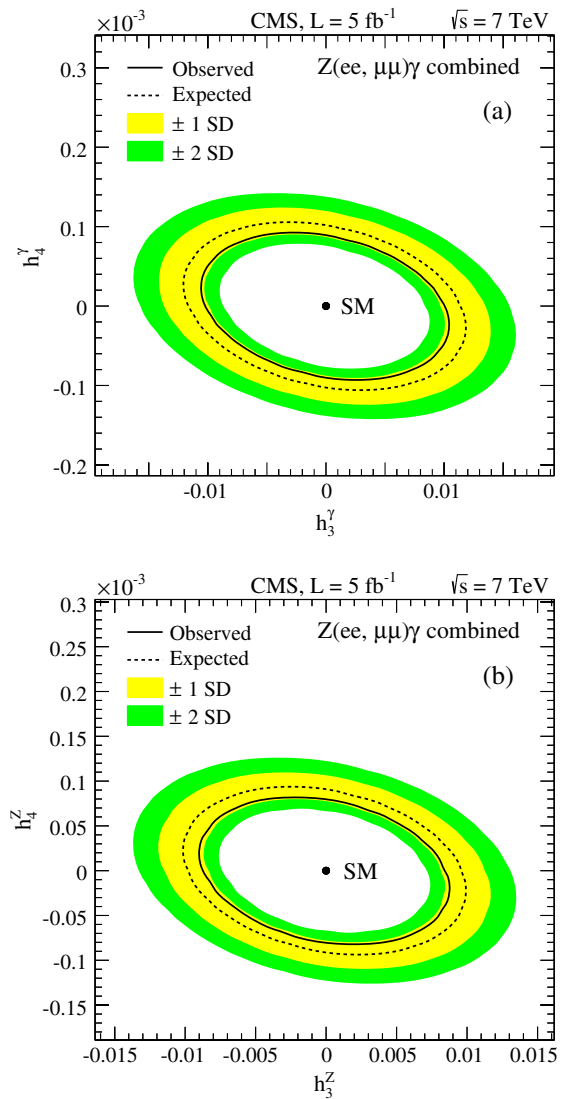


FIG. 12 (color online). Observed (solid curves) and expected (dashed curves) 95% C.L. exclusion contours for anomalous (a) $Z\gamma\gamma$ and (b) $ZZ\gamma$ couplings, with ± 1 and ± 2 standard deviation contours indicated by light and dark shaded bands, respectively.

B. ZZ γ and Z $\gamma\gamma$ couplings

The most general vertex function for ZZ γ [46] can be written as

$$\begin{aligned} \Gamma_{ZZ\gamma}^{\alpha\beta\mu}(q_1, q_2, p) = & \frac{p^2 - q_1^2}{m_Z^2} \left[h_1^Z (q_2^\mu g^{\alpha\beta} - q_2^\alpha g^{\mu\beta}) \right. \\ & + \frac{h_2^Z}{m_Z^2} p^\alpha [(p \cdot q_2) g^{\mu\beta} - g_2^\mu p^\beta] \\ & \left. + h_3^Z \epsilon^{\mu\alpha\beta\rho} q_{2\rho} + \frac{h_4^Z}{m_Z^2} p^\alpha \epsilon^{\mu\beta\rho\sigma} p_\rho q_{2\sigma} \right], \end{aligned} \quad (9)$$

with the Z $\gamma\gamma$ vertex obtained by the replacements

$$\frac{p^2 - q_1^2}{m_Z^2} \rightarrow \frac{p^2}{m_Z^2} \quad \text{and} \quad h_i^Z \rightarrow h_i^\gamma, \quad i = 1, \dots, 4. \quad (10)$$

The couplings h_i^V for $V = Z$ or γ and $i = 1, 2$ violate CP symmetry, while those with $i = 3, 4$ are CP even. Although at tree level all these couplings vanish in the SM, at the higher, one-loop level, the CP -conserving couplings are $\approx 10^{-4}$. As the sensitivity to CP -odd and CP -even couplings is the same when using p_T^γ to check for the presence of contributions from ATGCs, we interpret the results as limits on h_3^V and h_4^V only.

C. Search for anomalous couplings in $W\gamma$ and $Z\gamma$ production

To extract limits on the ATGCs, we simply count the yield of events in bins of p_T^γ . The 95% confidence level (C.L.) upper limits on values of ATGCs are set using the modified frequentist CL_s method [47].

As the simulation of the ATGC signal is not available in MADGRAPH, the signals are generated using the SHERPA MC program [18] to simulate $W\gamma$ + jets and $Z\gamma$ + jets with up to two jets in the final state.

For the $W\gamma$ analysis, we set one- and two-dimensional limits on each ATGC parameter $\Delta\kappa_\gamma$ and λ_γ , while g_1^Z is set to the SM value, assuming the “equal couplings” scenario of the LEP parameterization [48].

For the $Z\gamma$ analysis, we set h_1^V and h_2^V to the SM values, and we set two-dimensional limits on the h_3^V and h_4^V .

TABLE X. One-dimensional 95% C.L. limits on ATGCs for $W\gamma \rightarrow e\nu\gamma$, $W\gamma \rightarrow \mu\nu\gamma$, and for the combined analyses. The intervals shown represent the allowed ranges of the coupling parameters.

	$\Delta\kappa_\gamma$	λ_γ
$W\gamma \rightarrow e\nu\gamma$	$[-0.45, 0.36]$	$[-0.059, 0.046]$
$W\gamma \rightarrow \mu\nu\gamma$	$[-0.46, 0.34]$	$[-0.057, 0.045]$
$W\gamma \rightarrow \ell\nu\gamma$	$[-0.38, 0.29]$	$[-0.050, 0.037]$

TABLE XI. One-dimensional 95% C.L. limits on ATGCs for $Z\gamma \rightarrow ee\gamma$, $Z\gamma \rightarrow \mu\mu\gamma$, and for the combined analyses. The intervals shown represent the allowed ranges of the coupling parameters.

	$h_3^\gamma [10^{-2}]$	$h_4^\gamma [10^{-4}]$	$h_3^Z [10^{-2}]$	$h_4^Z [10^{-4}]$
$Z\gamma \rightarrow ee\gamma$	$[-1.3, 1.3]$	$[-1.1, 1.1]$	$[-1.1, 1.1]$	$[-1.0, 1.0]$
$Z\gamma \rightarrow \mu\mu\gamma$	$[-1.3, 1.3]$	$[-1.1, 1.2]$	$[-1.1, 1.1]$	$[-1.0, 1.1]$
$Z\gamma \rightarrow \ell\ell\gamma$	$[-1.0, 1.0]$	$[-0.9, 0.9]$	$[-0.9, 0.9]$	$[-0.8, 0.8]$

anomalous couplings, with $V = Z$ or γ . For limits set on the Z -type couplings, the γ couplings are set to their SM values—i.e., to zero—and vice versa. In this study, we follow the CMS convention of not suppressing the anomalous TGCs by an energy-dependent form factor.

The two-dimensional contours for upper limits at the 95% confidence level are given in Fig. 11 for the $W\gamma$, and in Fig. 12 for the $Z\gamma$ channels, with the corresponding one-dimensional limits listed in Table X for $W\gamma$ and in Table XI for $Z\gamma$.

VII. SUMMARY

We have presented updated measurements of the $V\gamma$ inclusive production cross sections in pp collisions at $\sqrt{s} = 7$ TeV, based on leptonic decays of EW vector bosons $W \rightarrow e\nu$, $W \rightarrow \mu\nu$, $Z \rightarrow ee$, and $Z \rightarrow \mu\mu$. The data were collected by the CMS experiment at the LHC in 2011 and correspond to an integrated luminosity of 5.0 fb^{-1} . A separation is required between the photon and the charged leptons in (η, ϕ) space of $\Delta R > 0.7$, and an additional requirement of $m_{\ell\ell} > 50 \text{ GeV}$ is placed on $Z\gamma$ candidates. The measured cross sections for $p_T^\gamma > 15 \text{ GeV}$, $\sigma(pp \rightarrow W\gamma) \times \mathcal{B}(W \rightarrow \ell\nu) = 37.0 \pm 0.8(\text{stat}) \pm 4.0(\text{syst}) \pm 0.8(\text{lum}) \text{ pb}$, and $\sigma(pp \rightarrow Z\gamma) \times \mathcal{B}(Z \rightarrow \ell\ell) = 5.33 \pm 0.08(\text{stat}) \pm 0.25(\text{syst}) \pm 0.12(\text{lum}) \text{ pb}$ are consistent with predictions of the SM; the ratio of these measurements, $6.9 \pm 0.2(\text{stat}) \pm 0.5(\text{syst})$, is also consistent with the SM value of 5.8 ± 0.1 predicted by MCFM. Measured cross sections for $p_T^\gamma > 60$ and $> 90 \text{ GeV}$ also agree with the SM. With no evidence observed for physics beyond the SM, we set the limits on anomalous $WW\gamma$, $ZZ\gamma$, and $Z\gamma\gamma$ couplings given in Tables X and XI.

ACKNOWLEDGMENTS

We congratulate our colleagues in the CERN accelerator departments for the excellent performance of the LHC and thank the technical and administrative staffs at CERN and at other CMS institutes for their contributions to the success of the CMS effort. In addition, we gratefully acknowledge the computing centers and personnel of the Worldwide LHC Computing Grid for delivering so effectively the computing infrastructure essential to our analyses. Finally,

we acknowledge the enduring support for the construction and operation of the LHC and the CMS detector provided by the following funding agencies: the Austrian Federal Ministry of Science, Research and Economy and the Austrian Science Fund; the Belgian Fonds de la Recherche Scientifique and Fonds voor Wetenschappelijk Onderzoek; the Brazilian funding agencies (CNPq, CAPES, FAPERJ, and FAPESP); the Bulgarian Ministry of Education, Youth and Science; CERN; the Chinese Academy of Sciences, Ministry of Science and Technology, and National Natural Science Foundation of China; the Colombian funding agency (COLCIENCIAS); the Croatian Ministry of Science, Education and Sport, and the Croatian Science Foundation; the Research Promotion Foundation, Cyprus; the Ministry of Education and Research, Estonian Research Council via IUT23-4 and IUT23-6 and European Regional Development Fund, Estonia; the Academy of Finland, Finnish Ministry of Education and Culture, and the Helsinki Institute of Physics; the Institut National de Physique Nucléaire et de Physique des Particules / CNRS, and Commissariat à l'Énergie Atomique et aux Énergies Alternatives / CEA, France; the Bundesministerium für Bildung und Forschung, Deutsche Forschungsgemeinschaft, and Helmholtz-Gemeinschaft Deutscher Forschungszentren, Germany; the General Secretariat for Research and Technology, Greece; the National Scientific Research Foundation and National Innovation Office, Hungary; the Department of Atomic Energy and the Department of Science and Technology, India; the Institute for Studies in Theoretical Physics and Mathematics, Iran; the Science Foundation, Ireland; the Istituto Nazionale di Fisica Nucleare, Italy; the Korean Ministry of Education, Science and Technology and the World Class University program of NRF, Republic of Korea; the Lithuanian Academy of Sciences; the Ministry of Education, and University of Malaya (Malaysia); the Mexican funding agencies (CINVESTAV, CONACYT, SEP, and UASLP-FAI); the Ministry of Business, Innovation and

Employment, New Zealand; the Pakistan Atomic Energy Commission; the Ministry of Science and Higher Education and the National Science Centre, Poland; the Fundação para a Ciência e a Tecnologia, Portugal; JINR, Dubna; the Ministry of Education and Science of the Russian Federation, the Federal Agency of Atomic Energy of the Russian Federation, the Russian Academy of Sciences, and the Russian Foundation for Basic Research; the Ministry of Education, Science and Technological Development of Serbia; the Secretaría de Estado de Investigación, Desarrollo e Innovación and Programa Consolider-Ingenio 2010, Spain; the Swiss funding agencies (ETH Board, ETH Zurich, PSI, SNF, UniZH, Canton Zurich, and SER); the Ministry of Science and Technology, Taipei; the Thailand Center of Excellence in Physics, the Institute for the Promotion of Teaching Science and Technology of Thailand, and the National Science and Technology Development Agency of Thailand; the Scientific and Technical Research Council of Turkey and the Turkish Atomic Energy Authority; the National Academy of Sciences of Ukraine, and State Fund for Fundamental Researches, Ukraine; the Science and Technology Facilities Council, United Kingdom; and the U.S. Department of Energy and the U.S. National Science Foundation. Individuals have received support from the Marie Curie program and the European Research Council and EPLANET (European Union); the Leventis Foundation; the A. P. Sloan Foundation; the Alexander von Humboldt Foundation; the Belgian Federal Science Policy Office; the Fonds pour la Formation à la Recherche dans l'Industrie et dans l'Agriculture (FRIA-Belgium); the Agentschap voor Innovatie door Wetenschap en Technologie (IWT-Belgium); the Ministry of Education, Youth and Sports (MEYS) of the Czech Republic; the Council of Science and Industrial Research, India; the Compagnia di San Paolo (Torino); and the HOMING PLUS program of the Foundation for Polish Science, cofinanced from the European Union Regional Development Fund; and the Thalis and Aristeia programs cofinanced by EU-ESF and the Greek NSRF.

APPENDIX: VARIOUS KINEMATIC DISTRIBUTIONS OF $V\gamma$ CANDIDATE EVENTS

The various kinematic distributions of the selected $W\gamma$ and $Z\gamma$ candidate events in data overlaid with the background predictions are shown in Figs. 13, 14, and 15.

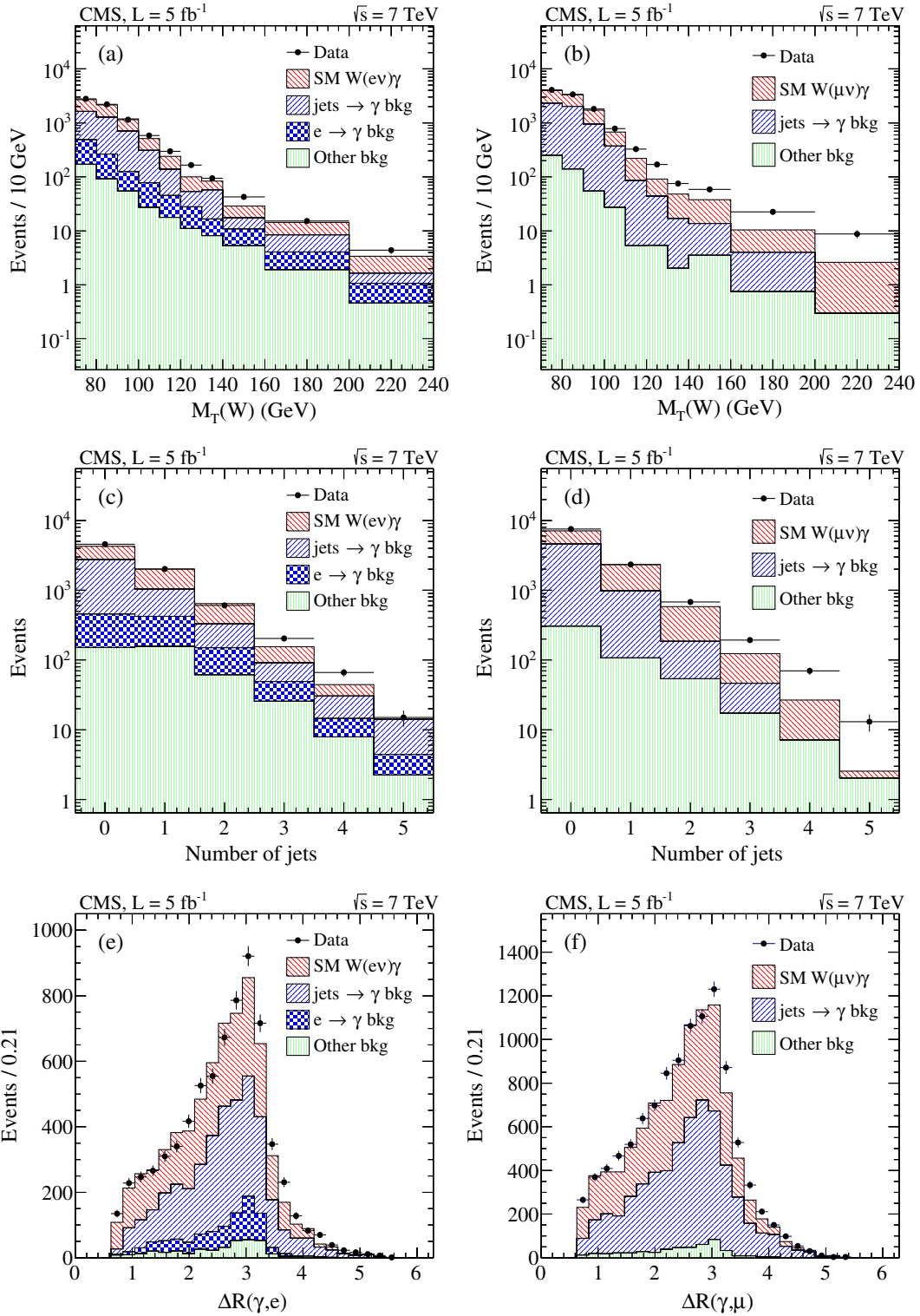


FIG. 13 (color online). Distributions in the W -boson transverse invariant mass for $W\gamma$ candidate events in data, with the signal and background MC simulation contributions to the (a) $W\gamma \rightarrow ev\gamma$ and (b) $W\gamma \rightarrow \mu\nu\gamma$ channels shown for comparison. The contributions for the number of jets with $p_T > 30$ GeV are given in (c) and (d), respectively. The separation in R between the charged lepton and the photon is given in (e) for the electron channel, and that for muon channel is illustrated in (f).

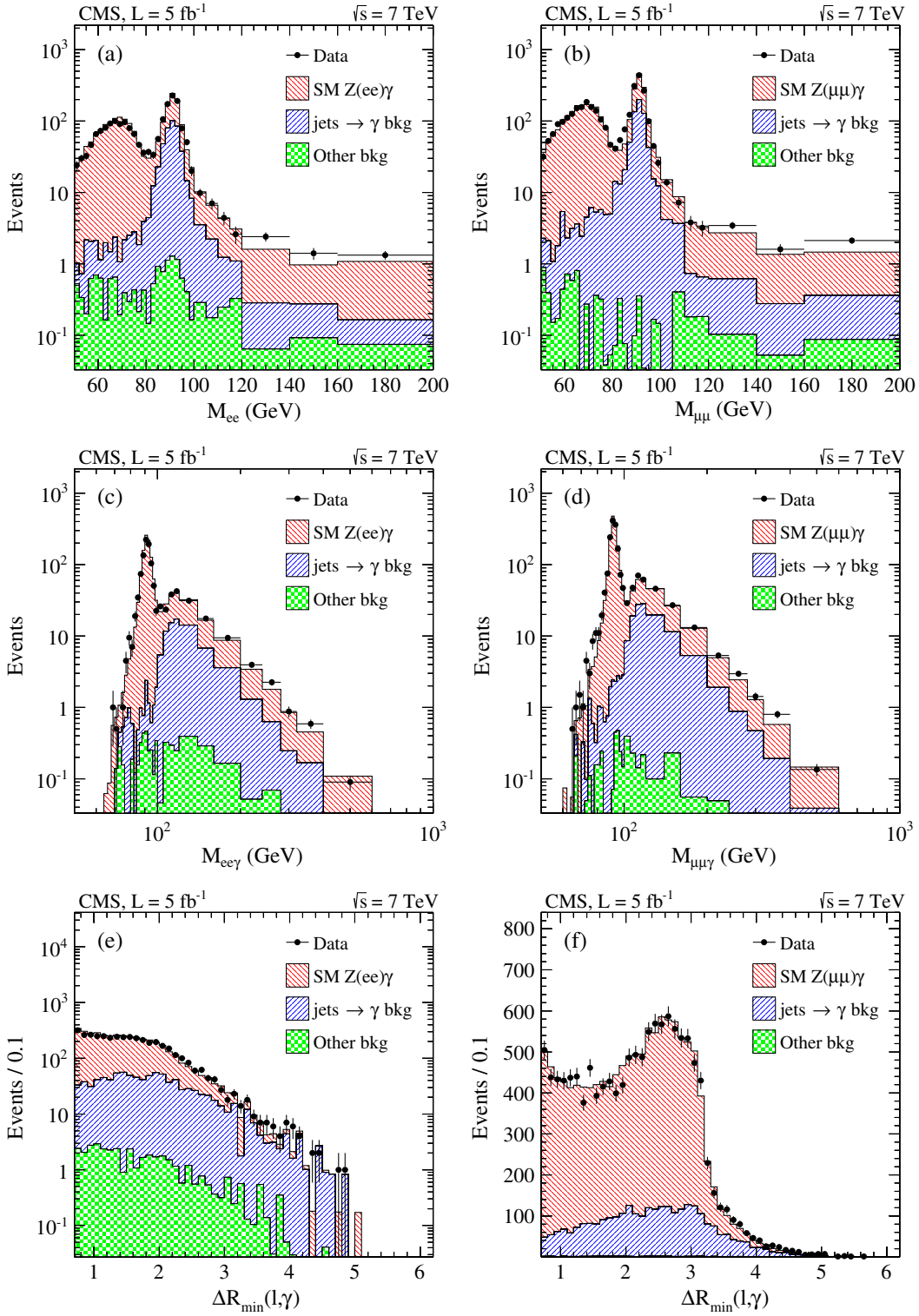


FIG. 14 (color online). Distributions in the dilepton invariant mass for $Z\gamma$ candidate events in data, with the signal and background MC simulation contributions to the (a) $Z\gamma \rightarrow ee\gamma$ and (b) $Z\gamma \rightarrow \mu\mu\gamma$ channels shown for comparison. The contributions for the dilepton-plus-photon invariant mass are given in (c) and (d). The smallest separation in R between any charged leptons and the photon is given in (e) for the electron channel, and that for muon channel is illustrated in (f).

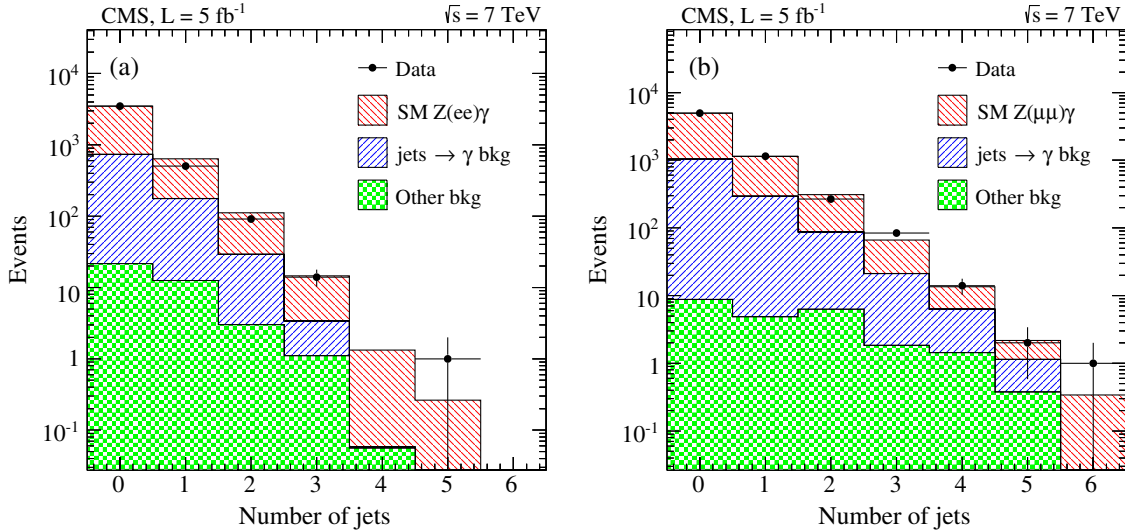


FIG. 15 (color online). Distributions in the number of jets with $p_T > 30$ GeV for $Z\gamma$ candidate events in data, with the signal and background MC simulation contributions to the (a) $Z\gamma \rightarrow ee\gamma$ and (b) $Z\gamma \rightarrow \mu\mu\gamma$ channels shown for comparison.

- [1] LEP Electroweak Working Group, arXiv:hep-ex/0612034v2.
- [2] P. Acciarri (L3 Collaboration), Phys. Lett. B **346**, 190 (1995).
- [3] P. Achard (L3 Collaboration), Phys. Lett. B **597**, 119 (2004).
- [4] G. Abbiendi (OPAL Collaboration), Eur. Phys. J. C **32**, 303 (2003).
- [5] V. M. Abazov *et al.* (D0 Collaboration), Phys. Rev. D **71**, 091108 (2005).
- [6] V. M. Abazov *et al.* (D0 Collaboration), Phys. Rev. Lett. **100**, 241805 (2008).
- [7] T. Aaltonen *et al.* (CDF Collaboration), Phys. Rev. D **82**, 031103 (2010).
- [8] V. M. Abazov *et al.* (D0 Collaboration), Phys. Lett. B **653**, 378 (2007).
- [9] V. M. Abazov *et al.* (D0 Collaboration), Phys. Rev. Lett. **102**, 201802 (2009).
- [10] CMS Collaboration, Phys. Lett. B **699**, 25 (2011).
- [11] CMS Collaboration, Phys. Lett. B **701**, 535 (2011).
- [12] ATLAS Collaboration, Phys. Rev. D **87**, 112003 (2013).
- [13] U. Baur, T. Han, and J. Ohnemus, Phys. Rev. D **48**, 5140 (1993).
- [14] U. Baur, T. Han, and J. Ohnemus, Phys. Rev. D **57**, 2823 (1998).
- [15] CMS Collaboration, JINST **3**, S08004 (2008).
- [16] J. Alwall, M. Herquet, F. Maltoni, and O. Mattelaer, J. High Energy Phys. **06** (2011) 128.
- [17] T. Sjöstrand, S. Mrenna, and P. Z. Skands, J. High Energy Phys. **05** (2006) 026.
- [18] T. Gleisberg, S. Hoeche, F. Krauss, M. Schonherr, S. Schumann, F. Siegert, and J. Winter, J. High Energy Phys. **02** (2009) 007.
- [19] J. M. Campbell, R. K. Ellis, and C. Williams, J. High Energy Phys. **07** (2011) 018.
- [20] J. M. Campbell and R. K. Ellis, Phys. Rev. D **60**, 113006 (1999).
- [21] P. M. Nadolsky, H.-L. Lai, Q.-H. Cao, J. Huston, J. Pumplin, D. Stump, W.-K. Tung, and C.-P. Yuan, Phys. Rev. D **78**, 013004 (2008).
- [22] J. Pumplin, D. R. Stump, J. Huston, H.-L. Lai, P. Nadolsky, and W.-K. Tung, J. High Energy Phys. **07** (2002) 012.
- [23] S. Agostinelli (GEANT4 Collaboration), Nucl. Instrum. Methods Phys. Res., Sect. A **506**, 250 (2003).
- [24] CMS Collaboration, JINST **7**, P10002 (2012).
- [25] CMS Collaboration, Phys. Rev. D **84**, 052011 (2011).
- [26] M. Cacciari, G. Salam, and G. Soyez, Eur. Phys. J. C **72**, 1896 (2012).
- [27] CMS Collaboration, J. High Energy Phys. **01** (2011) 080.
- [28] J. Everka, Ph.D. thesis, California Institute of Technology, 2013.
- [29] S. Chatrchyan (CMS Collaboration), J. High Energy Phys. **06** (2013) 081.
- [30] CMS Collaboration, CMS Physics Analysis Summary Report No. CMS-PAS-PFT-10-003, 2010, <http://cdsweb.cern.ch/record/1279347>.
- [31] K. Cranmer, Comput. Phys. Commun. **136**, 198 (2001).
- [32] J. Beringer *et al.* (Particle Data Group), Phys. Rev. D **86**, 010001 (2012).
- [33] T. Skwarnicki, Ph.D. thesis, DESY Internal No. DESY-F31-86-02, 1986.
- [34] R. W. Brown, D. Sahdev, and K. O. Mikaelian, Phys. Rev. D **20**, 1164 (1979).
- [35] K. O. Mikaelian, M. A. Samuel, and D. Sahdev, Phys. Rev. Lett. **43**, 746 (1979).
- [36] C. J. Goebel, F. Halzen, and J. P. Leveille, Phys. Rev. D **23**, 2682 (1981).
- [37] S. J. Brodsky and R. W. Brown, Phys. Rev. Lett. **49**, 966 (1982).
- [38] R. W. Brown, K. L. Kowalski, and S. J. Brodsky, Phys. Rev. D **28**, 624 (1983).
- [39] U. Baur, S. Errede, and G. Landsberg, Phys. Rev. D **50**, 1917 (1994).
- [40] CMS Collaboration, Phys. Lett. B **710**, 403 (2012).
- [41] CMS Collaboration, Phys. Lett. B **722**, 5 (2013).
- [42] CMS Collaboration, CMS Physics Analysis Summary Report No. CMS-PAS-SMP-12-008, 2012, <http://cdsweb.cern.ch/record/1434360>.

- [43] L. Lyons, G. Gibaut, and P. Clifford, *Nucl. Instrum. Methods Phys. Res., Sect. A* **270**, 110 (1988).
- [44] K. Hagiwara, R. D. Peccei, and D. Zeppenfeld, *Nucl. Phys. B* **282**, 253 (1987).
- [45] K. Hagiwara, J. Woodside, and D. Zeppenfeld, *Phys. Rev. D* **41**, 2113 (1990).
- [46] U. Baur and E. L. Berger, *Phys. Rev. D* **47**, 4889 (1993).
- [47] G. Cowan, K. Cranmer, E. Gross, and O. Vitells, *Eur. Phys. J. C* **71**, 1 (2011).
- [48] G. Gounaris, J.-L. Kneur, D. Zeppenfeld *et al.*, in *Physics at LEP2*, Vol. 1, edited by G. Altarelli and F. Zwirner (CERN, Geneva, 1996), p. 525.

S. Chatrchyan,¹ V. Khachatryan,¹ A. M. Sirunyan,¹ A. Tumasyan,¹ W. Adam,² T. Bergauer,² M. Dragicevic,² J. Erö,² C. Fabjan,^{2,b} M. Friedl,² R. Fröhwrith,^{2,b} V. M. Ghete,² N. Hörmann,² J. Hrubec,² M. Jeitler,^{2,b} W. Kiesenhofer,² V. Knünz,² M. Krämer,^{2,b} I. Krätschmer,² D. Liko,² I. Mikulec,² D. Rabady,^{2,c} B. Rahbaran,² C. Rohringer,² H. Rohringer,² R. Schöfbeck,² J. Strauss,² A. Taurok,² W. Treberer-Treberspurg,² W. Waltenberger,² C.-E. Wulz,^{2,b} V. Mossolov,³ N. Shumeiko,³ J. Suarez Gonzalez,³ S. Alderweireldt,⁴ M. Bansal,⁴ S. Bansal,⁴ T. Cornelis,⁴ E. A. De Wolf,⁴ X. Janssen,⁴ A. Knutsson,⁴ S. Luyckx,⁴ L. Mucibello,⁴ S. Ochesanu,⁴ B. Roland,⁴ R. Rougny,⁴ Z. Staykova,⁴ H. Van Haevermaet,⁴ P. Van Mechelen,⁴ N. Van Remortel,⁴ A. Van Spilbeeck,⁴ F. Blekman,⁵ S. Blyweert,⁵ J. D'Hondt,⁵ A. Kalogeropoulos,⁵ J. Keaveney,⁵ M. Maes,⁵ A. Olbrechts,⁵ S. Tavernier,⁵ W. Van Doninck,⁵ P. Van Mulders,⁵ G. P. Van Onsem,⁵ I. Villella,⁵ B. Clerbaux,⁶ G. De Lentdecker,⁶ L. Favart,⁶ A. P. R. Gay,⁶ T. Hreus,⁶ A. Léonard,⁶ P. E. Marage,⁶ A. Mohammadi,⁶ L. Perniè,⁶ T. Reis,⁶ T. Seva,⁶ L. Thomas,⁶ C. Vander Velde,⁶ P. Vanlaer,⁶ J. Wang,⁶ V. Adler,⁷ K. Beernaert,⁷ L. Benucci,⁷ A. Cimmino,⁷ S. Costantini,⁷ S. Dildick,⁷ G. Garcia,⁷ B. Klein,⁷ J. Lellouch,⁷ A. Marinov,⁷ J. Mccartin,⁷ A. A. Ocampo Rios,⁷ D. Ryckbosch,⁷ M. Sigamani,⁷ N. Strobbe,⁷ F. Thyssen,⁷ M. Tytgat,⁷ S. Walsh,⁷ E. Yazgan,⁷ N. Zaganidis,⁷ S. Basegmez,⁸ C. Beluffi,^{8,d} G. Bruno,⁸ R. Castello,⁸ A. Caudron,⁸ L. Ceard,⁸ C. Delaere,⁸ T. du Pree,⁸ D. Favart,⁸ L. Forthomme,⁸ A. Giannanco,^{8,e} J. Hollar,⁸ P. Jez,⁸ V. Lemaitre,⁸ J. Liao,⁸ O. Militaru,⁸ C. Nuttens,⁸ D. Pagano,⁸ A. Pin,⁸ K. Piotrkowski,⁸ A. Popov,^{8,f} M. Selvaggi,⁸ J. M. Vizan Garcia,⁸ N. Belyi,⁹ T. Caebergs,⁹ E. Daubie,⁹ G. H. Hammad,⁹ G. A. Alves,¹⁰ M. Correa Martins Junior,¹⁰ T. Martins,¹⁰ M. E. Pol,¹⁰ M. H. G. Souza,¹⁰ W. L. Aldá Júnior,¹¹ W. Carvalho,¹¹ J. Chinellato,^{11,g} A. Custódio,¹¹ E. M. Da Costa,¹¹ D. De Jesus Damiao,¹¹ C. De Oliveira Martins,¹¹ S. Fonseca De Souza,¹¹ H. Malbouisson,¹¹ M. Malek,¹¹ D. Matos Figueiredo,¹¹ L. Mundim,¹¹ H. Nogima,¹¹ W. L. Prado Da Silva,¹¹ A. Santoro,¹¹ A. Sznajder,¹¹ E. J. Tonelli Manganote,^{11,g} A. Vilela Pereira,¹¹ C. A. Bernardes,^{12b} F. A. Dias,^{12a,h} T. R. Fernandez Perez Tomei,^{12a} E. M. Gregores,^{12b} C. Lagana,^{12a} P. G. Mercadante,^{12b} S. F. Novaes,^{12a} Sandra S. Padula,^{12a} V. Genchev,^{13,c} P. Iaydjiev,^{13,c} S. Piperov,¹³ M. Rodozov,¹³ G. Sultanov,¹³ M. Vutova,¹³ A. Dimitrov,¹⁴ R. Hadjiiska,¹⁴ V. Kozuharov,¹⁴ L. Litov,¹⁴ B. Pavlov,¹⁴ P. Petkov,¹⁴ J. G. Bian,¹⁵ G. M. Chen,¹⁵ H. S. Chen,¹⁵ C. H. Jiang,¹⁵ D. Liang,¹⁵ S. Liang,¹⁵ X. Meng,¹⁵ J. Tao,¹⁵ J. Wang,¹⁵ X. Wang,¹⁵ Z. Wang,¹⁵ H. Xiao,¹⁵ M. Xu,¹⁵ C. Asawatangtrakuldee,¹⁶ Y. Ban,¹⁶ Y. Guo,¹⁶ Q. Li,¹⁶ W. Li,¹⁶ S. Liu,¹⁶ Y. Mao,¹⁶ S. J. Qian,¹⁶ D. Wang,¹⁶ L. Zhang,¹⁶ W. Zou,¹⁶ C. Avila,¹⁷ C. A. Carrillo Montoya,¹⁷ L. F. Chaparro Sierra,¹⁷ J. P. Gomez,¹⁷ B. Gomez Moreno,¹⁷ J. C. Sanabria,¹⁷ N. Godinovic,¹⁸ D. Lelas,¹⁸ R. Plestina,^{18,i} D. Polic,¹⁸ I. Puljak,¹⁸ Z. Antunovic,¹⁹ M. Kovac,¹⁹ V. Briglijevic,²⁰ S. Duric,²⁰ K. Kadija,²⁰ J. Luetic,²⁰ D. Mekterovic,²⁰ S. Morovic,²⁰ L. Tikvica,²⁰ A. Attikis,²¹ G. Mavromanolakis,²¹ J. Mousa,²¹ C. Nicolaou,²¹ F. Ptochos,²¹ P. A. Razis,²¹ M. Finger,²² M. Finger Jr.,²² A. A. Abdelalim,^{23,j} Y. Assran,^{23,k} S. Elgammal,^{23,j} A. Ellithi Kamel,^{23,l} M. A. Mahmoud,^{23,m} A. Radi,^{23,n,o} M. Kadastik,²⁴ M. Müntel,²⁴ M. Murumaa,²⁴ M. Raidal,²⁴ L. Rebane,²⁴ A. Tiko,²⁴ P. Eerola,²⁵ G. Fedi,²⁵ M. Voutilainen,²⁵ J. Hätkönen,²⁶ V. Karimäki,²⁶ R. Kinnunen,²⁶ M. J. Kortelainen,²⁶ T. Lampén,²⁶ K. Lassila-Perini,²⁶ S. Lehti,²⁶ T. Lindén,²⁶ P. Luukka,²⁶ T. Mäenpää,²⁶ T. Peltola,²⁶ E. Tuominen,²⁶ J. Tuominiemi,²⁶ E. Tuovinen,²⁶ L. Wendland,²⁶ T. Tuuva,²⁷ M. Besancon,²⁸ F. Couderc,²⁸ M. Dejardin,²⁸ D. Denegri,²⁸ B. Fabbro,²⁸ J. L. Faure,²⁸ F. Ferri,²⁸ S. Ganjour,²⁸ A. Givernaud,²⁸ P. Gras,²⁸ G. Hamel de Monchenault,²⁸ P. Jarry,²⁸ E. Locci,²⁸ J. Malcles,²⁸ L. Millischer,²⁸ A. Nayak,²⁸ J. Rander,²⁸ A. Rosowsky,²⁸ M. Titov,²⁸ S. Baffioni,²⁹ F. Beaudette,²⁹ L. Benhabib,²⁹ M. Bluj,^{29,p} P. Busson,²⁹ C. Charlot,²⁹ N. Daci,²⁹ T. Dahms,²⁹ M. Dalchenko,²⁹ L. Dobrzynski,²⁹ A. Florent,²⁹ R. Granier de Cassagnac,²⁹ M. Haguenauer,²⁹ P. Miné,²⁹ C. Mironov,²⁹ I. N. Naranjo,²⁹ M. Nguyen,²⁹ C. Ochando,²⁹ P. Paganini,²⁹ D. Sabes,²⁹ R. Salerno,²⁹ Y. Sirois,²⁹ C. Veelken,²⁹ A. Zabi,²⁹ J.-L. Agram,^{30,q} J. Andrea,³⁰ D. Bloch,³⁰ J.-M. Brom,³⁰ E. C. Chabert,³⁰ C. Collard,³⁰ E. Conte,^{30,q} F. Drouhin,^{30,q} J.-C. Fontaine,^{30,q} D. Gelé,³⁰ U. Goerlach,³⁰ C. Goetzmann,³⁰ P. Juillet,³⁰ A.-C. Le Bihan,³⁰ P. Van Hove,³⁰ S. Gadrat,³¹ S. Beauceron,³² N. Beaupere,³² G. Boudoul,³² S. Brochet,³² J. Chasserat,³² R. Chierici,³² D. Contardo,³² P. Depasse,³² H. El Mamouni,³² J. Fay,³² S. Gascon,³² M. Gouzevitch,³² B. Ille,³² T. Kurca,³² M. Lethuillier,³² L. Mirabito,³² S. Perries,³²

- L. Sgandurra,³² V. Sordini,³² Y. Tschudi,³² M. Vander Donckt,³² P. Verdier,³² S. Viret,³² Z. Tsamalaidze,^{33,r} C. Autermann,³⁴ S. Beranek,³⁴ B. Calpas,³⁴ M. Edelhoff,³⁴ L. Feld,³⁴ N. Heracleous,³⁴ O. Hindrichs,³⁴ K. Klein,³⁴ A. Ostapchuk,³⁴ A. Perieanu,³⁴ F. Raupach,³⁴ J. Sammet,³⁴ S. Schael,³⁴ D. Sprenger,³⁴ H. Weber,³⁴ B. Wittmer,³⁴ V. Zhukov,^{34,f} M. Ata,³⁵ J. Caudron,³⁵ E. Dietz-Laursonn,³⁵ D. Duchardt,³⁵ M. Erdmann,³⁵ R. Fischer,³⁵ A. Güth,³⁵ T. Hebbeker,³⁵ C. Heidemann,³⁵ K. Hoepfner,³⁵ D. Klingebiel,³⁵ P. Kreuzer,³⁵ M. Merschmeyer,³⁵ A. Meyer,³⁵ M. Olschewski,³⁵ K. Padeken,³⁵ P. Papacz,³⁵ H. Pieta,³⁵ H. Reithler,³⁵ S. A. Schmitz,³⁵ L. Sonnenschein,³⁵ J. Steggemann,³⁵ D. Teyssier,³⁵ S. Thüer,³⁵ M. Weber,³⁵ V. Cherepanov,³⁶ Y. Erdogan,³⁶ G. Flügge,³⁶ H. Geenen,³⁶ M. Geisler,³⁶ W. Haj Ahmad,³⁶ F. Hoehle,³⁶ B. Kargoll,³⁶ T. Kress,³⁶ Y. Kuessel,³⁶ J. Lingemann,^{36,c} A. Nowack,³⁶ I. M. Nugent,³⁶ L. Perchalla,³⁶ O. Pooth,³⁶ A. Stahl,³⁶ M. Aldaya Martin,³⁷ I. Asin,³⁷ N. Bartosik,³⁷ J. Behr,³⁷ W. Behrenhoff,³⁷ U. Behrens,³⁷ M. Bergholz,^{37,s} A. Bethani,³⁷ K. Borras,³⁷ A. Burgmeier,³⁷ A. Cakir,³⁷ L. Calligaris,³⁷ A. Campbell,³⁷ S. Choudhury,³⁷ F. Costanza,³⁷ C. Diez Pardos,³⁷ S. Dooling,³⁷ T. Dorland,³⁷ G. Eckerlin,³⁷ D. Eckstein,³⁷ G. Flucke,³⁷ A. Geiser,³⁷ I. Glushkov,³⁷ P. Gunnellini,³⁷ S. Habib,³⁷ J. Hauk,³⁷ G. Hellwig,³⁷ D. Horton,³⁷ H. Jung,³⁷ M. Kasemann,³⁷ P. Katsas,³⁷ C. Kleinwort,³⁷ H. Kluge,³⁷ M. Krämer,³⁷ D. Krücker,³⁷ E. Kuznetsova,³⁷ W. Lange,³⁷ J. Leonard,³⁷ K. Lipka,³⁷ W. Lohmann,^{37,s} B. Lutz,³⁷ R. Mankel,³⁷ I. Marfin,³⁷ I.-A. Melzer-Pellmann,³⁷ A. B. Meyer,³⁷ J. Mnich,³⁷ A. Mussgiller,³⁷ S. Naumann-Emme,³⁷ O. Novgorodova,³⁷ F. Nowak,³⁷ J. Olzem,³⁷ H. Perrey,³⁷ A. Petrukhin,³⁷ D. Pitzl,³⁷ R. Placakyte,³⁷ A. Raspereza,³⁷ P. M. Ribeiro Cipriano,³⁷ C. Riedl,³⁷ E. Ron,³⁷ M. Ö. Sahin,³⁷ J. Salfeld-Nebgen,³⁷ R. Schmidt,^{37,s} T. Schoerner-Sadenius,³⁷ N. Sen,³⁷ M. Stein,³⁷ R. Walsh,³⁷ C. Wissing,³⁷ V. Blobel,³⁸ H. Enderle,³⁸ J. Erfle,³⁸ E. Garutti,³⁸ U. Gebbert,³⁸ M. Görner,³⁸ M. Gosselink,³⁸ J. Haller,³⁸ K. Heine,³⁸ R. S. Höing,³⁸ G. Kaussen,³⁸ H. Kirschenmann,³⁸ R. Klanner,³⁸ R. Kogler,³⁸ J. Lange,³⁸ I. Marchesini,³⁸ T. Peiffer,³⁸ N. Pietsch,³⁸ D. Rathjens,³⁸ C. Sander,³⁸ H. Schettler,³⁸ P. Schleper,³⁸ E. Schlieckau,³⁸ A. Schmidt,³⁸ M. Schröder,³⁸ T. Schum,³⁸ M. Seidel,³⁸ J. Sibille,^{38,t} V. Sola,³⁸ H. Stadie,³⁸ G. Steinbrück,³⁸ J. Thomsen,³⁸ D. Troendle,³⁸ E. Usai,³⁸ L. Vanelderden,³⁸ C. Barth,³⁹ C. Baus,³⁹ J. Berger,³⁹ C. Böser,³⁹ E. Butz,³⁹ T. Chwalek,³⁹ W. De Boer,³⁹ A. Descroix,³⁹ A. Dierlamm,³⁹ M. Feindt,³⁹ M. Guthoff,^{39,c} F. Hartmann,^{39,c} T. Hauth,^{39,c} H. Held,³⁹ K. H. Hoffmann,³⁹ U. Husemann,³⁹ I. Katkov,^{39,f} J. R. Komaragiri,³⁹ A. Kornmayer,^{39,c} P. Lobelle Pardo,³⁹ D. Martschei,³⁹ Th. Müller,³⁹ M. Niegel,³⁹ A. Nürnberg,³⁹ O. Oberst,³⁹ J. Ott,³⁹ G. Quast,³⁹ K. Rabbertz,³⁹ F. Ratnikov,³⁹ S. Röcker,³⁹ F.-P. Schilling,³⁹ G. Schott,³⁹ H. J. Simonis,³⁹ F. M. Stober,³⁹ R. Ulrich,³⁹ J. Wagner-Kuhr,³⁹ S. Wayand,³⁹ T. Weiler,³⁹ M. Zeise,³⁹ G. Anagnostou,⁴⁰ G. Daskalakis,⁴⁰ T. Geralis,⁴⁰ S. Kesisoglou,⁴⁰ A. Kyriakis,⁴⁰ D. Loukas,⁴⁰ A. Markou,⁴⁰ C. Markou,⁴⁰ E. Ntomari,⁴⁰ L. Gouskos,⁴¹ A. Panagiotou,⁴¹ N. Saoulidou,⁴¹ E. Stiliaris,⁴¹ X. Aslanoglou,⁴² I. Evangelou,⁴² G. Flouris,⁴² C. Foudas,⁴² P. Kokkas,⁴² N. Manthos,⁴² I. Papadopoulos,⁴² E. Paradas,⁴² G. Bencze,⁴³ C. Hajdu,⁴³ P. Hidas,⁴³ D. Horvath,^{43,u} B. Radics,⁴³ F. Sikler,⁴³ V. Veszpremi,⁴³ G. Vesztergombi,^{43,v} A. J. Zsigmond,⁴³ N. Beni,⁴⁴ S. Czellar,⁴⁴ J. Molnar,⁴⁴ J. Palinkas,⁴⁴ Z. Szillasi,⁴⁴ J. Karancsi,⁴⁵ P. Raics,⁴⁵ Z. L. Trocsanyi,⁴⁵ B. Ujvari,⁴⁵ S. K. Swain,^{46,w} S. B. Beri,⁴⁷ V. Bhatnagar,⁴⁷ N. Dhingra,⁴⁷ R. Gupta,⁴⁷ M. Kaur,⁴⁷ M. Z. Mehta,⁴⁷ M. Mittal,⁴⁷ N. Nishu,⁴⁷ L. K. Saini,⁴⁷ A. Sharma,⁴⁷ J. B. Singh,⁴⁷ Ashok Kumar,⁴⁸ Arun Kumar,⁴⁸ S. Ahuja,⁴⁸ A. Bhardwaj,⁴⁸ B. C. Choudhary,⁴⁸ S. Malhotra,⁴⁸ M. Naimuddin,⁴⁸ K. Ranjan,⁴⁸ P. Saxena,⁴⁸ V. Sharma,⁴⁸ R. K. Shivpuri,⁴⁸ S. Banerjee,⁴⁹ S. Bhattacharya,⁴⁹ K. Chatterjee,⁴⁹ S. Dutta,⁴⁹ B. Gomber,⁴⁹ Sa. Jain,⁴⁹ Sh. Jain,⁴⁹ R. Khurana,⁴⁹ A. Modak,⁴⁹ S. Mukherjee,⁴⁹ D. Roy,⁴⁹ S. Sarkar,⁴⁹ M. Sharan,⁴⁹ A. P. Singh,⁴⁹ A. Abdulsalam,⁵⁰ D. Dutta,⁵⁰ S. Kailas,⁵⁰ V. Kumar,⁵⁰ A. K. Mohanty,^{50,c} L. M. Pant,⁵⁰ P. Shukla,⁵⁰ A. Topkar,⁵⁰ T. Aziz,⁵¹ R. M. Chatterjee,⁵¹ S. Ganguly,⁵¹ S. Ghosh,⁵¹ M. Guchait,^{51,x} A. Gurtu,^{51,y} G. Kole,⁵¹ S. Kumar,⁵¹ M. Maity,^{51,z} G. Majumder,⁵¹ K. Mazumdar,⁵¹ G. B. Mohanty,⁵¹ B. Parida,⁵¹ K. Sudhakar,⁵¹ N. Wickramage,^{51,aa} S. Banerjee,⁵² S. Dugad,⁵² H. Arfaei,⁵³ H. Bakhshiansohi,⁵³ S. M. Etesami,^{53,bb} A. Fahim,^{53,cc} H. Hesari,⁵³ A. Jafari,⁵³ M. Khakzad,⁵³ M. Mohammadi Najafabadi,⁵³ S. Paktnat Mehdiabadi,⁵³ B. Safarzadeh,^{53,dd} M. Zeinali,⁵³ M. Grunewald,⁵⁴ M. Abbrescia,^{55a,55b} L. Barbone,^{55a,55b} C. Calabria,^{55a,55b} S. S. Chhibra,^{55a,55b} A. Colaleo,^{55a} D. Creanza,^{55a,55c} N. De Filippis,^{55a,55c} M. De Palma,^{55a,55b} L. Fiore,^{55a} G. Iaselli,^{55a,55c} G. Maggi,^{55a,55c} M. Maggi,^{55a} B. Marangelli,^{55a,55b} S. My,^{55a,55c} S. Nuzzo,^{55a,55b} N. Pacifico,^{55a} A. Pompili,^{55a,55b} G. Pugliese,^{55a,55c} G. Selvaggi,^{55a,55b} L. Silvestris,^{55a} G. Singh,^{55a,55b} R. Venditti,^{55a,55b} P. Verwilligen,^{55a} G. Zito,^{55a} G. Abbiendi,^{56a} A. C. Benvenuti,^{56a} D. Bonacorsi,^{56a,56b} S. Braibant-Giacomelli,^{56a,56b} L. Brigliadori,^{56a,56b} R. Campanini,^{56a,56b} P. Capiluppi,^{56a,56b} A. Castro,^{56a,56b} F. R. Cavallo,^{56a} G. Codispoti,^{56a} M. Cuffiani,^{56a,56b} G. M. Dallavalle,^{56a} F. Fabbri,^{56a} A. Fanfani,^{56a,56b} D. Fasanella,^{56a,56b} P. Giacomelli,^{56a} C. Grandi,^{56a} L. Guiducci,^{56a,56b} S. Marcellini,^{56a} G. Masetti,^{56a,c} M. Meneghelli,^{56a,56b} A. Montanari,^{56a} F. L. Navarria,^{56a,56b} F. Odorici,^{56a} A. Perrotta,^{56a} F. Primavera,^{56a,56b} A. M. Rossi,^{56a,56b} T. Rovelli,^{56a,56b} G. P. Siroli,^{56a,56b} N. Tosi,^{56a,56b} R. Travaglini,^{56a,56b} S. Albergo,^{57a,57b} M. Chiorboli,^{57a,57b} S. Costa,^{57a,57b} F. Giordano,^{57a,c} R. Potenza,^{57a,57b} A. Tricomi,^{57a,57b} C. Tuve,^{57a,57b} G. Barbagli,^{58a} V. Ciulli,^{58a,58b} C. Civinini,^{58a} R. D'Alessandro,^{58a,58b}

- E. Focardi,^{58a,58b} S. Frosali,^{58a,58b} E. Gallo,^{58a} S. Gonzi,^{58a,58b} V. Gori,^{58a,58b} P. Lenzi,^{58a,58b} M. Meschini,^{58a} S. Paoletti,^{58a}
 G. Sguazzoni,^{58a} A. Tropiano,^{58a,58b} L. Benussi,⁵⁹ S. Bianco,⁵⁹ F. Fabbri,⁵⁹ D. Piccolo,⁵⁹ P. Fabbricatore,^{60a} R. Musenich,^{60a}
 S. Tosi,^{60a,60b} A. Benaglia,^{61a} F. De Guio,^{61a,61b} M. E. Dinardo,^{61a} S. Fiorendi,^{61a,61b} S. Gennai,^{61a} A. Ghezzi,^{61a,61b}
 P. Govoni,^{61a} M. T. Lucchini,^{61a,c} S. Malvezzi,^{61a} R. A. Manzoni,^{61a,61b,c} A. Martelli,^{61a,61b,c} D. Menasce,^{61a} L. Moroni,^{61a}
 M. Paganoni,^{61a,61b} D. Pedrini,^{61a} S. Ragazzi,^{61a,61b} N. Redaelli,^{61a} T. Tabarelli de Fatis,^{61a,61b} S. Buontempo,^{62a}
 N. Cavallo,^{62a,62c} A. De Cosa,^{62a,62b} F. Fabozzi,^{62a,62c} A. O. M. Iorio,^{62a,62b} L. Lista,^{62a} S. Meola,^{62a,62d,c} M. Merola,^{62a}
 P. Paolucci,^{62a,c} P. Azzi,^{63a} N. Bacchetta,^{63a} D. Bisello,^{63a,63b} A. Branca,^{63a,63b} R. Carlin,^{63a,63b} P. Checchia,^{63a} T. Dorigo,^{63a}
 U. Dosselli,^{63a} F. Fanzago,^{63a} M. Galanti,^{63a,63b,c} F. Gasparini,^{63a,63b} U. Gasparini,^{63a,63b} P. Giubilato,^{63a,63b} A. Gozzelino,^{63a}
 K. Kanishchhev,^{63a,63c} S. Lacaprara,^{63a} I. Lazzizzera,^{63a,63c} M. Margoni,^{63a,63b} A. T. Meneguzzo,^{63a,63b} M. Passaseo,^{63a}
 J. Pazzini,^{63a,63b} M. Pegoraro,^{63a} N. Pozzobon,^{63a,63b} P. Ronchese,^{63a,63b} M. Sgaravatto,^{63a} F. Simonetto,^{63a,63b} E. Torassa,^{63a}
 M. Tosi,^{63a,63b} P. Zotto,^{63a,63b} G. Zumerle,^{63a,63b} M. Gabusi,^{64a,64b} S. P. Ratti,^{64a,64b} C. Riccardi,^{64a,64b} P. Vitulo,^{64a,64b}
 M. Biasini,^{65a,65b} G. M. Bilei,^{65a} L. Fanò,^{65a,65b} P. Lariccia,^{65a,65b} G. Mantovani,^{65a,65b} M. Menichelli,^{65a} A. Nappi,^{65a,65b,a}
 F. Romeo,^{65a,65b} A. Saha,^{65a} A. Santocchia,^{65a,65b} A. Spiezia,^{65a,65b} K. Androsov,^{66a,ee} P. Azzurri,^{66a} G. Bagliesi,^{66a}
 J. Bernardini,^{66a} T. Boccali,^{66a} G. Broccolo,^{66a,66c} R. Castaldi,^{66a} R. T. D'Agnolo,^{66a,66c,c} R. Dell'Orso,^{66a} F. Fiori,^{66a,66c}
 L. Foà,^{66a,66c} A. Giassi,^{66a} M. T. Grippo,^{66a,ee} A. Kraan,^{66a} F. Ligabue,^{66a,66c} T. Lomtadze,^{66a} L. Martini,^{66a,ee}
 A. Messineo,^{66a,66b} F. Palla,^{66a} A. Rizzi,^{66a,66b} A. Savoy-Navarro,^{66a,ff} A. T. Serban,^{66a} P. Spagnolo,^{66a} P. Squillaciotti,^{66a}
 R. Tenchini,^{66a} G. Tonelli,^{66a,66b} A. Venturi,^{66a} P. G. Verdini,^{66a} C. Vernieri,^{66a,66c} L. Barone,^{67a,67b} F. Cavallari,^{67a}
 D. Del Re,^{67a,67b} M. Diemoz,^{67a} M. Grassi,^{67a,67b} E. Longo,^{67a,67b} F. Margaroli,^{67a,67b} P. Meridiani,^{67a} F. Michelini,^{67a,67b}
 S. Nourbakhsh,^{67a,67b} G. Organtini,^{67a,67b} R. Paramatti,^{67a} S. Rahatlou,^{67a,67b} C. Rovelli,^{67a} L. Soffi,^{67a,67b} N. Amapane,^{68a,68b}
 R. Arcidiacono,^{68a,68c} S. Argiro,^{68a,68b} M. Arneodo,^{68a,68c} C. Biino,^{68a} N. Cartiglia,^{68a} S. Casasso,^{68a,68b} M. Costa,^{68a,68b}
 N. Demaria,^{68a} C. Mariotti,^{68a} S. Maselli,^{68a} E. Migliore,^{68a,68b} V. Monaco,^{68a,68b} M. Musich,^{68a} M. M. Obertino,^{68a,68c}
 G. Ortona,^{68a,68b} N. Pastrone,^{68a} M. Pelliccioni,^{68a,c} A. Potenza,^{68a,68b} A. Romero,^{68a,68b} M. Ruspa,^{68a,68c} R. Sacchi,^{68a,68b}
 A. Solano,^{68a,68b} A. Staiano,^{68a} U. Tamponi,^{68a} S. Belforte,^{69a} V. Candelise,^{69a,69b} M. Casarsa,^{69a} F. Cossutti,^{69a,c}
 G. Della Ricca,^{69a,69b} B. Gobbo,^{69a} C. La Licata,^{69a,69b} M. Marone,^{69a,69b} D. Montanino,^{69a,69b} A. Penzo,^{69a} A. Schizzi,^{69a,69b}
 A. Zanetti,^{69a} S. Chang,⁷⁰ T. Y. Kim,⁷⁰ S. K. Nam,⁷⁰ D. H. Kim,⁷¹ G. N. Kim,⁷¹ J. E. Kim,⁷¹ D. J. Kong,⁷¹ Y. D. Oh,⁷¹
 H. Park,⁷¹ D. C. Son,⁷¹ J. Y. Kim,⁷² Zero J. Kim,⁷² S. Song,⁷² S. Choi,⁷³ D. Gyun,⁷³ B. Hong,⁷³ M. Jo,⁷³ H. Kim,⁷³
 T. J. Kim,⁷³ K. S. Lee,⁷³ S. K. Park,⁷³ Y. Roh,⁷³ M. Choi,⁷⁴ J. H. Kim,⁷⁴ C. Park,⁷⁴ I. C. Park,⁷⁴ S. Park,⁷⁴ G. Ryu,⁷⁴ Y. Choi,⁷⁵
 Y. K. Choi,⁷⁵ J. Goh,⁷⁵ M. S. Kim,⁷⁵ E. Kwon,⁷⁵ B. Lee,⁷⁵ J. Lee,⁷⁵ S. Lee,⁷⁵ H. Seo,⁷⁵ I. Yu,⁷⁵ I. Grigelionis,⁷⁶
 A. Juodagalvis,⁷⁶ H. Castilla-Valdez,⁷⁷ E. De La Cruz-Burelo,⁷⁷ I. Heredia-de La Cruz,^{77,gg} R. Lopez-Fernandez,⁷⁷
 J. Martínez-Ortega,⁷⁷ A. Sanchez-Hernandez,⁷⁷ L. M. Villasenor-Cendejas,⁷⁷ S. Carrillo Moreno,⁷⁸ F. Vazquez Valencia,⁷⁸
 H. A. Salazar Ibarguen,⁷⁹ E. Casimiro Linares,⁸⁰ A. Morelos Pineda,⁸⁰ M. A. Reyes-Santos,⁸⁰ D. Krofcheck,⁸¹ A. J. Bell,⁸²
 P. H. Butler,⁸² R. Doesburg,⁸² S. Reucroft,⁸² H. Silverwood,⁸² M. Ahmad,⁸³ M. I. Asghar,⁸³ J. Butt,⁸³ H. R. Hoorani,⁸³
 S. Khalid,⁸³ W. A. Khan,⁸³ T. Khurshid,⁸³ S. Qazi,⁸³ M. A. Shah,⁸³ M. Shoaib,⁸³ H. Bialkowska,⁸⁴ B. Boimska,⁸⁴
 T. Frueboes,⁸⁴ M. Górski,⁸⁴ M. Kazana,⁸⁴ K. Nawrocki,⁸⁴ K. Romanowska-Rybinska,⁸⁴ M. Szleper,⁸⁴ G. Wrochna,⁸⁴
 P. Zalewski,⁸⁴ G. Brona,⁸⁵ K. Bunkowski,⁸⁵ M. Cwiok,⁸⁵ W. Dominik,⁸⁵ K. Doroba,⁸⁵ A. Kalinowski,⁸⁵ M. Konecki,⁸⁵
 J. Krolikowski,⁸⁵ M. Misiura,⁸⁵ W. Wolszczak,⁸⁵ N. Almeida,⁸⁶ P. Bargassa,⁸⁶ C. Beirão Da Cruz E Silva,⁸⁶ P. Faccioli,⁸⁶
 P. G. Ferreira Parracho,⁸⁶ M. Gallinaro,⁸⁶ F. Nguyen,⁸⁶ J. Rodrigues Antunes,⁸⁶ J. Seixas,^{86,c} J. Varela,⁸⁶ P. Vischia,⁸⁶
 S. Afanasiev,⁸⁷ P. Bunin,⁸⁷ I. Golutvin,⁸⁷ I. Gorbunov,⁸⁷ A. Kamenev,⁸⁷ V. Karjavin,⁸⁷ V. Konoplyanikov,⁸⁷ G. Kozlov,⁸⁷
 A. Lanev,⁸⁷ A. Malakhov,⁸⁷ V. Matveev,⁸⁷ P. Moisenz,⁸⁷ V. Palichik,⁸⁷ V. Perelygin,⁸⁷ S. Shmatov,⁸⁷ N. Skatchkov,⁸⁷
 V. Smirnov,⁸⁷ A. Zarubin,⁸⁷ S. Evstyukhin,⁸⁸ V. Golovtsov,⁸⁸ Y. Ivanov,⁸⁸ V. Kim,⁸⁸ P. Levchenko,⁸⁸ V. Murzin,⁸⁸
 V. Oreshkin,⁸⁸ I. Smirnov,⁸⁸ V. Sulimov,⁸⁸ L. Uvarov,⁸⁸ S. Vavilov,⁸⁸ A. Vorobyev,⁸⁸ An. Vorobyev,⁸⁸ Yu. Andreev,⁸⁹
 A. Dermenev,⁸⁹ S. Gninenko,⁸⁹ N. Golubev,⁸⁹ M. Kirsanov,⁸⁹ N. Krasnikov,⁸⁹ A. Pashenkov,⁸⁹ D. Tlisov,⁸⁹ A. Toropin,⁸⁹
 V. Epshteyn,⁹⁰ M. Erofeeva,⁹⁰ V. Gavrilov,⁹⁰ N. Lychkovskaya,⁹⁰ V. Popov,⁹⁰ G. Safronov,⁹⁰ S. Semenov,⁹⁰ A. Spiridonov,⁹⁰
 V. Stolin,⁹⁰ E. Vlasov,⁹⁰ A. Zhokin,⁹⁰ V. Andreev,⁹¹ M. Azarkin,⁹¹ I. Dremin,⁹¹ M. Kirakosyan,⁹¹ A. Leonidov,⁹¹
 G. Mesyats,⁹¹ S. V. Rusakov,⁹¹ A. Vinogradov,⁹¹ A. Belyaev,⁹² E. Boos,⁹² V. Bunichev,⁹² M. Dubinin,^{92,h} L. Dudko,⁹²
 A. Gribushin,⁹² V. Klyukhin,⁹² O. Kodolova,⁹² I. Lokhtin,⁹² A. Markina,⁹² S. Obraztsov,⁹² S. Petrushanko,⁹² V. Savrin,⁹²
 A. Snigirev,⁹² I. Azhgirey,⁹³ I. Bayshev,⁹³ S. Bitioukov,⁹³ V. Kachanov,⁹³ A. Kalinin,⁹³ D. Konstantinov,⁹³ V. Krychkine,⁹³
 V. Petrov,⁹³ R. Ryutin,⁹³ A. Sobol,⁹³ L. Tourtchanovitch,⁹³ S. Troshin,⁹³ N. Tyurin,⁹³ A. Uzunian,⁹³ A. Volkov,⁹³
 P. Adzic,^{94,hh} M. Djordjevic,⁹⁴ M. Ekmedzic,⁹⁴ D. Krpic,^{94,hh} J. Milosevic,⁹⁴ M. Aguilar-Benitez,⁹⁵ J. Alcaraz Maestre,⁹⁵

- C. Battilana,⁹⁵ E. Calvo,⁹⁵ M. Cerrada,⁹⁵ M. Chamizo Llatas,^{95,c} N. Colino,⁹⁵ B. De La Cruz,⁹⁵ A. Delgado Peris,⁹⁵
 D. Domínguez Vázquez,⁹⁵ C. Fernandez Bedoya,⁹⁵ J. P. Fernández Ramos,⁹⁵ A. Ferrando,⁹⁵ J. Flix,⁹⁵ M. C. Fouz,⁹⁵
 P. Garcia-Abia,⁹⁵ O. Gonzalez Lopez,⁹⁵ S. Goy Lopez,⁹⁵ J. M. Hernandez,⁹⁵ M. I. Josa,⁹⁵ G. Merino,⁹⁵
 E. Navarro De Martino,⁹⁵ J. Puerta Pelayo,⁹⁵ A. Quintario Olmeda,⁹⁵ I. Redondo,⁹⁵ L. Romero,⁹⁵ J. Santaolalla,⁹⁵
 M. S. Soares,⁹⁵ C. Willmott,⁹⁵ C. Albajar,⁹⁶ J. F. de Trocóniz,⁹⁶ H. Brun,⁹⁷ J. Cuevas,⁹⁷ J. Fernandez Menendez,⁹⁷
 S. Folgueras,⁹⁷ I. Gonzalez Caballero,⁹⁷ L. Lloret Iglesias,⁹⁷ J. Piedra Gomez,⁹⁷ J. A. Brochero Cifuentes,⁹⁸ I. J. Cabrillo,⁹⁸
 A. Calderon,⁹⁸ S. H. Chuang,⁹⁸ J. Duarte Campderros,⁹⁸ M. Fernandez,⁹⁸ G. Gomez,⁹⁸ J. Gonzalez Sanchez,⁹⁸
 A. Graziano,⁹⁸ C. Jorda,⁹⁸ A. Lopez Virto,⁹⁸ J. Marco,⁹⁸ R. Marco,⁹⁸ C. Martinez Rivero,⁹⁸ F. Matorras,⁹⁸
 F. J. Munoz Sanchez,⁹⁸ T. Rodrigo,⁹⁸ A. Y. Rodriguez-Marrero,⁹⁸ A. Ruiz-Jimeno,⁹⁸ L. Scodellaro,⁹⁸ I. Vila,⁹⁸
 R. Vilar Cortabitarte,⁹⁸ D. Abbaneo,⁹⁹ E. Auffray,⁹⁹ G. Auzinger,⁹⁹ M. Bachtis,⁹⁹ P. Baillon,⁹⁹ A. H. Ball,⁹⁹ D. Barney,⁹⁹
 J. Bendavid,⁹⁹ J. F. Benitez,⁹⁹ C. Bernet,^{99,i} G. Bianchi,⁹⁹ P. Bloch,⁹⁹ A. Bocci,⁹⁹ A. Bonato,⁹⁹ O. Bondu,⁹⁹ C. Botta,⁹⁹
 H. Breuker,⁹⁹ T. Camporesi,⁹⁹ G. Cerminara,⁹⁹ T. Christiansen,⁹⁹ J. A. Coarasa Perez,⁹⁹ S. Colafranceschi,^{99,ii}
 D. d'Enterria,⁹⁹ A. Dabrowski,⁹⁹ A. David,⁹⁹ A. De Roeck,⁹⁹ S. De Visscher,⁹⁹ S. Di Guida,⁹⁹ M. Dobson,⁹⁹
 N. Dupont-Sagorin,⁹⁹ A. Elliott-Peisert,⁹⁹ J. Eugster,⁹⁹ W. Funk,⁹⁹ G. Georgiou,⁹⁹ M. Giffels,⁹⁹ D. Gigi,⁹⁹ K. Gill,⁹⁹
 D. Giordano,⁹⁹ M. Girone,⁹⁹ M. Giunta,⁹⁹ F. Gleje,⁹⁹ R. Gomez-Reino Garrido,⁹⁹ S. Gowdy,⁹⁹ R. Guida,⁹⁹ J. Hammer,⁹⁹
 M. Hansen,⁹⁹ P. Harris,⁹⁹ C. Hartl,⁹⁹ A. Hinzmann,⁹⁹ V. Innocente,⁹⁹ P. Janot,⁹⁹ E. Karavakis,⁹⁹ K. Kousouris,⁹⁹
 K. Krajczar,⁹⁹ P. Lecoq,⁹⁹ Y.-J. Lee,⁹⁹ C. Lourenço,⁹⁹ N. Magini,⁹⁹ M. Malberti,⁹⁹ L. Malgeri,⁹⁹ M. Mannelli,⁹⁹ L. Masetti,⁹⁹
 F. Meijers,⁹⁹ S. Mersi,⁹⁹ E. Meschi,⁹⁹ R. Moser,⁹⁹ M. Mulders,⁹⁹ P. Musella,⁹⁹ E. Nesvold,⁹⁹ L. Orsini,⁹⁹
 E. Palencia Cortezon,⁹⁹ E. Perez,⁹⁹ L. Perrozzi,⁹⁹ A. Petrilli,⁹⁹ A. Pfeiffer,⁹⁹ M. Pierini,⁹⁹ M. Pimiä,⁹⁹ D. Piparo,⁹⁹
 M. Plagge,⁹⁹ L. Quertenmont,⁹⁹ A. Racz,⁹⁹ W. Reece,⁹⁹ G. Rolandi,^{99,ii} M. Rovere,⁹⁹ H. Sakulin,⁹⁹ F. Santanastasio,⁹⁹
 C. Schäfer,⁹⁹ C. Schwick,⁹⁹ I. Segoni,⁹⁹ S. Sekmen,⁹⁹ A. Sharma,⁹⁹ P. Siegrist,⁹⁹ P. Silva,⁹⁹ M. Simon,⁹⁹ P. Sphicas,^{99,kk}
 D. Spiga,⁹⁹ M. Stoye,⁹⁹ A. Tsirou,⁹⁹ G. I. Veres,^{99,v} J. R. Vlimant,⁹⁹ H. K. Wöhri,⁹⁹ S. D. Worm,^{99,ii} W. D. Zeuner,⁹⁹
 W. Bertl,¹⁰⁰ K. Deiters,¹⁰⁰ W. Erdmann,¹⁰⁰ K. Gabathuler,¹⁰⁰ R. Horisberger,¹⁰⁰ Q. Ingram,¹⁰⁰ H. C. Kaestli,¹⁰⁰ S. König,¹⁰⁰
 D. Kotlinski,¹⁰⁰ U. Langenegger,¹⁰⁰ D. Renker,¹⁰⁰ T. Rohe,¹⁰⁰ F. Bachmair,¹⁰¹ L. Bäni,¹⁰¹ L. Bianchini,¹⁰¹ P. Bortignon,¹⁰¹
 M. A. Buchmann,¹⁰¹ B. Casal,¹⁰¹ N. Chanon,¹⁰¹ A. Deisher,¹⁰¹ G. Dissertori,¹⁰¹ M. Dittmar,¹⁰¹ M. Donegà,¹⁰¹ M. Dünser,¹⁰¹
 P. Eller,¹⁰¹ K. Freudenreich,¹⁰¹ C. Grab,¹⁰¹ D. Hits,¹⁰¹ P. Lecomte,¹⁰¹ W. Lustermann,¹⁰¹ B. Mangano,¹⁰¹ A. C. Marini,¹⁰¹
 P. Martinez Ruiz del Arbol,¹⁰¹ N. Mohr,¹⁰¹ F. Moortgat,¹⁰¹ C. Nägeli,^{101,mm} P. Nef,¹⁰¹ F. Nessi-Tedaldi,¹⁰¹ F. Pandolfi,¹⁰¹
 L. Pape,¹⁰¹ F. Pauss,¹⁰¹ M. Peruzzi,¹⁰¹ F. J. Ronga,¹⁰¹ M. Rossini,¹⁰¹ L. Sala,¹⁰¹ A. K. Sanchez,¹⁰¹ A. Starodumov,^{101,nn}
 B. Stieger,¹⁰¹ M. Takahashi,¹⁰¹ L. Tauscher,^{101,a} A. Thea,¹⁰¹ K. Theofilatos,¹⁰¹ D. Treille,¹⁰¹ C. Urscheler,¹⁰¹ R. Wallny,¹⁰¹
 H. A. Weber,¹⁰¹ C. Amsler,^{102,oo} V. Chiochia,¹⁰² C. Favaro,¹⁰² M. Ivova Rikova,¹⁰² B. Kilminster,¹⁰² B. Millan Mejias,¹⁰²
 P. Otiougova,¹⁰² P. Robmann,¹⁰² H. Snoek,¹⁰² S. Taroni,¹⁰² S. Tupputi,¹⁰² M. Verzetti,¹⁰² M. Cardaci,¹⁰³ K. H. Chen,¹⁰³
 C. Ferro,¹⁰³ C. M. Kuo,¹⁰³ S. W. Li,¹⁰³ W. Lin,¹⁰³ Y. J. Lu,¹⁰³ R. Volpe,¹⁰³ S. S. Yu,¹⁰³ P. Bartalini,¹⁰⁴ P. Chang,¹⁰⁴
 Y. H. Chang,¹⁰⁴ Y. W. Chang,¹⁰⁴ Y. Chao,¹⁰⁴ K. F. Chen,¹⁰⁴ C. Dietz,¹⁰⁴ U. Grundler,¹⁰⁴ W.-S. Hou,¹⁰⁴ Y. Hsiung,¹⁰⁴
 K. Y. Kao,¹⁰⁴ Y. J. Lei,¹⁰⁴ R.-S. Lu,¹⁰⁴ D. Majumder,¹⁰⁴ E. Petrakou,¹⁰⁴ X. Shi,¹⁰⁴ J. G. Shiu,¹⁰⁴ Y. M. Tzeng,¹⁰⁴ M. Wang,¹⁰⁴
 B. Asavapibhop,¹⁰⁵ N. Suwonjandee,¹⁰⁵ A. Adiguzel,¹⁰⁶ M. N. Bakirci,^{106,pp} S. Cerci,^{106,qq} C. Dozen,¹⁰⁶ I. Dumanoglu,¹⁰⁶
 E. Eskut,¹⁰⁶ S. Giris,¹⁰⁶ G. Gokbulut,¹⁰⁶ E. Gurpinar,¹⁰⁶ I. Hos,¹⁰⁶ E. E. Kangal,¹⁰⁶ A. Kayis Topaksu,¹⁰⁶ G. Onengut,^{106,rr}
 K. Ozdemir,¹⁰⁶ S. Ozturk,^{106,pp} A. Polatoz,¹⁰⁶ K. Sogut,^{106,ss} D. Sunar Cerci,^{106,qq} B. Tali,^{106,qq} H. Topakli,^{106,pp} M. Vergili,¹⁰⁶
 I. V. Akin,¹⁰⁷ T. Aliev,¹⁰⁷ B. Bilin,¹⁰⁷ S. Bilmis,¹⁰⁷ M. Deniz,¹⁰⁷ H. Gamsizkan,¹⁰⁷ A. M. Guler,¹⁰⁷ G. Karapinar,^{107,tt}
 K. Ocalan,¹⁰⁷ A. Ozpineci,¹⁰⁷ M. Serin,¹⁰⁷ R. Sever,¹⁰⁷ U. E. Surat,¹⁰⁷ M. Yalvac,¹⁰⁷ M. Zeyrek,¹⁰⁷ E. Gürmez,¹⁰⁸
 B. Isildak,^{108,uu} M. Kaya,^{108,vv} O. Kaya,^{108,vv} S. Ozkorucuklu,^{108,ww} N. Sonmez,^{108,xx} H. Bahtiyar,^{109,yy} E. Barlas,¹⁰⁹
 K. Cankocak,¹⁰⁹ Y. O. Günaydin,^{109,zz} F. I. Vardarli,¹⁰⁹ M. Yücel,¹⁰⁹ L. Levchuk,¹¹⁰ P. Sorokin,¹¹⁰ J. J. Brooke,¹¹¹
 E. Clement,¹¹¹ D. Cussans,¹¹¹ H. Flacher,¹¹¹ R. Frazier,¹¹¹ J. Goldstein,¹¹¹ M. Grimes,¹¹¹ G. P. Heath,¹¹¹ H. F. Heath,¹¹¹
 L. Kreczko,¹¹¹ S. Metson,¹¹¹ D. M. Newbold,^{111,ii} K. Nirunpong,¹¹¹ A. Poll,¹¹¹ S. Senkin,¹¹¹ V. J. Smith,¹¹¹ T. Williams,¹¹¹
 L. Basso,^{112,aaa} K. W. Bell,¹¹² A. Belyaev,^{112,aaa} C. Brew,¹¹² R. M. Brown,¹¹² D. J. A. Cockerill,¹¹² J. A. Coughlan,¹¹²
 K. Harder,¹¹² S. Harper,¹¹² J. Jackson,¹¹² E. Olaiya,¹¹² D. Petyt,¹¹² B. C. Radburn-Smith,¹¹²
 C. H. Shepherd-Themistocleous,¹¹² I. R. Tomalin,¹¹² W. J. Womersley,¹¹² R. Bainbridge,¹¹³ O. Buchmuller,¹¹³ D. Burton,¹¹³
 D. Colling,¹¹³ N. Cripps,¹¹³ M. Cutajar,¹¹³ P. Dauncey,¹¹³ G. Davies,¹¹³ M. Della Negra,¹¹³ W. Ferguson,¹¹³ J. Fulcher,¹¹³
 D. Futyan,¹¹³ A. Gilbert,¹¹³ A. Guneratne Bryer,¹¹³ G. Hall,¹¹³ Z. Hatherell,¹¹³ J. Hays,¹¹³ G. Iles,¹¹³ M. Jarvis,¹¹³
 G. Karapostoli,¹¹³ M. Kenzie,¹¹³ R. Lane,¹¹³ R. Lucas,^{113,ii} L. Lyons,¹¹³ A.-M. Magnan,¹¹³ J. Marrouche,¹¹³ B. Mathias,¹¹³

- R. Nandi,¹¹³ J. Nash,¹¹³ A. Nikitenko,^{113,nn} J. Pela,¹¹³ M. Pesaresi,¹¹³ K. Petridis,¹¹³ M. Pioppi,^{113,bbb} D. M. Raymond,¹¹³ S. Rogerson,¹¹³ A. Rose,¹¹³ C. Seez,¹¹³ P. Sharp,^{113,a} A. Sparrow,¹¹³ A. Tapper,¹¹³ M. Vazquez Acosta,¹¹³ T. Virdee,¹¹³ S. Wakefield,¹¹³ N. Wardle,¹¹³ T. Whyntie,¹¹³ M. Chadwick,¹¹⁴ J. E. Cole,¹¹⁴ P. R. Hobson,¹¹⁴ A. Khan,¹¹⁴ P. Kyberd,¹¹⁴ D. Leggat,¹¹⁴ D. Leslie,¹¹⁴ W. Martin,¹¹⁴ I. D. Reid,¹¹⁴ P. Symonds,¹¹⁴ L. Teodorescu,¹¹⁴ M. Turner,¹¹⁴ J. Dittmann,¹¹⁵ K. Hatakeyama,¹¹⁵ A. Kasmi,¹¹⁵ H. Liu,¹¹⁵ T. Scarborough,¹¹⁵ O. Charaf,¹¹⁶ S. I. Cooper,¹¹⁶ C. Henderson,¹¹⁶ P. Rumerio,¹¹⁶ A. Avetisyan,¹¹⁷ T. Bose,¹¹⁷ C. Fantasia,¹¹⁷ A. Heister,¹¹⁷ P. Lawson,¹¹⁷ D. Lazic,¹¹⁷ J. Rohlf,¹¹⁷ D. Sperka,¹¹⁷ J. St. John,¹¹⁷ L. Sulak,¹¹⁷ J. Alimena,¹¹⁸ S. Bhattacharya,¹¹⁸ G. Christopher,¹¹⁸ D. Cutts,¹¹⁸ Z. Demiragli,¹¹⁸ A. Ferapontov,¹¹⁸ A. Garabedian,¹¹⁸ U. Heintz,¹¹⁸ S. Jabeen,¹¹⁸ G. Kukartsev,¹¹⁸ E. Laird,¹¹⁸ G. Landsberg,¹¹⁸ M. Luk,¹¹⁸ M. Narain,¹¹⁸ M. Segala,¹¹⁸ T. Sinthuprasith,¹¹⁸ T. Speer,¹¹⁸ R. Breedon,¹¹⁹ G. Breto,¹¹⁹ M. Calderon De La Barca Sanchez,¹¹⁹ S. Chauhan,¹¹⁹ M. Chertok,¹¹⁹ J. Conway,¹¹⁹ R. Conway,¹¹⁹ P. T. Cox,¹¹⁹ R. Erbacher,¹¹⁹ M. Gardner,¹¹⁹ R. Houtz,¹¹⁹ W. Ko,¹¹⁹ A. Kopecky,¹¹⁹ R. Lander,¹¹⁹ O. Mall,¹¹⁹ T. Miceli,¹¹⁹ R. Nelson,¹¹⁹ D. Pellett,¹¹⁹ F. Ricci-Tam,¹¹⁹ B. Rutherford,¹¹⁹ M. Searle,¹¹⁹ J. Smith,¹¹⁹ M. Squires,¹¹⁹ M. Tripathi,¹¹⁹ S. Wilbur,¹¹⁹ R. Yohay,¹¹⁹ V. Andreev,¹²⁰ D. Cline,¹²⁰ R. Cousins,¹²⁰ S. Erhan,¹²⁰ P. Everaerts,¹²⁰ C. Farrell,¹²⁰ M. Felcini,¹²⁰ J. Hauser,¹²⁰ M. Ignatenko,¹²⁰ C. Jarvis,¹²⁰ G. Rakness,¹²⁰ P. Schlein,^{120,a} E. Takasugi,¹²⁰ P. Traczyk,¹²⁰ V. Valuev,¹²⁰ M. Weber,¹²⁰ J. Babb,¹²¹ R. Clare,¹²¹ J. Ellison,¹²¹ J. W. Gary,¹²¹ G. Hanson,¹²¹ H. Liu,¹²¹ O. R. Long,¹²¹ A. Luthra,¹²¹ H. Nguyen,¹²¹ S. Paramesvaran,¹²¹ J. Sturdy,¹²¹ S. Sumowidagdo,¹²¹ R. Wilken,¹²¹ S. Wimpenny,¹²¹ W. Andrews,¹²² J. G. Branson,¹²² G. B. Cerati,¹²² S. Cittolin,¹²² D. Evans,¹²² A. Holzner,¹²² R. Kelley,¹²² M. Lebourgeois,¹²² J. Letts,¹²² I. Macneill,¹²² S. Padhi,¹²² C. Palmer,¹²² G. Petrucciani,¹²² M. Pieri,¹²² M. Sani,¹²² V. Sharma,¹²² S. Simon,¹²² E. Sudano,¹²² M. Tadel,¹²² Y. Tu,¹²² A. Vartak,¹²² S. Wasserbaech,^{122,ccc} F. Würthwein,¹²² A. Yagil,¹²² J. Yoo,¹²² D. Barge,¹²³ R. Bellan,¹²³ C. Campagnari,¹²³ M. D'Alfonso,¹²³ T. Danielson,¹²³ K. Flowers,¹²³ P. Geffert,¹²³ C. George,¹²³ F. Golf,¹²³ J. Incandela,¹²³ C. Justus,¹²³ P. Kalavase,¹²³ D. Kovalskyi,¹²³ V. Krutelyov,¹²³ S. Lowette,¹²³ R. Magaña Villalba,¹²³ N. Mccoll,¹²³ V. Pavlunin,¹²³ J. Ribnik,¹²³ J. Richman,¹²³ R. Rossin,¹²³ D. Stuart,¹²³ W. To,¹²³ C. West,¹²³ A. Apresyan,¹²⁴ A. Bornheim,¹²⁴ J. Bunn,¹²⁴ Y. Chen,¹²⁴ E. Di Marco,¹²⁴ J. Duarte,¹²⁴ D. Kcira,¹²⁴ Y. Ma,¹²⁴ A. Mott,¹²⁴ H. B. Newman,¹²⁴ C. Rogan,¹²⁴ M. Spiropulu,¹²⁴ V. Timciuc,¹²⁴ J. Veverka,¹²⁴ R. Wilkinson,¹²⁴ S. Xie,¹²⁴ Y. Yang,¹²⁴ R. Y. Zhu,¹²⁴ V. Azzolini,¹²⁵ A. Calamba,¹²⁵ R. Carroll,¹²⁵ T. Ferguson,¹²⁵ Y. Iiyama,¹²⁵ D. W. Jang,¹²⁵ Y. F. Liu,¹²⁵ M. Paulini,¹²⁵ J. Russ,¹²⁵ H. Vogel,¹²⁵ I. Vorobiev,¹²⁵ J. P. Cumalat,¹²⁶ B. R. Drell,¹²⁶ W. T. Ford,¹²⁶ A. Gaz,¹²⁶ E. Luiggi Lopez,¹²⁶ U. Nauenberg,¹²⁶ J. G. Smith,¹²⁶ K. Stenson,¹²⁶ K. A. Ulmer,¹²⁶ S. R. Wagner,¹²⁶ J. Alexander,¹²⁷ A. Chatterjee,¹²⁷ N. Eggert,¹²⁷ L. K. Gibbons,¹²⁷ W. Hopkins,¹²⁷ A. Khukhunaishvili,¹²⁷ B. Kreis,¹²⁷ N. Mirman,¹²⁷ G. Nicolas Kaufman,¹²⁷ J. R. Patterson,¹²⁷ A. Ryd,¹²⁷ E. Salvati,¹²⁷ W. Sun,¹²⁷ W. D. Teo,¹²⁷ J. Thom,¹²⁷ J. Thompson,¹²⁷ J. Tucker,¹²⁷ Y. Weng,¹²⁷ L. Winstrom,¹²⁷ P. Wittich,¹²⁷ D. Winn,¹²⁸ S. Abdullin,¹²⁹ M. Albrow,¹²⁹ J. Anderson,¹²⁹ G. Apollinari,¹²⁹ L. A. T. Bauerick,¹²⁹ A. Beretvas,¹²⁹ J. Berryhill,¹²⁹ P. C. Bhat,¹²⁹ K. Burkett,¹²⁹ J. N. Butler,¹²⁹ V. Chetluru,¹²⁹ H. W. K. Cheung,¹²⁹ F. Chlebana,¹²⁹ S. Cihangir,¹²⁹ V. D. Elvira,¹²⁹ I. Fisk,¹²⁹ J. Freeman,¹²⁹ Y. Gao,¹²⁹ E. Gottschalk,¹²⁹ L. Gray,¹²⁹ D. Green,¹²⁹ O. Gutsche,¹²⁹ D. Hare,¹²⁹ R. M. Harris,¹²⁹ J. Hirschauer,¹²⁹ B. Hooberman,¹²⁹ S. Jindariani,¹²⁹ M. Johnson,¹²⁹ U. Joshi,¹²⁹ B. Klima,¹²⁹ S. Kunori,¹²⁹ S. Kwan,¹²⁹ J. Linacre,¹²⁹ D. Lincoln,¹²⁹ R. Lipton,¹²⁹ J. Lykken,¹²⁹ K. Maeshima,¹²⁹ J. M. Marraffino,¹²⁹ V. I. Martinez Outschoorn,¹²⁹ S. Maruyama,¹²⁹ D. Mason,¹²⁹ P. McBride,¹²⁹ K. Mishra,¹²⁹ S. Mrenna,¹²⁹ Y. Musienko,^{129,ddd} C. Newman-Holmes,¹²⁹ V. O'Dell,¹²⁹ O. Prokofyev,¹²⁹ N. Ratnikova,¹²⁹ E. Sexton-Kennedy,¹²⁹ S. Sharma,¹²⁹ W. J. Spalding,¹²⁹ L. Spiegel,¹²⁹ L. Taylor,¹²⁹ S. Tkaczyk,¹²⁹ N. V. Tran,¹²⁹ L. Uplegger,¹²⁹ E. W. Vaandering,¹²⁹ R. Vidal,¹²⁹ J. Whitmore,¹²⁹ W. Wu,¹²⁹ F. Yang,¹²⁹ J. C. Yun,¹²⁹ D. Acosta,¹³⁰ P. Avery,¹³⁰ D. Bourilkov,¹³⁰ M. Chen,¹³⁰ T. Cheng,¹³⁰ S. Das,¹³⁰ M. De Gruttola,¹³⁰ G. P. Di Giovanni,¹³⁰ D. Dobur,¹³⁰ A. Drozdetskiy,¹³⁰ R. D. Field,¹³⁰ M. Fisher,¹³⁰ Y. Fu,¹³⁰ I. K. Furic,¹³⁰ J. Hugon,¹³⁰ B. Kim,¹³⁰ J. Konigsberg,¹³⁰ A. Korytov,¹³⁰ A. Kropivnitskaya,¹³⁰ T. Kypreos,¹³⁰ J. F. Low,¹³⁰ K. Matchev,¹³⁰ P. Milenovic,^{130,eee} G. Mitselmakher,¹³⁰ L. Muniz,¹³⁰ R. Remington,¹³⁰ A. Rinkevicius,¹³⁰ N. Skhirtladze,¹³⁰ M. Snowball,¹³⁰ J. Yelton,¹³⁰ M. Zakaria,¹³⁰ V. Gaultney,¹³¹ S. Hewamanage,¹³¹ S. Linn,¹³¹ P. Markowitz,¹³¹ G. Martinez,¹³¹ J. L. Rodriguez,¹³¹ T. Adams,¹³² A. Askew,¹³² J. Bochenek,¹³² J. Chen,¹³² B. Diamond,¹³² S. V. Gleyzer,¹³² J. Haas,¹³² S. Hagopian,¹³² V. Hagopian,¹³² K. F. Johnson,¹³² H. Prosper,¹³² V. Veeraraghavan,¹³² M. Weinberg,¹³² M. M. Baarmand,¹³³ B. Dorney,¹³³ M. Hohlmann,¹³³ H. Kalakhety,¹³³ F. Yumiceva,¹³³ M. R. Adams,¹³⁴ L. Apanasevich,¹³⁴ V. E. Bazterra,¹³⁴ R. R. Betts,¹³⁴ I. Bucinskaite,¹³⁴ J. Callner,¹³⁴ R. Cavanaugh,¹³⁴ O. Evdokimov,¹³⁴ L. Gauthier,¹³⁴ C. E. Gerber,¹³⁴ D. J. Hofman,¹³⁴ S. Khalatyan,¹³⁴ P. Kurt,¹³⁴ F. Lacroix,¹³⁴ D. H. Moon,¹³⁴ C. O'Brien,¹³⁴ C. Silkworth,¹³⁴ D. Strom,¹³⁴ P. Turner,¹³⁴ N. Varelas,¹³⁴ U. Akgun,¹³⁵ E. A. Albayrak,^{135,yy} B. Bilki,^{135,fff} W. Clarida,¹³⁵ K. Dilsiz,¹³⁵ F. Duru,¹³⁵ S. Griffiths,¹³⁵ J.-P. Merlo,¹³⁵ H. Mermerkaya,^{135,ggg} A. Mestvirishvili,¹³⁵ A. Moeller,¹³⁵ J. Nachtman,¹³⁵ C. R. Newsom,¹³⁵

- H. Ogul,¹³⁵ Y. Onel,¹³⁵ F. Ozok,^{135,yy} S. Sen,¹³⁵ P. Tan,¹³⁵ E. Tiras,¹³⁵ J. Wetzel,¹³⁵ T. Yetkin,^{135,hhh} K. Yi,¹³⁵ B. A. Barnett,¹³⁶
 B. Blumenfeld,¹³⁶ S. Bolognesi,¹³⁶ D. Fehling,¹³⁶ G. Giurgiu,¹³⁶ A. V. Gritsan,¹³⁶ G. Hu,¹³⁶ P. Maksimovic,¹³⁶ M. Swartz,¹³⁶
 A. Whitbeck,¹³⁶ P. Baringer,¹³⁷ A. Bean,¹³⁷ G. Benelli,¹³⁷ R. P. Kenny III,¹³⁷ M. Murray,¹³⁷ D. Noonan,¹³⁷ S. Sanders,¹³⁷
 R. Stringer,¹³⁷ J. S. Wood,¹³⁷ A. F. Barfuss,¹³⁸ I. Chakaberia,¹³⁸ A. Ivanov,¹³⁸ S. Khalil,¹³⁸ M. Makouski,¹³⁸ Y. Maravin,¹³⁸
 S. Shrestha,¹³⁸ I. Svintradze,¹³⁸ J. Gronberg,¹³⁹ D. Lange,¹³⁹ F. Rebassoo,¹³⁹ D. Wright,¹³⁹ A. Baden,¹⁴⁰ B. Calvert,¹⁴⁰
 S. C. Eno,¹⁴⁰ J. A. Gomez,¹⁴⁰ N. J. Hadley,¹⁴⁰ R. G. Kellogg,¹⁴⁰ T. Kolberg,¹⁴⁰ Y. Lu,¹⁴⁰ M. Marionneau,¹⁴⁰
 A. C. Mignerey,¹⁴⁰ K. Pedro,¹⁴⁰ A. Peterman,¹⁴⁰ A. Skuja,¹⁴⁰ J. Temple,¹⁴⁰ M. B. Tonjes,¹⁴⁰ S. C. Tonwar,¹⁴⁰ A. Apyan,¹⁴¹
 G. Bauer,¹⁴¹ W. Busza,¹⁴¹ I. A. Cali,¹⁴¹ M. Chan,¹⁴¹ L. Di Matteo,¹⁴¹ V. Dutta,¹⁴¹ G. Gomez Ceballos,¹⁴¹ M. Goncharov,¹⁴¹
 D. Gulhan,¹⁴¹ Y. Kim,¹⁴¹ M. Klute,¹⁴¹ Y. S. Lai,¹⁴¹ A. Levin,¹⁴¹ P. D. Luckey,¹⁴¹ T. Ma,¹⁴¹ S. Nahm,¹⁴¹ C. Paus,¹⁴¹
 D. Ralph,¹⁴¹ C. Roland,¹⁴¹ G. Roland,¹⁴¹ G. S. F. Stephans,¹⁴¹ F. Stöckli,¹⁴¹ K. Sumorok,¹⁴¹ D. Velicanu,¹⁴¹ R. Wolf,¹⁴¹
 B. Wyslouch,¹⁴¹ M. Yang,¹⁴¹ Y. Yilmaz,¹⁴¹ A. S. Yoon,¹⁴¹ M. Zanetti,¹⁴¹ V. Zhukova,¹⁴¹ B. Dahmes,¹⁴² A. De Benedetti,¹⁴²
 G. Franzoni,¹⁴² A. Gude,¹⁴² J. Haupt,¹⁴² S. C. Kao,¹⁴² K. Klapoetke,¹⁴² Y. Kubota,¹⁴² J. Mans,¹⁴² N. Pastika,¹⁴² R. Rusack,¹⁴²
 M. Sasseville,¹⁴² A. Singovsky,¹⁴² N. Tambe,¹⁴² J. Turkewitz,¹⁴² L. M. Cremaldi,¹⁴³ R. Kroeger,¹⁴³ L. Perera,¹⁴³
 R. Rahmat,¹⁴³ D. A. Sanders,¹⁴³ D. Summers,¹⁴³ E. Avdeeva,¹⁴⁴ K. Bloom,¹⁴⁴ S. Bose,¹⁴⁴ D. R. Claes,¹⁴⁴ A. Dominguez,¹⁴⁴
 M. Eads,¹⁴⁴ R. Gonzalez Suarez,¹⁴⁴ J. Keller,¹⁴⁴ I. Kravchenko,¹⁴⁴ J. Lazo-Flores,¹⁴⁴ S. Malik,¹⁴⁴ F. Meier,¹⁴⁴ G. R. Snow,¹⁴⁴
 J. Dolen,¹⁴⁵ A. Godshalk,¹⁴⁵ I. Iashvili,¹⁴⁵ S. Jain,¹⁴⁵ A. Kharchilava,¹⁴⁵ A. Kumar,¹⁴⁵ S. Rappoccio,¹⁴⁵ Z. Wan,¹⁴⁵
 G. Alverson,¹⁴⁶ E. Barberis,¹⁴⁶ D. Baumgartel,¹⁴⁶ M. Chasco,¹⁴⁶ J. Haley,¹⁴⁶ A. Massironi,¹⁴⁶ D. Nash,¹⁴⁶ T. Orimoto,¹⁴⁶
 D. Trocino,¹⁴⁶ D. Wood,¹⁴⁶ J. Zhang,¹⁴⁶ A. Anastassov,¹⁴⁷ K. A. Hahn,¹⁴⁷ A. Kubik,¹⁴⁷ L. Lusito,¹⁴⁷ N. Mucia,¹⁴⁷
 N. Odell,¹⁴⁷ B. Pollack,¹⁴⁷ A. Pozdnyakov,¹⁴⁷ M. Schmitt,¹⁴⁷ S. Stoynev,¹⁴⁷ K. Sung,¹⁴⁷ M. Velasco,¹⁴⁷ S. Won,¹⁴⁷
 D. Berry,¹⁴⁸ A. Brinkerhoff,¹⁴⁸ K. M. Chan,¹⁴⁸ M. Hildreth,¹⁴⁸ C. Jessop,¹⁴⁸ D. J. Karmgard,¹⁴⁸ J. Kolb,¹⁴⁸ K. Lannon,¹⁴⁸
 W. Luo,¹⁴⁸ S. Lynch,¹⁴⁸ N. Marinelli,¹⁴⁸ D. M. Morse,¹⁴⁸ T. Pearson,¹⁴⁸ M. Planer,¹⁴⁸ R. Ruchti,¹⁴⁸ J. Slaunwhite,¹⁴⁸
 N. Valls,¹⁴⁸ M. Wayne,¹⁴⁸ M. Wolf,¹⁴⁸ L. Antonelli,¹⁴⁹ B. Bylsma,¹⁴⁹ L. S. Durkin,¹⁴⁹ C. Hill,¹⁴⁹ R. Hughes,¹⁴⁹ K. Kotov,¹⁴⁹
 T. Y. Ling,¹⁴⁹ D. Puigh,¹⁴⁹ M. Rodenburg,¹⁴⁹ G. Smith,¹⁴⁹ C. Vuosalo,¹⁴⁹ G. Williams,¹⁴⁹ B. L. Winer,¹⁴⁹ H. Wolfe,¹⁴⁹
 E. Berry,¹⁵⁰ P. Elmer,¹⁵⁰ V. Halyo,¹⁵⁰ P. Hebda,¹⁵⁰ J. Hegeman,¹⁵⁰ A. Hunt,¹⁵⁰ P. Jindal,¹⁵⁰ S. A. Koay,¹⁵⁰ P. Lujan,¹⁵⁰
 D. Marlow,¹⁵⁰ T. Medvedeva,¹⁵⁰ M. Mooney,¹⁵⁰ J. Olsen,¹⁵⁰ P. Piroué,¹⁵⁰ X. Quan,¹⁵⁰ A. Raval,¹⁵⁰ H. Saka,¹⁵⁰
 D. Stickland,¹⁵⁰ C. Tully,¹⁵⁰ J. S. Werner,¹⁵⁰ S. C. Zenz,¹⁵⁰ A. Zuranski,¹⁵⁰ E. Brownson,¹⁵¹ A. Lopez,¹⁵¹ H. Mendez,¹⁵¹
 J. E. Ramirez Vargas,¹⁵¹ E. Alagoz,¹⁵² D. Benedetti,¹⁵² G. Bolla,¹⁵² D. Bortoletto,¹⁵² M. De Mattia,¹⁵² A. Everett,¹⁵²
 Z. Hu,¹⁵² M. Jones,¹⁵² K. Jung,¹⁵² O. Koybasi,¹⁵² M. Kress,¹⁵² N. Leonardo,¹⁵² D. Lopes Pegna,¹⁵² V. Maroussov,¹⁵²
 P. Merkel,¹⁵² D. H. Miller,¹⁵² N. Neumeister,¹⁵² I. Shipsey,¹⁵² D. Silvers,¹⁵² A. Svyatkovskiy,¹⁵² M. Vidal Marono,¹⁵²
 F. Wang,¹⁵² W. Xie,¹⁵² L. Xu,¹⁵² H. D. Yoo,¹⁵² J. Zablocki,¹⁵² Y. Zheng,¹⁵² S. Guragain,¹⁵³ N. Parashar,¹⁵³ A. Adair,¹⁵⁴
 B. Akgun,¹⁵⁴ K. M. Ecklund,¹⁵⁴ F. J. M. Geurts,¹⁵⁴ W. Li,¹⁵⁴ B. P. Padley,¹⁵⁴ R. Redjimi,¹⁵⁴ J. Roberts,¹⁵⁴ J. Zabel,¹⁵⁴
 B. Betchart,¹⁵⁵ A. Bodek,¹⁵⁵ R. Covarelli,¹⁵⁵ P. de Barbaro,¹⁵⁵ R. Demina,¹⁵⁵ Y. Eshaq,¹⁵⁵ T. Ferbel,¹⁵⁵ A. Garcia-Bellido,¹⁵⁵
 P. Goldenzweig,¹⁵⁵ J. Han,¹⁵⁵ A. Harel,¹⁵⁵ D. C. Miner,¹⁵⁵ G. Petrillo,¹⁵⁵ D. Vishnevskiy,¹⁵⁵ M. Zielinski,¹⁵⁵ A. Bhatti,¹⁵⁶
 R. Ciesielski,¹⁵⁶ L. Demortier,¹⁵⁶ K. Goulianios,¹⁵⁶ G. Lungu,¹⁵⁶ S. Malik,¹⁵⁶ C. Mesropian,¹⁵⁶ S. Arora,¹⁵⁷ A. Barker,¹⁵⁷
 J. P. Chou,¹⁵⁷ C. Contreras-Campana,¹⁵⁷ E. Contreras-Campana,¹⁵⁷ D. Duggan,¹⁵⁷ D. Ferencek,¹⁵⁷ Y. Gershtein,¹⁵⁷
 R. Gray,¹⁵⁷ E. Halkiadakis,¹⁵⁷ D. Hidas,¹⁵⁷ A. Lath,¹⁵⁷ S. Panwalkar,¹⁵⁷ M. Park,¹⁵⁷ R. Patel,¹⁵⁷ V. Rekovic,¹⁵⁷ J. Robles,¹⁵⁷
 S. Salur,¹⁵⁷ S. Schnetzer,¹⁵⁷ C. Seitz,¹⁵⁷ S. Somalwar,¹⁵⁷ R. Stone,¹⁵⁷ S. Thomas,¹⁵⁷ M. Walker,¹⁵⁷ G. Cerizza,¹⁵⁸
 M. Hollingsworth,¹⁵⁸ K. Rose,¹⁵⁸ S. Spanier,¹⁵⁸ Z. C. Yang,¹⁵⁸ A. York,¹⁵⁸ O. Bouhali,^{159,iii} R. Eusebi,¹⁵⁹ W. Flanagan,¹⁵⁹
 J. Gilmore,¹⁵⁹ T. Kamon,^{159,iiii} V. Khotilovich,¹⁵⁹ R. Montalvo,¹⁵⁹ I. Osipenkov,¹⁵⁹ Y. Pakhotin,¹⁵⁹ A. Perloff,¹⁵⁹ J. Roe,¹⁵⁹
 A. Safonov,¹⁵⁹ T. Sakuma,¹⁵⁹ I. Suarez,¹⁵⁹ A. Tatarinov,¹⁵⁹ D. Toback,¹⁵⁹ N. Akchurin,¹⁶⁰ J. Damgov,¹⁶⁰ C. Dragoiu,¹⁶⁰
 P. R. Dudero,¹⁶⁰ C. Jeong,¹⁶⁰ K. Kovitanggoon,¹⁶⁰ S. W. Lee,¹⁶⁰ T. Libeiro,¹⁶⁰ I. Volobouev,¹⁶⁰ E. Appelt,¹⁶¹
 A. G. Delannoy,¹⁶¹ S. Greene,¹⁶¹ A. Gurrola,¹⁶¹ W. Johns,¹⁶¹ C. Maguire,¹⁶¹ Y. Mao,¹⁶¹ A. Melo,¹⁶¹ M. Sharma,¹⁶¹
 P. Sheldon,¹⁶¹ B. Snook,¹⁶¹ S. Tuo,¹⁶¹ J. Velkovska,¹⁶¹ M. W. Arenton,¹⁶² S. Boutle,¹⁶² B. Cox,¹⁶² B. Francis,¹⁶²
 J. Goodell,¹⁶² R. Hirosky,¹⁶² A. Ledovskoy,¹⁶² C. Lin,¹⁶² C. Neu,¹⁶² J. Wood,¹⁶² S. Gollapinni,¹⁶³ R. Harr,¹⁶³
 P. E. Karchin,¹⁶³ C. Kottachchi Kankamage Don,¹⁶³ P. Lamichhane,¹⁶³ A. Sakharov,¹⁶³ D. A. Belknap,¹⁶⁴ L. Borrello,¹⁶⁴
 D. Carlsmith,¹⁶⁴ M. Cepeda,¹⁶⁴ S. Dasu,¹⁶⁴ E. Friis,¹⁶⁴ M. Grothe,¹⁶⁴ R. Hall-Wilton,¹⁶⁴ M. Herndon,¹⁶⁴ A. Hervé,¹⁶⁴
 K. Kaadze,¹⁶⁴ P. Klabbers,¹⁶⁴ J. Klukas,¹⁶⁴ A. Lanaro,¹⁶⁴ R. Loveless,¹⁶⁴ A. Mohapatra,¹⁶⁴ M. U. Mozer,¹⁶⁴ I. Ojalvo,¹⁶⁴
 G. A. Pierro,¹⁶⁴ G. Polese,¹⁶⁴ I. Ross,¹⁶⁴ A. Savin,¹⁶⁴ W. H. Smith¹⁶⁴ and J. Swanson¹⁶⁴

(CMS Collaboration)

- ¹*Yerevan Physics Institute, Yerevan, Armenia*
²*Institut für Hochenergiephysik der OeAW, Wien, Austria*
³*National Centre for Particle and High Energy Physics, Minsk, Belarus*
⁴*Universiteit Antwerpen, Antwerpen, Belgium*
⁵*Vrije Universiteit Brussel, Brussel, Belgium*
⁶*Université Libre de Bruxelles, Bruxelles, Belgium*
⁷*Ghent University, Ghent, Belgium*
⁸*Université Catholique de Louvain, Louvain-la-Neuve, Belgium*
⁹*Université de Mons, Mons, Belgium*
¹⁰*Centro Brasileiro de Pesquisas Fisicas, Rio de Janeiro, Brazil*
¹¹*Universidade do Estado do Rio de Janeiro, Rio de Janeiro, Brazil*
^{12a}*Universidade Estadual Paulista, São Paulo, Brazil*
^{12b}*Universidade Federal do ABC, São Paulo, Brazil*
¹³*Institute for Nuclear Research and Nuclear Energy, Sofia, Bulgaria*
¹⁴*University of Sofia, Sofia, Bulgaria*
¹⁵*Institute of High Energy Physics, Beijing, China*
¹⁶*State Key Laboratory of Nuclear Physics and Technology, Peking University, Beijing, China*
¹⁷*Universidad de Los Andes, Bogota, Colombia*
¹⁸*Technical University of Split, Split, Croatia*
¹⁹*University of Split, Split, Croatia*
²⁰*Institute Rudjer Boskovic, Zagreb, Croatia*
²¹*University of Cyprus, Nicosia, Cyprus*
²²*Charles University, Prague, Czech Republic*
²³*Academy of Scientific Research and Technology of the Arab Republic of Egypt,
Egyptian Network of High Energy Physics, Cairo, Egypt*
²⁴*National Institute of Chemical Physics and Biophysics, Tallinn, Estonia*
²⁵*Department of Physics, University of Helsinki, Helsinki, Finland*
²⁶*Helsinki Institute of Physics, Helsinki, Finland*
²⁷*Lappeenranta University of Technology, Lappeenranta, Finland*
²⁸*DSM/IRFU, CEA/Saclay, Gif-sur-Yvette, France*
²⁹*Laboratoire Leprince-Ringuet, Ecole Polytechnique, IN2P3-CNRS, Palaiseau, France*
³⁰*Institut Pluridisciplinaire Hubert Curien, Université de Strasbourg,
Université de Haute Alsace Mulhouse, CNRS/IN2P3, Strasbourg, France*
³¹*Centre de Calcul de l'Institut National de Physique Nucléaire et de Physique des Particules,
CNRS/IN2P3, Villeurbanne, France*
³²*Université de Lyon, Université Claude Bernard Lyon 1, CNRS-IN2P3,
Institut de Physique Nucléaire de Lyon, Villeurbanne, France*
³³*Institute of High Energy Physics and Informatization, Tbilisi State University, Tbilisi, Georgia*
³⁴*RWTH Aachen University, I. Physikalisches Institut, Aachen, Germany*
³⁵*RWTH Aachen University, III. Physikalisches Institut A, Aachen, Germany*
³⁶*RWTH Aachen University, III. Physikalisches Institut B, Aachen, Germany*
³⁷*Deutsches Elektronen-Synchrotron, Hamburg, Germany*
³⁸*University of Hamburg, Hamburg, Germany*
³⁹*Institut für Experimentelle Kernphysik, Karlsruhe, Germany*
⁴⁰*Institute of Nuclear and Particle Physics (INPP), NCSR Demokritos, Aghia Paraskevi, Greece*
⁴¹*University of Athens, Athens, Greece*
⁴²*University of Ioánnina, Ioánnina, Greece*
⁴³*KFKI Research Institute for Particle and Nuclear Physics, Budapest, Hungary*
⁴⁴*Institute of Nuclear Research ATOMKI, Debrecen, Hungary*
⁴⁵*University of Debrecen, Debrecen, Hungary*
⁴⁶*National Institute of Science Education and Research, Bhubaneswar, India*
⁴⁷*Panjab University, Chandigarh, India*
⁴⁸*University of Delhi, Delhi, India*
⁴⁹*Saha Institute of Nuclear Physics, Kolkata, India*
⁵⁰*Bhabha Atomic Research Centre, Mumbai, India*
⁵¹*Tata Institute of Fundamental Research—EHEP, Mumbai, India*
⁵²*Tata Institute of Fundamental Research—HECR, Mumbai, India*
⁵³*Institute for Research in Fundamental Sciences (IPM), Tehran, Iran*

- ⁵⁴*University College Dublin, Dublin, Ireland*
^{55a}*INFN Sezione di Bari, Bari, Italy*
^{55b}*Università di Bari, Bari, Italy*
^{55c}*Politecnico di Bari, Bari, Italy*
^{56a}*INFN Sezione di Bologna, Bologna, Italy*
^{56b}*Università di Bologna, Bologna, Italy*
^{57a}*INFN Sezione di Catania, Catania, Italy*
^{57b}*Università di Catania, Catania, Italy*
^{58a}*INFN Sezione di Firenze, Firenze, Italy*
^{58b}*Università di Firenze, Firenze, Italy*
⁵⁹*INFN Laboratori Nazionali di Frascati, Frascati, Italy*
^{60a}*INFN Sezione di Genova, Genova, Italy*
^{60b}*Università di Genova, Genova, Italy*
^{61a}*INFN Sezione di Milano-Bicocca, Milano, Italy*
^{61b}*Università di Milano-Bicocca, Milano, Italy*
^{62a}*INFN Sezione di Napoli, Napoli, Italy*
^{62b}*Università di Napoli 'Federico II', Napoli, Italy*
^{62c}*Università della Basilicata (Potenza), Napoli, Italy*
^{62d}*Università G. Marconi (Roma), Napoli, Italy*
^{63a}*INFN Sezione di Padova, Padova, Italy*
^{63b}*Università di Padova, Padova, Italy*
^{63c}*Università di Trento (Trento), Padova, Italy*
^{64a}*INFN Sezione di Pavia, Pavia, Italy*
^{64b}*Università di Pavia, Pavia, Italy*
^{65a}*INFN Sezione di Perugia*
^{65b}*Università di Perugia*
^{66a}*INFN Sezione di Pisa, Pisa, Italy*
^{66b}*Università di Pisa, Pisa, Italy*
^{66c}*Scuola Normale Superiore di Pisa, Pisa, Italy*
^{67a}*INFN Sezione di Roma, Roma, Italy*
^{67b}*Università di Roma, Roma, Italy*
^{68a}*INFN Sezione di Torino, Torino, Italy*
^{68b}*Università di Torino, Torino, Italy*
^{68c}*Università del Piemonte Orientale (Novara), Torino, Italy*
^{69a}*INFN Sezione di Trieste, Trieste, Italy*
^{69b}*Università di Trieste, Trieste, Italy*
⁷⁰*Kangwon National University, Chunchon, Korea*
⁷¹*Kyungpook National University, Daegu, Korea*
⁷²*Chonnam National University, Institute for Universe and Elementary Particles, Kwangju, Korea*
⁷³*Korea University, Seoul, Korea*
⁷⁴*University of Seoul, Seoul, Korea*
⁷⁵*Sungkyunkwan University, Suwon, Korea*
⁷⁶*Vilnius University, Vilnius, Lithuania*
⁷⁷*Centro de Investigacion y de Estudios Avanzados del IPN, Mexico City, Mexico*
⁷⁸*Universidad Iberoamericana, Mexico City, Mexico*
⁷⁹*Benemerita Universidad Autónoma de Puebla, Puebla, Mexico*
⁸⁰*Universidad Autónoma de San Luis Potosí, San Luis Potosí, Mexico*
⁸¹*University of Auckland, Auckland, New Zealand*
⁸²*University of Canterbury, Christchurch, New Zealand*
⁸³*National Centre for Physics, Quaid-I-Azam University, Islamabad, Pakistan*
⁸⁴*National Centre for Nuclear Research, Swierk, Poland*
⁸⁵*Institute of Experimental Physics, Faculty of Physics, University of Warsaw, Warsaw, Poland*
⁸⁶*Laboratório de Instrumentação e Física Experimental de Partículas, Lisboa, Portugal*
⁸⁷*Joint Institute for Nuclear Research, Dubna, Russia*
⁸⁸*Petersburg Nuclear Physics Institute, Gatchina (St. Petersburg), Russia*
⁸⁹*Institute for Nuclear Research, Moscow, Russia*
⁹⁰*Institute for Theoretical and Experimental Physics, Moscow, Russia*
⁹¹*P.N. Lebedev Physical Institute, Moscow, Russia*
⁹²*Skobeltsyn Institute of Nuclear Physics, Lomonosov Moscow State University, Moscow, Russia*
⁹³*State Research Center of Russian Federation, Institute for High Energy Physics, Protvino, Russia*

- ⁹⁴*University of Belgrade, Faculty of Physics and Vinca Institute of Nuclear Sciences, Belgrade, Serbia*
⁹⁵*Centro de Investigaciones Energéticas Medioambientales y Tecnológicas (CIEMAT), Madrid, Spain*
⁹⁶*Universidad Autónoma de Madrid, Madrid, Spain*
⁹⁷*Universidad de Oviedo, Oviedo, Spain*
⁹⁸*Instituto de Física de Cantabria (IFCA), CSIC-Universidad de Cantabria, Santander, Spain*
⁹⁹*CERN, European Organization for Nuclear Research, Geneva, Switzerland*
¹⁰⁰*Paul Scherrer Institut, Villigen, Switzerland*
¹⁰¹*Institute for Particle Physics, ETH Zurich, Zurich, Switzerland*
¹⁰²*Universität Zürich, Zurich, Switzerland*
¹⁰³*National Central University, Chung-Li, Taiwan*
¹⁰⁴*National Taiwan University (NTU), Taipei, Taiwan*
¹⁰⁵*Chulalongkorn University, Bangkok, Thailand*
¹⁰⁶*Cukurova University, Adana, Turkey*
¹⁰⁷*Middle East Technical University, Physics Department, Ankara, Turkey*
¹⁰⁸*Bogazici University, Istanbul, Turkey*
¹⁰⁹*Istanbul Technical University, Istanbul, Turkey*
¹¹⁰*National Scientific Center, Kharkov Institute of Physics and Technology, Kharkov, Ukraine*
¹¹¹*University of Bristol, Bristol, United Kingdom*
¹¹²*Rutherford Appleton Laboratory, Didcot, United Kingdom*
¹¹³*Imperial College, London, United Kingdom*
¹¹⁴*Brunel University, Uxbridge, United Kingdom*
¹¹⁵*Baylor University, Waco, USA*
¹¹⁶*The University of Alabama, Tuscaloosa, USA*
¹¹⁷*Boston University, Boston, USA*
¹¹⁸*Brown University, Providence, USA*
¹¹⁹*University of California, Davis, Davis, USA*
¹²⁰*University of California, Los Angeles, USA*
¹²¹*University of California, Riverside, Riverside, USA*
¹²²*University of California, San Diego, La Jolla, USA*
¹²³*University of California, Santa Barbara, Santa Barbara, USA*
¹²⁴*California Institute of Technology, Pasadena, USA*
¹²⁵*Carnegie Mellon University, Pittsburgh, USA*
¹²⁶*University of Colorado at Boulder, Boulder, USA*
¹²⁷*Cornell University, Ithaca, USA*
¹²⁸*Fairfield University, Fairfield, USA*
¹²⁹*Fermi National Accelerator Laboratory, Batavia, USA*
¹³⁰*University of Florida, Gainesville, USA*
¹³¹*Florida International University, Miami, USA*
¹³²*Florida State University, Tallahassee, USA*
¹³³*Florida Institute of Technology, Melbourne, USA*
¹³⁴*University of Illinois at Chicago (UIC), Chicago, USA*
¹³⁵*The University of Iowa, Iowa City, USA*
¹³⁶*Johns Hopkins University, Baltimore, USA*
¹³⁷*The University of Kansas, Lawrence, USA*
¹³⁸*Kansas State University, Manhattan, USA*
¹³⁹*Lawrence Livermore National Laboratory, Livermore, USA*
¹⁴⁰*University of Maryland, College Park, USA*
¹⁴¹*Massachusetts Institute of Technology, Cambridge, USA*
¹⁴²*University of Minnesota, Minneapolis, USA*
¹⁴³*University of Mississippi, Oxford, USA*
¹⁴⁴*University of Nebraska-Lincoln, Lincoln, USA*
¹⁴⁵*State University of New York at Buffalo, Buffalo, USA*
¹⁴⁶*Northeastern University, Boston, USA*
¹⁴⁷*Northwestern University, Evanston, USA*
¹⁴⁸*University of Notre Dame, Notre Dame, USA*
¹⁴⁹*The Ohio State University, Columbus, USA*
¹⁵⁰*Princeton University, Princeton, USA*
¹⁵¹*University of Puerto Rico, Mayaguez, USA*
¹⁵²*Purdue University, West Lafayette, USA*
¹⁵³*Purdue University Calumet, Hammond, USA*

¹⁵⁴*Rice University, Houston, USA*¹⁵⁵*University of Rochester, Rochester, USA*¹⁵⁶*The Rockefeller University, New York, USA*¹⁵⁷*Rutgers, The State University of New Jersey, Piscataway, USA*¹⁵⁸*University of Tennessee, Knoxville, USA*¹⁵⁹*Texas A&M University, College Station, USA*¹⁶⁰*Texas Tech University, Lubbock, USA*¹⁶¹*Vanderbilt University, Nashville, USA*¹⁶²*University of Virginia, Charlottesville, USA*¹⁶³*Wayne State University, Detroit, USA*¹⁶⁴*University of Wisconsin, Madison, USA*^aDeceased.^bAlso at Vienna University of Technology, Vienna, Austria.^cAlso at CERN, European Organization for Nuclear Research, Geneva, Switzerland.^dAlso at Institut Pluridisciplinaire Hubert Curien, Université de Strasbourg, Université de Haute Alsace Mulhouse, CNRS/IN2P3, Strasbourg, France.^eAlso at National Institute of Chemical Physics and Biophysics, Tallinn, Estonia.^fAlso at Skobeltsyn Institute of Nuclear Physics, Lomonosov Moscow State University, Moscow, Russia.^gAlso at Universidade Estadual de Campinas, Campinas, Brazil.^hAlso at California Institute of Technology, Pasadena, USA.ⁱAlso at Laboratoire Leprince-Ringuet, Ecole Polytechnique, IN2P3-CNRS, Palaiseau, France.^jAlso at Zewail City of Science and Technology, Zewail, Egypt.^kAlso at Suez Canal University, Suez, Egypt.^lAlso at Cairo University, Cairo, Egypt.^mAlso at Fayoum University, El-Fayoum, Egypt.ⁿAlso at British University in Egypt, Cairo, Egypt.^oAlso at Ain Shams University, Cairo, Egypt.^pAlso at National Centre for Nuclear Research, Swierk, Poland.^qAlso at Université de Haute Alsace, Mulhouse, France.^rAlso at Joint Institute for Nuclear Research, Dubna, Russia.^sAlso at Brandenburg University of Technology, Cottbus, Germany.^tAlso at The University of Kansas, Lawrence, USA.^uAlso at Institute of Nuclear Research ATOMKI, Debrecen, Hungary.^vAlso at Eötvös Loránd University, Budapest, Hungary.^wAlso at Tata Institute of Fundamental Research—EHEP, Mumbai, India.^xAlso at Tata Institute of Fundamental Research—HECR, Mumbai, India.^yAlso at King Abdulaziz University, Jeddah, Saudi Arabia.^zAlso at University of Visva-Bharati, Santiniketan, India.^{aa}Also at University of Ruhuna, Matara, Sri Lanka.^{bb}Also at Isfahan University of Technology, Isfahan, Iran.^{cc}Also at Sharif University of Technology, Tehran, Iran.^{dd}Also at Plasma Physics Research Center, Science and Research Branch, Islamic Azad University, Tehran, Iran.^{ee}Also at Università degli Studi di Siena, Siena, Italy.^{ff}Also at Purdue University, West Lafayette, USA.^{gg}Also at Universidad Michoacana de San Nicolas de Hidalgo, Morelia, Mexico.^{hh}Also at Faculty of Physics, University of Belgrade, Belgrade, Serbia.ⁱⁱAlso at Facoltà Ingegneria, Università di Roma, Roma, Italy.^{jj}Also at Scuola Normale e Sezione dell'INFN, Pisa, Italy.^{kk}Also at University of Athens, Athens, Greece.^{ll}Also at Rutherford Appleton Laboratory, Didcot, United Kingdom.^{mm}Also at Paul Scherrer Institut, Villigen, Switzerland.ⁿⁿAlso at Institute for Theoretical and Experimental Physics, Moscow, Russia.^{oo}Also at Albert Einstein Center for Fundamental Physics, Bern, Switzerland.^{pp}Also at Gaziosmanpasa University, Tokat, Turkey.^{qq}Also at Adiyaman University, Adiyaman, Turkey.^{rr}Also at Cag University, Mersin, Turkey.^{ss}Also at Mersin University, Mersin, Turkey.^{tt}Also at Izmir Institute of Technology, Izmir, Turkey.^{uu}Also at Ozyegin University, Istanbul, Turkey.

^{vv} Also at Kafkas University, Kars, Turkey.

^{ww} Also at Suleyman Demirel University, Isparta, Turkey.

^{xx} Also at Ege University, Izmir, Turkey.

^{yy} Also at Mimar Sinan University, Istanbul, Istanbul, Turkey.

^{zz} Also at Kahramanmaraş Sütçü Imam University, Kahramanmaraş, Turkey.

^{aaa} Also at School of Physics and Astronomy, University of Southampton, Southampton, United Kingdom.

^{bbb} Also at INFN Sezione di Perugia, Università di Perugia, Perugia, Italy.

^{ccc} Also at Utah Valley University, Orem, USA.

^{ddd} Also at Institute for Nuclear Research, Moscow, Russia.

^{eee} Also at University of Belgrade, Faculty of Physics and Vinca Institute of Nuclear Sciences, Belgrade, Serbia.

^{fff} Also at Argonne National Laboratory, Argonne, USA.

^{ggg} Also at Erzincan University, Erzincan, Turkey.

^{hhh} Also at Yildiz Technical University, Istanbul, Turkey.

ⁱⁱⁱ Also at Texas A&M University at Qatar, Doha, Qatar.

^{jjj} Also at Kyungpook National University, Daegu, Korea.